PROJECT HEGAASUS

Loughborough University, UK
Powertrain Department
Aircraft Systems Department
Business and Sales Department

Virginia Tech, USA
Structures Department
Aircraft Performance Department
Modelling Department

HYBRID ELECTRIC GENERAL AVIATION AIRCRAFT

2018 AIAA UNDERGRADUATE DESIGN COMPETITION

HAMSTERWORKS

HAMSTERWORKS DESIGN TEAM

Sammi Rocker (USA)
Design and Modelling
AIAA – 543803

Daniel Guerrero (UK)
Aircraft Integration
AIAA – 921916

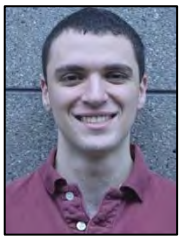

Kyle Silva (USA)
Landing Gear & Certification
AIAA –921097

Ashley Peyton-Bruhl (UK)
Business & Sales
AIAA – 921913

Danny Fritsch (USA)
Flight Physics
AIAA-921435

Nathaniel Marsh (UK)
Propulsion Design
AIAA-921919

Troy Bergin (USA)
Structural Design
AIAA – 736794

Jennifer Glover (UK)
Powertrain Design
AIAA - 921554

Alexander Mclean (USA)
Stability & Performance
AIAA - 921291

Dhirun Mistry (UK)
Avionic Systems
AIAA – 921917

Pradeep Raj, Ph.D. (USA)
Virginia Tech Advisor

James Knowles, Ph.D. (UK)
Loughborough University Advisor

CONTENTS

LIST OF FIGURES

LIST OF TABLES

LIST OF ABBREVIATIONS

Abbreviation	Description
ACARE	Advisory Council for Aviation Research and innovation in Europe
AIAA	American Institute for Aeronautics and Astronautics
AMSL	Above Mean Sea Level
EIS	Entry into Service
GA	General Aviation
HEGAA	Hybrid Electric General Aviation Aircraft
ICAO CAEP	International Civil Aviation Organization - Committee on Aviation Environmental Protection
LD	Landing
MG	Milestone Gate
MLW	Maximum Landing Weight
MTOW	Maximum Take Off Weight
NACA	National Advisory Committee for Aeronautics
OWE	Operating Weight Empty
PLI	Product Liability Insurance
QDF	Quantity Discount Factor
RFP	Request for Proposal
SFC	Specific Fuel Consumption
TO	Take Off
ISA	International Standard Atmosphere
ICE	Internal Combustion Engine
EHA	Electro Hydrostatic Actuation
GEN	Generator
TRU	Transformer Rectifier Unit
INV	Invertor
BAT	Battery

1. EXECUTIVE SUMMARY

In response to the AIAA 2017-2018 Undergraduate Team Aircraft Design Competition Request for Proposal, a new family of hybrid electric general aviation aircraft has been developed to meet the diverse needs of the everyday aviator, implementing cutting-edge hybrid electric propulsion technology to offer the owner unparalleled savings and uncompromising performance. The HamsterWorks team introduces Project HEGAAsus: the future of general aviation. The proposed family consists of a four and six seat variant, which will enter service in 2028 and 2030, respectively.

The HEGAAsus' cost-saving operation is made possible by complementing the reliability and availability of jet fuel with growing energy density of new battery technology: its Higgs V6 engine is designed for a 200+ knot cruise, and retractable twin electric wing propulsors provide power augmentation for an aggressive take-off and climb from improved or unimproved runways, allowing the HEGAAsus to service even the 56 percent of private and public-use airports that are unpaved or less than 3000 feet. With an engine sized to work most efficiently for cruise and state-of-the-art electric propulsion components, it can perform its long-range mission with 60 percent of the combustion fuel consumption of current high-performance general aviation aircraft like the Cessna TTx and Piper Seneca, truly setting the HEGAAsus apart from the competition. This tri-propeller configuration is electrically coupled and, with FAR Part 23's newly flexible requirements on the demonstrated compliance of asymmetric thrust avoidance, allows for a single-engine rated pilot, making up 87 percent of the global general aviation community, to operate the HEGAAsus with ease.

The HamsterWorks team is always looking toward the future, so to compete with expected fast-paced technology developments, the HEGAAsus was designed with upgradability in mind. Its fly-by-light system architecture will enable future autonomous functionality with redundant fiber optic cables which reduce weight and increase reliability. The design also integrates convenient replacement of batteries as energy densities improve, grouping them in modules no heavier than the 50 kg lifting limit specified by workplace regulation entities. These features come packaged in a light-weight composite airframe that has a 95 percent part commonality by weight between the four and six seat variants, allowing for cost-effective production. All of this leads to a competitive sticker price in the future general aviation market, and 20-year lifetime cost savings of $400,000 and $620,000 for the four and six seat variants, relative to their primary combustion-only competition.

The HEGAAsus meets and, in many cases, exceeds the performance of current GA aircraft and the requirements outlined in the RFP. A summary of the aircraft performance and demonstration of compliance is shown in Table 1.

Table 1 - Aircraft performance summary

RFP performance requirement			Compliance		
Requirement statement	**4-seat**	**6-seat**	**4-seat**	**6-seat**	**Reference**
Cruise Speed [kts]	Target 200 Min 174		219	216	6.4.1
Still Air Range – with IFR reserves [nmi]	1000	750	1127	1106	6.4.3
Minimum Initial Climb Rate - ISA sea level [fpm]	1800	1500	2561	2351	6.4.2
Takeoff Field Length [ft] • Dry pavement, ISA sea level to 50ft obstacle	1500	1800	1413	1499	6.4.4
Landing Field Length [ft] • Dry pavement, ISA sea level to 50ft obstacle	1500	1800	1474	1607	6.4.5
Cargo volume per passenger [cuft]	4	4	7	4.7	7.2

The analysis and validation in the sections below demonstrate that the HEGAAsus offers what HamsterWorks believes to be the best solution to the AIAA's request for proposal and has benefitted greatly from unique perspectives brought to the project by the international collaboration between Virginia Tech and Loughborough University. The HEGAAsus was designed with international scope, playing a role in the identification of growing markets of general aviation outside of the US, as well as the consideration of international environmental policy expectations which make a hybrid electric aircraft with the HEGAAsus' specialized features a highly sought-after product.

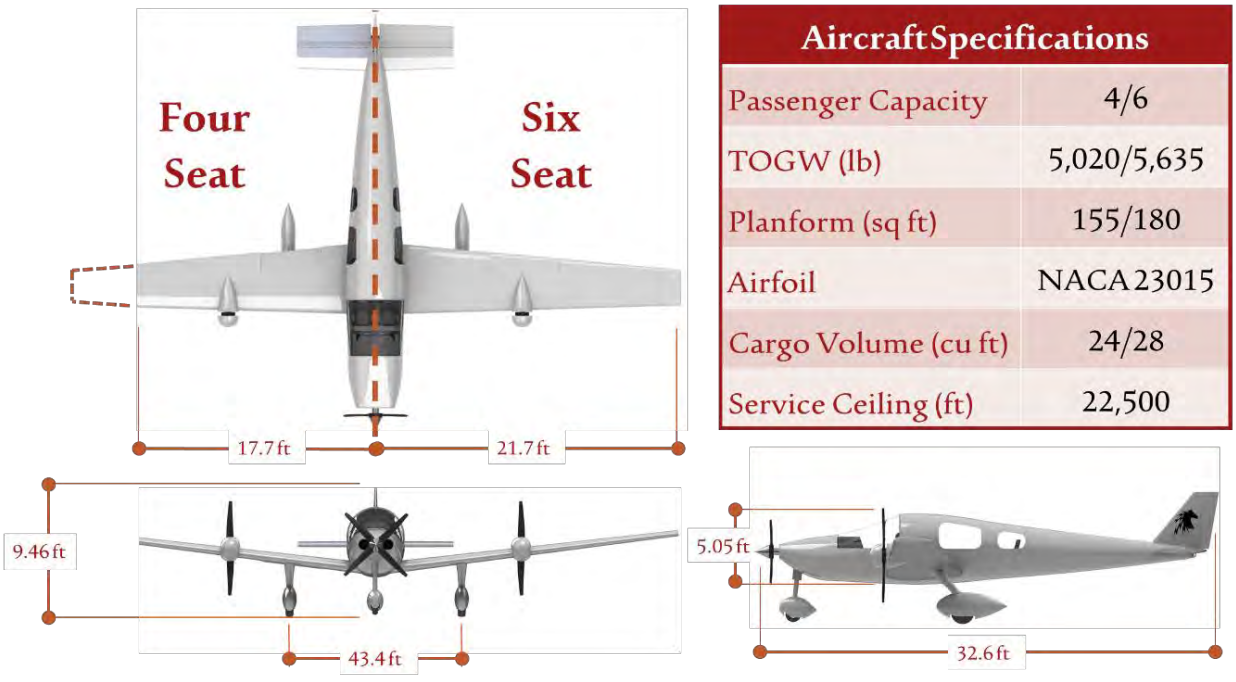

Figure 1 - Final 3-view of four and six seat variants

2. REQUIREMENTS IDENTIFICATION

To provide a means of verifying the RFP requirements and to ensure a design optimized for the customer, an analysis of the GA market was completed. The analysis is described here and includes: competitor placement, emerging disruptive technologies, customer specific requirements and concludes with a requirements statement and definition of the design mission profile.

2.1. Market Analysis

Market analysis was a key tool in verifying the RFP design point and confirming the potential for a profitable business. The standard approach to market research includes the collection of primary survey data from the customer. It was possible to collect some first-hand data from GA pilots during a visit to Virginia Tech Montgomery Executive Airport. However, most research was restricted to specialty magazines, forums and the competitor manufacturers' advertising, due to time and financial constraints. Both sources of information were interpreted to elicit customer requirements, with the aim of validating the design point.

2.1.1. Market potential

An analysis of the market potential suggested that an aging GA aircraft fleet coupled with major improvements in propulsive technology offer a promising business case for entering the GA market. A survey of existing aircraft [2] (Piper Seneca, Cessna 206 and Beechcraft 36) showed that the average age of these aircraft will be ~50 years at the target RFP EIS dates of 2028 and 2030, as shown in Figure 2. This position is supported by the 2011 FAA statistical data book and industry outlook, which identifies that the average piston engine aircraft age in 2010 was 42 years [3]. Assuming a maximum life of 60 years [4] provides a requirement to replace these aircraft at the RFP EIS dates.

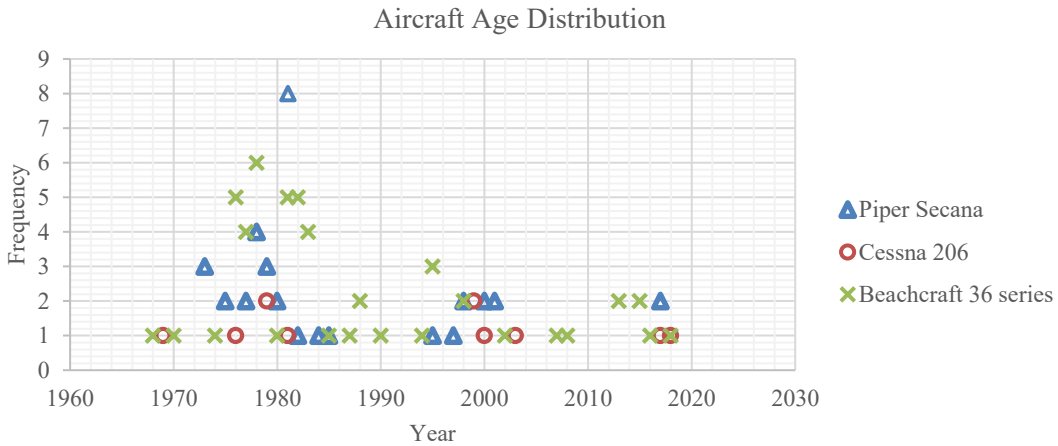

Figure 2 - Survey of second hand aircraft age [2]

Offering an innovative propulsive technology and a niche set of desirable attributes could generate its own new market in the GA sector. For example, the 2011 FAA industry outlook predicts market growth for long-range large cabin GA aircraft. Traditionally, this sector demand is met by business jets. However, the high-performance specification of the RFP requirements may offer these customers a lower cost alternative.

Another indication of the potential demand for hybrid technology is the growth in the hybrid automobile sector. The hybrid car market was valued at US$ 102.88 Billion in 2015 and is predicted to grow to US$ 398.90 billion by 2024 [5]. While the GA market is smaller in terms of sales volume, such growth in the auto industry suggests a desire for hybrid technology in the population.

2.1.2. Analysis of competitor aircraft

To understand the HEGAAsus family market placement and to identify key comparators for use in later design work, an analysis of range and cruise speed for existing 4 and 6-seat aircraft was undertaken [6]. Figure 3 shows the comparator speed and range data, with the RFP target and minimum design point overlaid.

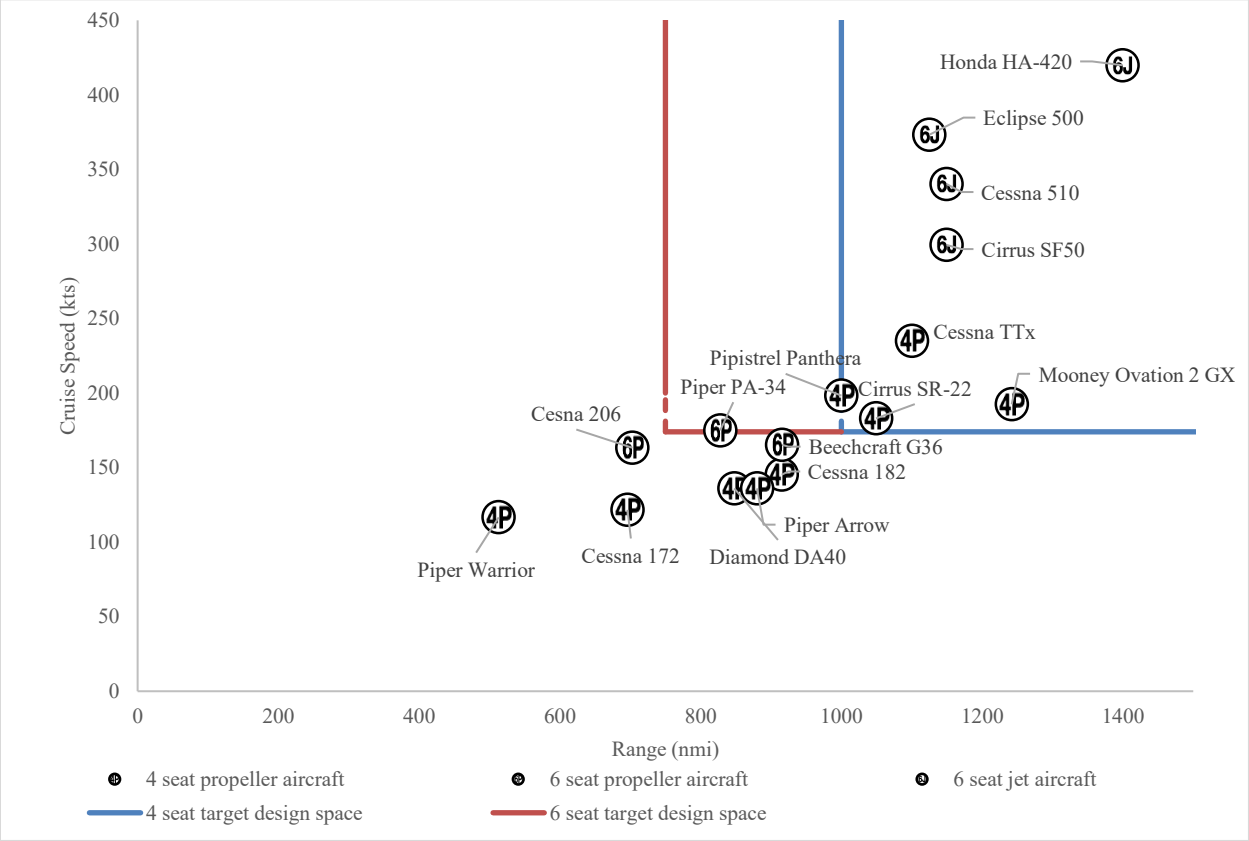

Figure 3 – Comparator range and speed placement

As shown by Figure 3 the RFP target cruise speed and range are most closely aligned with propeller GA aircraft, with the gas turbine powered aircraft sampled exceeding the design requirements significantly. This analysis shows that the HEGAAsus family occupies the high-performance end of propeller GA aircraft, a key point to be used in the concept generation phase of design. In addition to this, the key comparators for range and cruise speed were also be identified as:

- 4-seat aircraft –Pipistrel Panthera, Cirrus SR22T and Cessna TTx
- 6-seat aircraft – Beechcraft G36 and Piper PA-34

2.2. New Technology Analysis

2.2.1. Introduction to hybrid vehicles

A hybrid electric vehicle is defined by its combination of multiple power sources delivering desirable performance improvements. There are three general hybrid configurations: separated parallel, collated parallel and serial. A visual comparison of the three configurations can be seen in Figure 6, Figure 4 and Figure 5 [7]. A parallel hybrid system is characterized by a direct mechanical link between the combustion engine and the propulsion unit, with either a shared (collated parallel) or separate (separated parallel) power shaft driven by an electrical system.

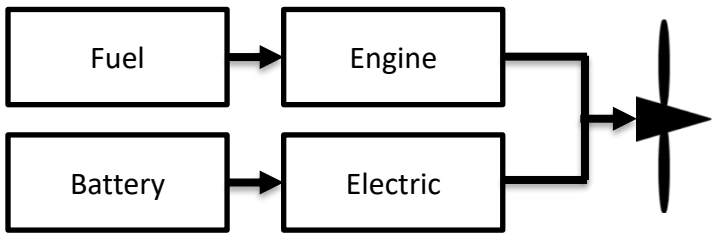

Figure 4 - Collated parallel hybrid system architecture

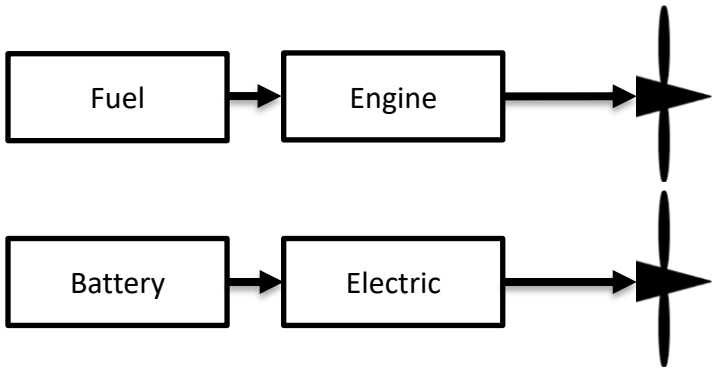

Figure 5 - Separated parallel hybrid system architecture

A serial hybrid system is characterized by a combustion engine delivering power to generate electricity, but not having a direct mechanical link to propulsion units.

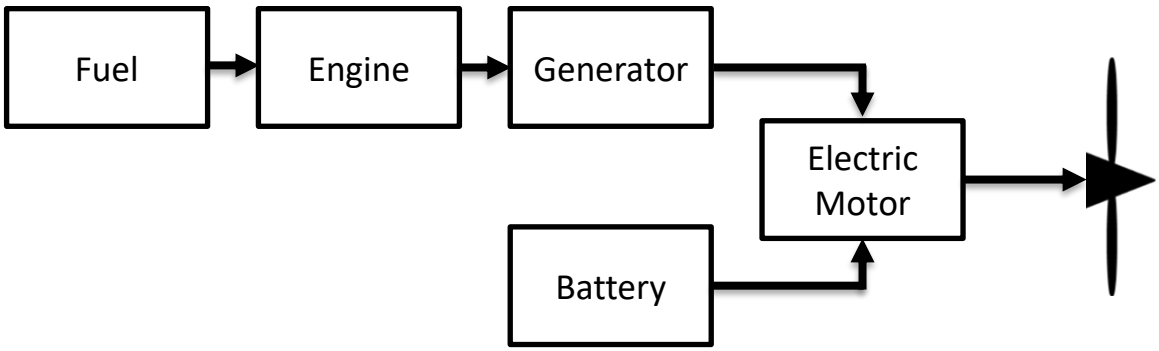

Figure 6 - Serial hybrid system architecture

2.2.2. Technology demonstrators

A key motivation for the RFP is the consistent increasing trend in the electrification of aircraft, with greater investment from industry leaders such as Airbus, Siemens and Rolls-Royce. While there are currently no commercial hybrid or fully electric aircraft, technology demonstrators have provided case studies for propulsion system development. A collaboration between Diamond Aircraft and Siemens produced the serial hybrid DA36 E-Star demonstrator, first flown in 2011 (Figure 7 a) [8]. This was a single seat motor glider, with a MTOW of 930 kg and a max take-off power of 70 kW. The hybrid drive cut emissions by 25%, permitted quiet take-off and landing, and demonstrated inflight recharging. However, the difference between the HEGAAsus and DA36 mission profiles limit the applicability of the project. As such, only the fundamentals of the drivetrain architecture can be applied to the design of the HEGAAsus.

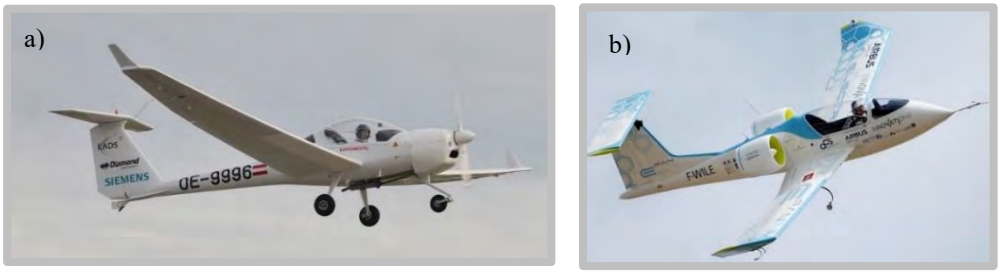

Figure 7 - DA36 demonstrator aircraft and E-Fan

Airbus, have produced a two seat, all-electric ducted fan demonstrator - E-Fan 2.0 (Figure 7 b)[9], [10]. Although the project demonstrated an all-electric aircraft, there was a hybrid variant planned for first flight in 2019. The E-Fan 4.0 was expected to carry 4 passengers for 2 to 3.5 hours, using a serial hybrid range extender powertrain model. In this configuration, the ducted fans can be powered by either battery power or directly from the internal combustion engine driven generator.

More novel propulsion architectures exist, such as the Airbus E-thrust concept. The 120-seat regional jet sized aircraft has electric ducted fans (EDF) buried in the wing roots and a gas turbine located in the rear fuselage [11]. Batteries supply the EDFs in takeoff and climb, while the gas turbine provides battery recharge and cruise power via generators. The NASA SCEPTOR concept is an all-electric technology demonstrator vehicle employing 2 wingtip mounted cruise propellers and 12 small leading edge distributed propellers. The small propellers increase lift during take-off and landing by increasing the relative velocity across the wing to produce higher lift from the smaller wing. The small propellers are switched off to optimize the cruise performance [12]. The Boeing XV-24a Lightning Strike is a vertical take-off and landing vehicle with distributed propulsion and tilt wing and canard, powered by a serial hybrid powertrain. This project has flight demonstrated a subscale model [13].

These case studies show that there are different hybrid architectures available to the HEGAAsus. As demonstrated by the E-Thrust and SCEPTOR projects, the concept of using the hybrid system to optimize cruise and take off power is popular. A full trade study will be conducted using influence from this study to identify the best architecture to meet the HEGAAsus mission requirements.

2.2.3. Distributed electric propulsion

Distributed electric propulsion (DEP) is another example of a novel aircraft configuration. It is predicted that fuel-burn savings can be achieved by using DEP; a key selling point for the HEGAASUS concept. As illustrated in Figure 8, DEP is characterized by an array of small propulsion units distributed along the aircraft, particularly the wing. [14]

Figure 8 - DEP shown on the NASA SCEPTOR[12]

Aerodynamic theory suggests that by inducing a larger dynamic pressure across the wing using the propeller-induced flow, higher lifting performance can be realized. A direct benefit of the increase in apparent velocity over the wing is the potential to reduce the wing size, necessary to provide the appropriate lifting performance. The limitation of this configuration is the increase in system complexity, manufacturing and maintenance costs. Additionally, as the subject of active early research it is unlikely that the technology readiness level (TRL) is sufficient for certification within the timeframe of the RFP EIS dates.

2.2.4. Batteries

Lithium-ion it is the predominant battery chemistry in the personal electronic device and electric automotive industry power source market, due to its high energy density and relative safety. For an aircraft, reducing weight is one of the primary design drivers to ensure the vehicle efficiency. As batteries were expected to contribute significantly to the HEGAAsus family aircraft weight, it was necessary to identify if other emerging battery technologies could meet the requirements of the HEGAAsus design. The trade study findings are summarized in

Table 2.

Table 2 - Battery technology research

Battery	Company	Specific energy (Wh/lb)	Current TRL	Projected TRL 2024
Current Li-Ion	Tesla [15]	115	9	9
Li-Ion with Ultrathin Li-Foil Anode	MIT SolidEnergy Systems [16]	230	5	8
Solid State Battery	University of Texas - Austin [17]	340	4	7
Graphene-Polymer	Grabat Graphenano [18]	455	3	6

The key design drivers for battery selection were specific energy and TRL. To meet the RFP EIS and certification requirements, it was assumed that the battery technology must be expected to achieve TRL level of 8 or above by 2024. Unlike fuel, battery weight does not decrease during use. Therefore, minimizing battery weight is a primary design driver for a hybrid or electric aircraft. The highest possible specific energy is preferable as this will deliver the HEGAAsus mission profile energy requirement with the minimum battery weight. Current lithium-ion chemistry is approaching its maximum theoretic specific energies, which is two orders of magnitude lower than fuel. However, SolidEnergy Systems has demonstrated higher specific energies in lithium-ion batteries using lithium-foil anodes. They have published considerable research on the demonstration of the technology capabilities and expect to begin electric vehicle battery production by the end of 2018 [16]. As the solid-state and graphene-polymer batteries not demonstrating a suitable expected TRL level to meet EIS, and the verified large-scale production capability of Li-Foil Anode batteries, the SolidEngery batteries were selected as the preferred battery cell.

2.3. Requirements Validation

2.3.1. Mission comparison

The AIAA RFP requires the 4-seat aircraft to fly 1000nmi and the 6-seat aircraft to fly 750mmi. As the higher range requirement, a validation study for the 4-seat was undertaken by examining potential routes from several major cities. *Figure 9* shows the current average 4-seat aircraft (range 800nmi) and the 1000nmi design point. The RFP range greater penetration into Europe from London. However, the benefit of the additional range is the realized for Trans-American crossings by reducing the number of layovers. For example, when traveling from Las Vegas to Miami or New York only one stop is required rather than two. For the reasons above, the requirement for 1000nmi is valid.

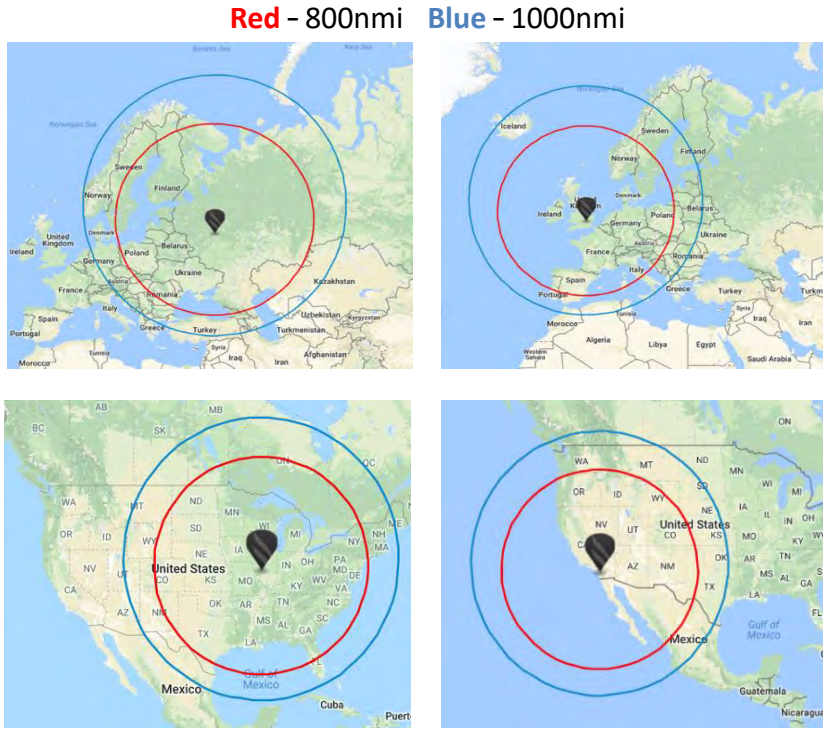

Figure 9 - Potential aircraft missions

2.3.2. Cruise altitude selection

The mission cruise altitude was set at 21,500/22,500 E/W ft above sea level. The HEGAAsus features a 3.35 psi differential pressurization system. A human needs supplemental oxygen if they spend thirty minutes or more at or above an altitude of 12,500 ft [19]. Using this partial pressurization system, a passenger in the HEGAAsus will feel 12,500 ft at a true altitude of 23,000 ft. At a cruise altitude of 22,500 ft the HEGAAsus passengers can fly comfortably

with no need for supplemental oxygen while experiencing significantly improved cruise speed and range over a cruising altitude below 12,500 ft.

2.3.3. Customer requirements

To elicit customer requirements, the questions shown in table 3 were posed with regards to both general aviation and identified direct comparators [20]–[28].

Table 3 - Customer requirements

Investigating question	Key competitors
What is the typical use of 4/6-seat aircraft?	• "Staycation" holidays and adventure trips (golfing/ fishing/ skiing) • Continental travel: Europe or North America • Small portion of the market for commercial flight offering rental or sharing
Who are the typical users of 4/6-seat aircraft?	• The highest proportion of pilots for GA are aged between 50-54[3] • Generally for family use or business professionals
How would a hybrid aircraft be a selling point?	• Reduced maintenance and operating costs, see section 4.1.1 for more detail • New technological advancement in aviation industry • Reduced fuel burn and environmental impact

From the analysis shown in Table 3, several conclusions were drawn and customer specific requirements generated. To ensure the final product is customer focused, the requirements shown below are to be considered at all relevant design decisions and validated where appropriate.

- **Large baggage space:**

  The baggage space requirement of 4 cubic feet per passenger, equivalent to a large hiking rucksack, does not fully align with the customer requirements. A larger baggage space would be desirable.

- **Excellent safety and reliability:**

  Only certified and TRL level 8-9 technology (by 2024) to be specified to ensure the safety and reliability of the aircraft at EIS and to conform to FAA requirements.

- **Luxury interior and aesthetically pleasing:**

  Design time dedicated to render a commercially appealing aircraft, improving the sales potential.

2.4. Final Requirements Statement and Mission Profile

This section concludes on the market and technological research conducted and discusses the validity of the key requirements from the RFP. Alterations to the RFP requirements are outlined in Table 4. Figure 10 shows the HEGAAsus design mission profile.

Table 4 - Requirements statement

Requirement	Justification
Hybrid propulsion	The use of a hybrid system will be a necessary minimum to meet the emissions and noise requirements set out by ICAO CAEP [29].
Range and cruise speed	Requirements for range and cruise speed align with our key competitors, suggesting there is a market for an aircraft with this performance.
Technology readiness	For EIS in 2028 and allowing a 4-year certification process, any new technology should be at a minimum TRL level of 8 or 9 by 2024.
Seat Variant Commonality	75% commonality between the 4 and 6-seat variants will be a necessary minimum to ensure a profitable manufacturing process. A 90% or higher commonality is desirable.
Flying in known icing conditions / All runway surface operation / VFR and IFR	The requirements for operation on all runway surfaces, flying in known icing conditions and operation under VFR and IFR all agree with the customer wants to use the aircraft for adventure use.
Baggage space	The baggage space requirement of 4 cubic feet per passenger, equivalent to a large hiking rucksack, is deemed a minimum. A baggage space of 6 cubic feet per passenger or higher is desirable.

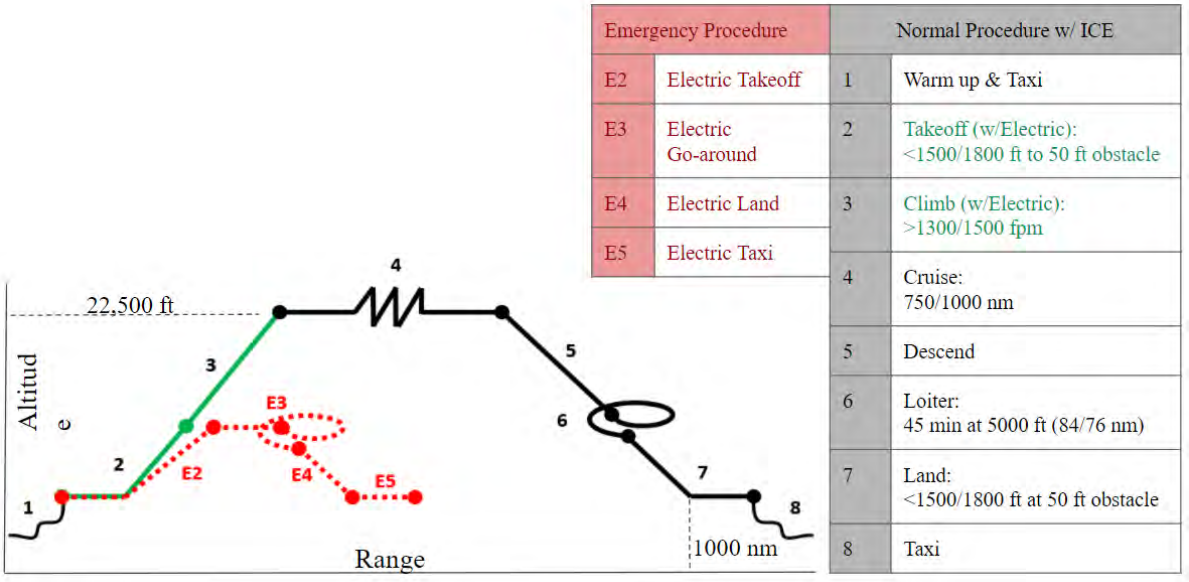

Figure 10 - Mission profile

3. CONCEPTUAL DESIGN

To reach the final preferred concept, it is necessary to follow a process of concept generation, down selection and preliminary sizing. The concept selection process was unconventional due to the trans-Atlantic team working in parallel at this stage. Due to scheduling differences between the institutions Both teams followed their own down selection process until two preferred concepts were generated. From here both concepts were merged to a final preferred concept.

3.1. Preferred Concept

Taking both preferred concepts, a trade study was undertaken to identify the best aspects of both designs. These aspects were collated to form the final preferred concept, informed by the assessment of relevant technologies completed previously. Following initial sizing the two preferred concepts are presented in Figure 11. The trade study comparing the preferred concepts and identifying the chosen design aspects for the final preferred concept is shown in Table 5.

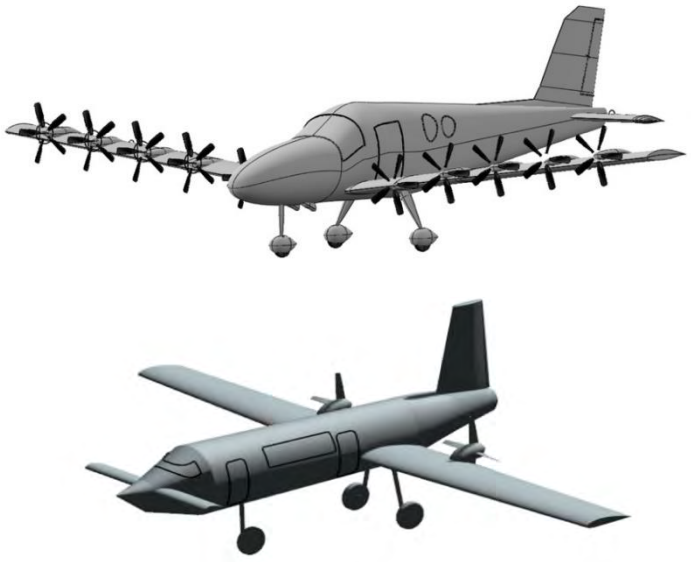

Figure 11 - Preferred concepts (VT top / LU bottom)

Table 5 - Final preferred concept selection

Features	VT	LU	Final preferred design
Fuselage	Upswept	Upswept	**Upswept** • Raises the horizontal stabilizer out of wing wake
Wing	Low wing Dihedral	Low wing Dihedral	**Low wing with Dihedral** • Recovery stability • Visually appealing
Vertical and horizonal stabilizer	Conventional	Canard	**Conventional** • Better aerodynamics performance for stall
Propulsion systems	DEP	Twin pusher	**Twin tractor** • More realistic TRL • Current precedent for certification • Ease of maintenance
Landing gear	Fixed Tricycle	Retractable Tricycle	**Fixed Tricycle** • Fixed reduce complexity and insurance cost • Tricycle safer then tail-dragger configuration

Taking the conclusions of the trade study, the final preferred concept is shown in Figure 12, with preliminary sizing shown in Table 6. This design offers several advantages over other concepts such as:

- Low dihedral wing and convectional tail plane for aerodynamics stability.
- Propulsive system offering ease of certification, maintenance and control.
- Aesthetically appealing aircraft profile.

Figure 12 - Final preferred concept

Table 6 - Final preferred concept preliminary sizing

Sizing Variable	4-seat	6-seat
Gross takeoff weight [lb]	4400	6600
Wing span [ft]	37	45
Power [hp]	310	465

1.1. Virginia Tech Down Selection Process

The Virginia Tech (VT) team followed a qualitative down selection process. All initial concepts were reduced to three candidate concepts by team assessment of each concept against the RFP and customer requirements. Following this a selection matrix was used to determine the preferred concept. Seven key grading criteria with an importance weighing out of 100% were used align with the importance of the requirements outlined by the RFP and customer. Table 7, presents the results of this assessment and the VT preferred concept.

Table 7 - VT stage 2 concept down select matrix

		Concepts		
	Weighting			
Aesthetic	0.11	37	**86**	58
Safety	0.21	42	**80**	78
Stability	0.15	86	**65**	84
Authority	0.15	47	**86**	59
Ease of Licensing	0.13	66	**30**	30
Maintenance	0.17	65	**68**	46
Manufacturability	0.09	84	**58**	71
	Total	*59*	***69***	*62*

1.2. Loughborough University Down Selection Process

The Loughborough University (LU) team used a similar down selection process, however the weighted selection matrix was used first to down select from all initial concepts to three candidate concepts. All initial concept were benchmarked against a comparator aircraft, the Pipistrel Panthera,[20] and graded out of 5, where a score of 3 indicated the concept was no better than the benchmark aircraft. Table 8 presents the results of this and the three candidate concepts. Following this the top three scoring aircraft were qualitatively analyzed against the RFP to generate the final LU preferred concept, which was selected as concept 1.

Table 8 - LU stage 1 concept down selection matrix

	Criteria	Weight	Concept													Pipistrel Panthera
			1	2	3	4	5	6	7	8	9	10	11	12	13	
Voice of the Customer	Mission compatibility	0.05	**2**	3	2	4	2	2	4	2	**5**	5	1	**4**	1	3
	Cabin	0.15	**4**	3	4	5	5	5	4	5	**3**	3	3	**5**	4	1
	Ease of flight	0.1	**2**	4	4	1	4	4	3	2	**5**	4	3	**4**	1	4
	Operations	0.2	**4**	3	2	1	1	2	2	2	**5**	5	3	**3**	2	4
Design	Certification	0.15	**4**	3	2	2	4	1	2	1	**3**	3	2	**3**	2	5
	Manufacturing	0.15	**3**	3	2	1	3	2	3	2	**4**	4	2	**4**	1	3
	Aerodynamic performance	0.2	**3**	2	3	2	3	3	4	5	**1**	1	3	**2**	4	2
		Total	**3.35**	2.90	2.70	2.10	3.10	2.70	3.05	2.90	**3.45**	3.35	2.60	**3.40**	2.40	3.10

1.3. Constraints sizing

First estimates for weight, wing area and power were calculated to allow preliminary sizing of the preferred concept. A constraints diagram, Figure 13, was generated using equations derived by Raymer [30]. The design space is indicated by the non-grey region. Assuming an empty weight and fuel weight fraction of 0.6 and 0.2, estimated from comparator aircraft, yields a gross take-off weight of 4400lb and 6600lb for the 4 and 6-seat aircraft. At the initial design point the wing area and power requirements are 138 / 206ft^2 and 310 / 465hp for the 4 and 6-seat aircraft respectively.

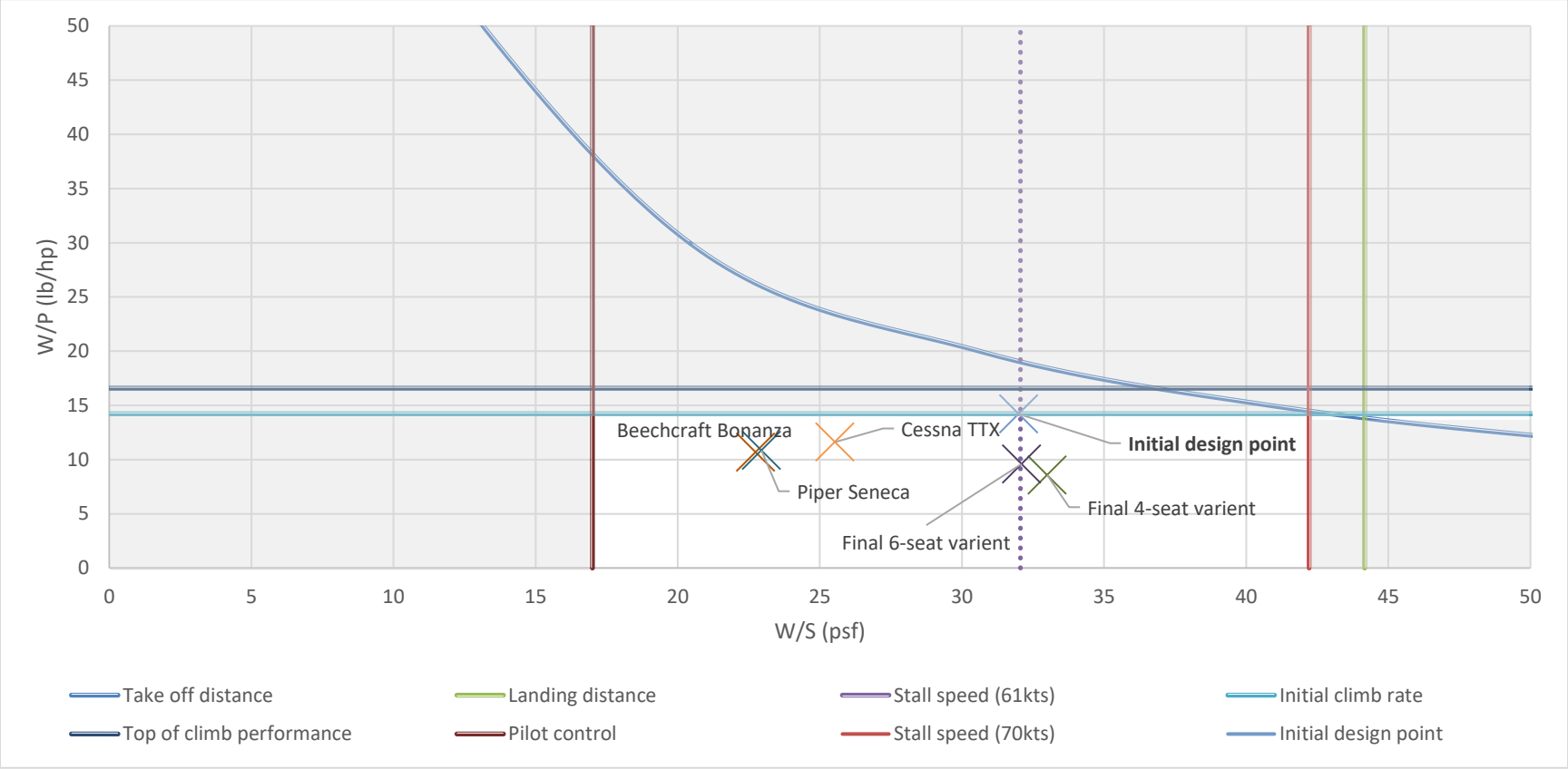

Figure 13 - Constraints diagram with overlaid competitor design point

2. CLASS I DESIGN

The initial design sizing was generated using well established class I type methods, using additional assumptions where appropriate to account for the improvements in technology between the time of writing of the literature and the entry into service of the aircraft. Any assumptions made are discussed where appropriate.

2.1. Powertrain and Energy Storage

2.1.1. Hybrid architecture selection

The first step to specifying the powertrain architecture was to decide which of the three hybrid systems would be deployed on the HEGAAsus. An estimate of the electric and combustion powertrain efficiencies for each hybrid configuration was calculated using component efficiency values from literature [31]–[36]. This is shown by the efficiency breakdown diagrams in Figure 14, *Figure 15* and *Figure 16*. Additionally, a qualitative analysis of the different architectures was undertaken, with the results presented in Table 9.

Figure 14 - Serial hybrid efficiency breakdown

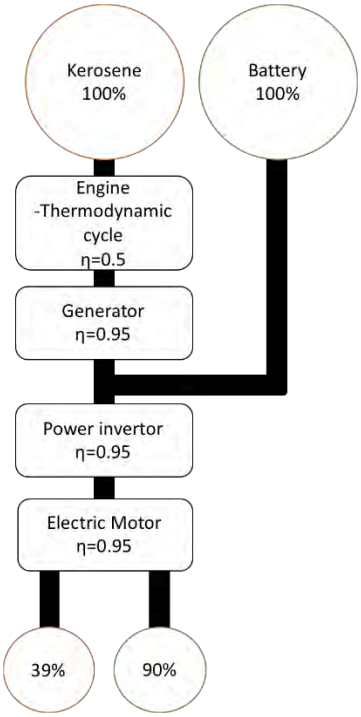

Figure 15 - Connected parallel hybrid efficiency breakdown

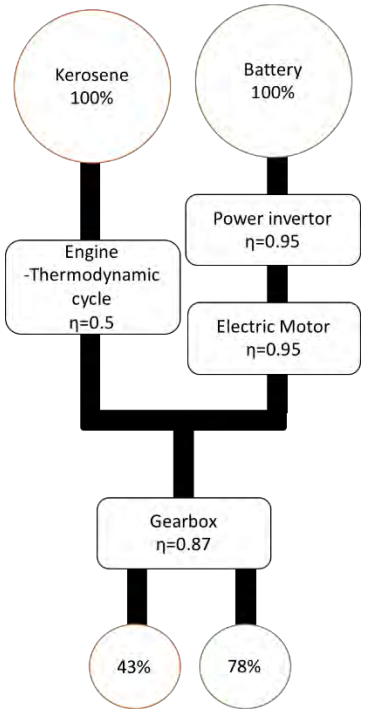

Figure 16 - Separated parallel hybrid efficiency breakdown

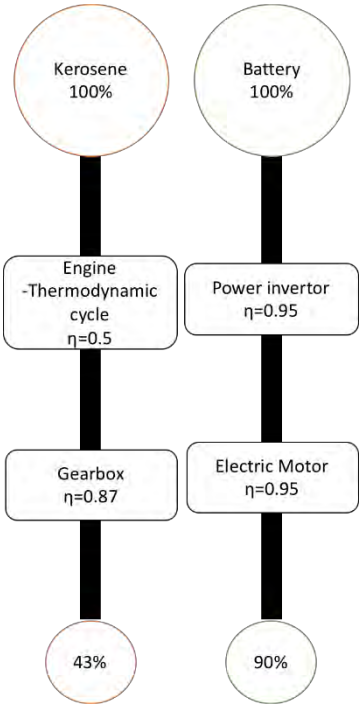

Table 9 - Qualitative analysis of hybrid architectures

	Parallel		Serial
	Collated	**Separate**	
Advantages	• Allows optimization of combustion engine for the cruise condition by augmenting with electric power. • Smaller combustion engine reduces weight and cost	• Allows optimization of combustion engine for the cruise condition by augmenting with electric power. • Smaller combustion engine reduces weight and cost	• In flight battery charging. • Structural location flexibility. • Potential for fully electric powered flight phases (reduced emissions and noise).
Disadvantages	• Complexity in power source control system • Additional weight and inefficiency from coupling gearbox	• Complexity in power source control system • Additional system required for inflight charging.	• Electric motor must be rated for highest power requirement. • Requires more components therefore increased weight • Large accumulation of inefficiency for energy from combustion engine.

The trade study showed that a separated parallel configuration offers the best powertrain efficiency for both the electric and combustion energy sources. Additional benefits were found in the reduced mass of the engine due to the configuration offering higher efficiencies and the removal of the need for a gearbox and clutch, which would add additional weight and mechanical complexity.

2.1.2. Energy storage sizing

With the hybrid architecture determined as separated parallel, a trade study was performed to determine the most efficient way to divide the mission energy requirements between the two systems. Some of the different methods considered were:

- 1. All electric taxi, takeoff, and climb, ICE for cruise
- 2. All electric cruise, ICE supplementation for takeoff and climb
- 3. Fixed percentage motor power through mission duration (10%, 20%, and 30% electric power tested)
- 4. ICE sized for cruise, supplemental power from electric motors for takeoff and climb

The mission energy requirement was calculated using the Cessna 400 as a baseline. Knowing the throttle settings and time in each flight phase from the Cessna 400 pilot's operating handbook [37], the total mechanical energy needed for each phase of the mission was calculated. These values were then scaled by the MTOW so as to adjust for the

difference in weight between the Cessna 400 and the HEGAAsus, to obtain a total mission requirement of 1610 kWh. The required energy was divided according to each hybrid utilization option and the resulting motor and combustion engine (CE) energies were converted into corresponding battery and fuel masses. The presented study was completed for the 6-seat aircraft, as a common propulsion system that had sufficient power and energy for the 6-seat mission would fulfill the requirements for the 4-seat.

Table 10 - Energy utilization trade study for 6-seat variant

Energy usage option	Required power (hp)		Mass (lb)		
	Motor	CE	Battery	Fuel	Total
1	634	335	295	524	819
2	335	634	4510	194	4,704
3	63 / 127 / 189	571 / 508 / 445	700 / 1399 / 2,098	490 / 437 / 382	1190/1836/ 2480
4	317	443	310	473	783

The trade study shows that energy utilization options 2 and 3 result in having to carry significantly more weight, due to the low energy density of batteries relative to fuel. Options 1 and 4 offer similar masse, however, utilizing both propulsion systems during takeoff and climb provides redundancies that increase the safety of the HEGAAsus as well as decreasing the takeoff distance and increasing the climb rate, as seen in section 6. The improved performance and safety was deemed more than sufficient justification for the 36 lb increase in weight.

Consideration was also made for the option for in flight recharging. A qualitative study was undertaken to understand the relationship between charge time and the additional ICE power and required generator capacity. These are summarized in Table 11. [38]–[41]. To charge the batteries in flight during the RFP required mission would require a significant increase to the specified ICE power. Additionally, a weight penalty (~240 lb) would be incurred by the increase in required fuel and recharging generators. For this reason, the base model HEGAAsus does not feature an inflight recharging system. However, it will be offered as an option with the compromise of decreased aircraft performance.

Table 11 - Battery recharge study

Charging condition	Charge time	Generator capacity	Additional power required by ICE
Maximum (581V, 200A)	1.4 hours	123kw	55%
Wall mounted charger (240V, 90A)	7.3 hours	23kw	10%

2.2. Material Selection

To determine the airframe material of choice, a trade study comparing aircraft grade aluminum and carbon fiber based composites was completed. Table 12 summarize properties of the materials considered in the trade study. As shown by Table 12, the benefit of composites is their high strength to weight ratios. This allows for a strong and light airframe, which is an enabler for the implementation of the heavier hybrid powertrain whilst maintaining acceptable aircraft weight. Carbon-epoxy composites are also resistant to corrosion that affects metal based components. Carbon fiber has been proven in service, with manufacturers including Boeing, Airbus, and Diamond delivering aircraft with an increasing percentage of composite forming the airframe [42]. Table 12 shows the material properties for two carbon fibers: HexPly 8552 [43] and Toray-3900 [44] (the composite material used by the Boeing787 [45]). Both materials are high strength and damage resistant, specifically designed for aerospace applications. The material properties were calculated using the rule of mixtures, and assuming the composites to be quasi-isentropic. Based on material properties and with the recommendation of an industrial expert [46] the HexPly 8552 IM7 was selected due to its prevalence and low cost.

Table 12 - Materials trade study properties [45]

	Material type	**Density [lb/in3]**	**0°Tensile Modulus [msi]**	**90°Tensile Modulus [msi]**	**0°Tensile Strength [ksi]**	**90°Tensile Strength [ksi]**
Aluminum 6160	Metallic	0.0975	10	10	40	40
Toray 3900	Composite	0.0446	21.5	12	430	8.75
HexPly 8552 – IM7	Composite	0.0470	23.7	1.5	386	10

2.3. Wing Sizing

The aim of the Class I wing design was to determine the wing loading and initial planform. As seen in the sizing constraints, Figure 13, a low wing loading is desirable for reducing the takeoff and landing distance and stall speed, but a high wing loading is desirable for increasing cruise speed and range. During conversations with general aviation pilots and engineers, a lower limit of 17 psf was suggested to provide the pilot with adequate control in gusty conditions. Figure 17 shows the relationship between wing loading and best-range cruise speed.

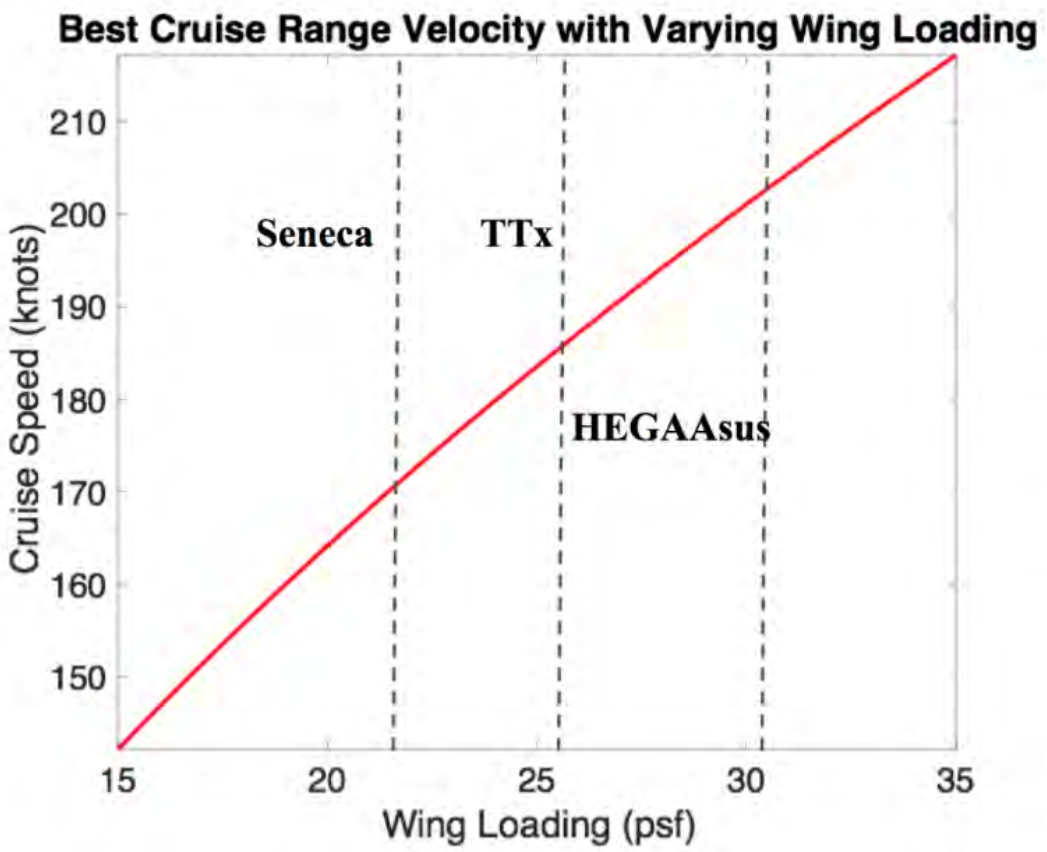

Figure 17- Best cruise range velocity with varying wing loading

Taking this lower limit and Figure 17, which shows the relationship between wing loading and cruise speed, it was clear that a higher wing loading resulted in better cruise performance. However, this has negative impacts on the load carried by wing structures, increases the stall speed, and increases the takeoff and landing distances. As the airframe is manufactured from composite materials, with a high strength to weight ratio, it was deemed that a higher wing loading would be possible without adversely affecting the airframe weight. Additionally, takeoff and landing distance could be improved with the use of high-lift devices. The Cessna TTx [47] and Piper Seneca [48] have wing loadings of 25.5 and 21.1 psf. Seeking the advantages of a higher wing loading, 30 psf was selected for the class I wing loading.

Having estimated the gross takeoff weight of both variants, a wing loading of 30 psf yields a wing planform area of 146 and 220 ft^2 for the four and 6-seat variants. With the aim to design a common wing, an intermediate value of 175ft^2 was chosen. At this stage in the design process a rectangular wing planform was assumed with a 175 ft^2 reference area and 5 ft chord. Consideration was made to the dihedral angle; according to the relationship developed by Scholz, the Oswald efficiency factor increases exponentially with dihedral angle while the lift is virtually unaffected [49].

However, increasing the dihedral angle increases the root bending moment. By balancing considerations from both a performance and structural standpoint, a dihedral angle of 7° was chosen.

2.4. Empennage sizing

Without knowing certain specifics of the aircraft, including CG location and precise wing location, the initial empennage size was determined using comparator aircraft. It is useful to design the tail based on two non-dimensional parameters known as the tail volume ratio, defined in equations (1) and (2), and the aspect ratio, defined in equation (3) where c is a chord length, b is a span, S is an area, and l represents tail moment arms to the center of gravity.

$$V_H = \frac{S_h l_h}{S_{ref} c_{ref}} \tag{1}$$

$$V_V = \frac{S_v l_v}{S_{ref} b_{ref}} \tag{2}$$

$$AR = \frac{b^2}{S} \tag{3}$$

Table 13 shows typical tail volume ratios and aspect ratios for general aviation aircraft from Nicolai [50] and Sadraey. [51]. Typical horizontal aspect ratios range from 3-5 and vertical aspect ratios range from 1-2. Utilizing these two parameters, the basic geometry of the empennage can be defined.

Table 13- Typical volume ratios and aspect ratios from GA aircraft

Aircraft	V_H	V_V	AR_H	AR_V
Comparators	0.6 – 0.9	0.037-0.047	3-5	1-2
HEGAAsus	0.8	0.04	3	1

2.5. Fuselage sizing

With consideration to aerodynamic performance, the main design driver for the fuselage is the fineness ratio (length/max width). According to Scholz, the lowest friction drag on a fuselage occurs at a fineness ratio of 6 [50]. However, a higher fineness ratio increases the moment arm of the tail surfaces, meaning that they can be made smaller and lighter. Based on these considerations and a study of comparator fuselages, it was decided that the fineness ratio should be constrained to between 5 and 7.

In addition to aerodynamic performance considerations, the fuselage must provide sufficient internal volume to accommodate the crew, payload, and subsystems. To meet these requirements, it was decided that the cabin height and width must be greater than 4 ft. The fuselage profile must also provide an appropriate pilot field of view.

The final fuselage design is shown in Figure 18. The fuselage meets the design requirements with a fineness ratio of 5.88, a cabin height of 4.04 ft, a cabin width of 4.13 ft, and a 28 cubic foot cargo hold.

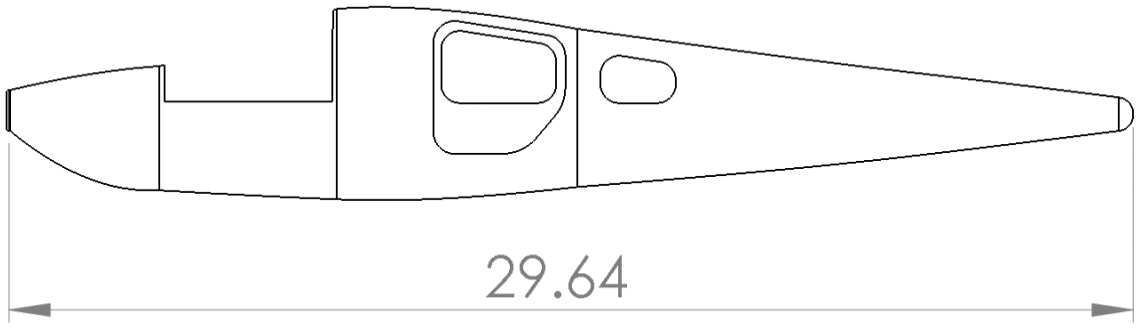

Figure 18 - HEGAAsus fuselage profile

2.6. Class I Weight Estimate

To determine the aircraft's empty weight, the class I method outlined in Roskam's Aircraft Design [52] was used. Component weight fractions of comparator aircraft including the Beechcraft J35, Cessna 210J, Beechcraft G-50TB, Beechcraft Travel Air, and the Cessna 31 were used in the analysis. Class I component weights were estimated from the average of the comparator component weight fractions and the MTOW calculated in section 3.4, 4,400 and 6,600lbs for the 4 and 6-seat aircraft respectively.

A weight reduction factor of 0.6 was applied to all structural components to account for the use of carbon fiber in the HEGAAsus. The reduction factor was calculated by taking the ratio of the tensile modulus and density of Hex Ply 855T and Aluminum 6061 [45]. To account for the hybrid powertrain, weights were estimated for each hybrid component[31]–[36]. The battery and fuel weights calculated in section 4.1 were included as known weights. The complete class I mass breakdown is shown in Table 14.

Table 14 - Class I weight estimate

Component		4-seat (lbf)	6-seat (lbf)
Group 1- Structure Weight	Wing	322.25	322.25
	Empennage	73.60	73.60
	Nacelle	91.14	91.14
	Fuselage	260.05	260.05
	Landing Gear	197.29	197.29
Group 2- Powertrain Weight	Engine	268	268
	Engine Install	5.74	5.74
	Propeller (combined)	203.84	203.84
	Fuel System	96.62	96.62
	Generator/Alternator	110	110
	Controller	55	55
	Inverter	55	55
	Cables	55	55
	Motors	220	220
	Motor Install	4.7	4.7
Group 3- Fixed Equipment Weight	Flight Controls	108.62	108.62
	Hydraulic Systems	99.19	99.19
	Electrical Systems	153.9	153.9
	Electronics	25.66	25.66
	Avionics	57.90	57.90
	Air Systems	52.82	52.82
	Furnishings	198.4	297.84
	Paint	40.85	40.85
	Trapped Fuel & Oil	74.96	74.96
Empty Weight		**2830.53**	**2929.97**
Group 4 – Variable mission weights	Payload	879.64	1320.57
	Fuel	387	473
	Batteries	146	310
Max takeoff weight		**4243.17**	**5033.54**

3. CLASS II DESIGN

This chapter develops the design from a class I level to class II and includes: specification of hybrid powertrain components and subsystem architectures including energy storage and thermal management, development of the wing and empennage design, and specification of key structural architecture.

3.1. Powertrain

3.1.1. Drivetrain component specification

The combustion engine power requirements were set by a refined iteration of the analysis conducted in section 4.1 following improved estimates for aircraft performance during the initial design phase. The required combustion engine power is 288hp and total motor power is 314hp.

Combustion engine

Specification of the combustion engine required two engine types to be considered: internal combustion engine (ICE) and turboprop (TBP). A qualitative analysis is shown in Table 15.

Table 15 - Combustion engine down selection

Engine Type	Advantage	Disadvantage
ICE	• Cheaper • Compatible with more fuel types • Easier to maintain • Small area footprint	• Lower power to weight ratio • Limited choice in power requirement
TBP	• Higher power to weight ratio • More efficient at higher speeds/altitudes	• Expensive • Large area footprint • Increased maintenance

The ICE is the preferred option due to the increased fuel compatibility and ease of maintenance. This consideration will make the aircraft more suitable for sale in emerging markets such as India, where GA maintenance bases are less readily available [53]. The final ICE specification was made using an engine trade study, the results of which are shown in Table 16. This study focused on comparing competitor aircraft engines to identify the optimal compromise between engine physical size (a project design driver) and running cost (a customer requirement), whilst meeting the minimum required 288hp.

Table 16 - Internal combustion engine selection

Engine Name [31], [34], [54]–[63]	**Centurion 3.0**	**Continental IO 360**	**Continental TSIO**	**Continental IO-550-C**	**EPS**	**RED A05**	**Higgs Diesel E330**
Engine Type	Diesel	Avgas	Avgas	Av gas	Diesel	Diesel	Diesel
Turbo	Twin	~	~	Twin	~	~	~
Power (hp)	271	164	308	430	350	300	470
Cost $	89,000	-	72,400	-	94,120	170,000	-
Aircraft	Cessna 182	Seneca	Cessna TTX	Beech Baron G58	Cirrus SR22	-	-
Aircraft Cost (M$)	-	-	0.81	1.40	0.54	-	-
Weight (lbs)	583	343	633	495	624	578	305
Volume (ft^3)	17.6	20.0	31.9	15.5	-	16.2	-
Power/Weight (hp/lb)	0.46	0.64	0.49	0.87	0.56	0.52	1.56
Specific fuel cost ($/hr)	80	-	175	160	65	78	70
Specific fuel consumption (lb/hp hr)	0.388	0.523	0.664	0.671	0.315	0.362	0.398

The preferred ICE was the Higgs Diesel E330 due its low power to weight ratio and specific fuel cost. This engine is new to the market, with certification starting in 2016, but is low risk to 2028 EIS. The power output exceeds what is required by the HEGAAsus, so a single de-rated engine to be mounted in the aircraft nose was specified. The Higgs engine also offers several advantages over conventional engines due to its step piston design, including:

- High durability with low exhaust emissions
- Compact low mass design
- Extended oil change periods (oil does not degrade)
- Extended maintenance intervals (less parts to maintain)

Motors

Initially three principal categories of electric motors, including: brush DC, brushless DC and AC induction motors were considered. A trade study analysis the benefits of relative performance, cost, and maintenance of each in terms of market averages, shown in Table 17 [64]–[66].

Table 17 - DC vs AC motor trade study

Property	Brush DC	Brushless DC	AC Induction
Efficiency	Motor: 80% Controller: 95% **Net: 75%**	Motor: 93% Controller: 97% **Net: 90%**	Motor: 91% Controller: 97% **Net: 88%**
Wear/Service	Brushes; Bearings	Bearings	Bearings
Specific Cost ($ per kW)	**Low** – inexpensive components	**High**- permanent magnets cost > $50/kg	**Medium** – cheap motor, expensive inverter
Thermal Management	**High** – windings on rotor and commutator	**Medium** – Windings on stator, low magnet heating	**Medium** – Windings on stator, current in rotor needs cooling
Lifespan	**Short** – brush wear, potential for overdrive	**Medium** – potential for overdrive	**Long** – rugged and frequency controls (not current controls)

DC brushless motors and AC induction motors out-perform a brush DC design. An AC induction motors can offer additional benefits can make it better suited for aviation applications, including lower specific energy cost and a longer and more robust lifespan. With hybrid electric aviation being an emerging industry, there is limited choice of FAA certified electric motors available. Table 18 shows the two electric motors considered for the HEGAAsus design [32][67].

Table 18 - Technical AC induction motor details

Property	DA36 E-Star Motor	Siemens SP260D
Current	AC	AC
Permanent electrical power	95 hp	350 hp
Maximum continuous speed	2,500 rpms	2,500 rpms
Continuous torque	70	1,000 Nm
Total weight including airscrew bearings	30 lbs	110 lbs
Motor efficiency	90 %	95 %

There was only one motor that met the power requirement - the Siemens SP260D. With the ICE mounted in the nose of the aircraft, two wing-mounted SP260D motors was the most appropriate design to maintain propulsion symmetry. Although this far exceeds the required power, it was deemed possible due to the light weight design of the SP260D. Furthermore, the motor configuration yields additional benefits. The configuration provides propulsion redundancy in the case of an internal combustion engine or motor failure during operation, with the capability of continued flight on either system alone. Furthermore, as sufficiently high energy density batteries become available, an all-electric variant of the aircraft will be possible with no change to the electric motors.

3.1.2. Propeller design

Utilizing the design ethos of a main nose-mounted propeller augmented with two wing-mounted propellers for take-off and climb, allows the propellers to be designed to achieve maximum efficiency at their intended operational power. Additionally, it is necessary to specify a folding mechanism for the wing propellers to reduce drag during cruise when the augmented power is not required.

The wing propellers are each required to deliver a propulsive power of 157hp, for both variants. At this power, fixed pitch, variable speed models offer a lighter-weight system than variable pitch models [36]. To simplify the use of a folding system, a two-blade design has been chosen as this allows a symmetrical retraction. The design point of 157hp was chosen to match the maximum efficiency speed of the electric motors of 2300rpm. The propellers were then sized using an initial sizing algorithm presented in [68], as equation (4) below, which yields a propeller diameter of 1.7m, with a 90'' pitch.

$$D = 0.4591\sqrt[4]{P} \tag{4}$$

The main nose propeller is required to provide a propulsive power of 288hp. Above 200hp fixed speed, variable pitch propellers offer a greater efficiency and lower overall system weight than fixed pitch variants [68]. The use of an electrically actuated variable pitch mechanism offers the opportunity for greater and easier integration to the FADEC system and greater integration to future autonomy modules, as well as a lighter weight solution than traditional hydraulic controls [36]. Sizing the nose propeller required the consideration of ground clearance, landing gear length and propeller tip speed. To meet these constraints, it was necessary to utilize a four-blade design. Using actuator disk theory [68] a propeller diameter of 1.93m was calculated, this propeller design gave a predicted cruise propulsive efficiency of η=0.82.

3.1.3. FADEC control

The propulsion system is controlled by a full authority digital engine controller (FADEC). This system automatically controls the engine and motor power output, propeller pitch and propeller deployment depending on the selected flight phase and requested thrust setting. The advantages of using FADEC include: increased fuel efficiency, simpler controls (replacing mixture, power and throttle controls with a single throttle lever) and automatic workarounds in emergency situations. For example, in the event of ICE failure during cruise, it would automatically deploy the wing motors, reducing the pilot workload in critical scenarios.

3.1.4. Powertrain system layout

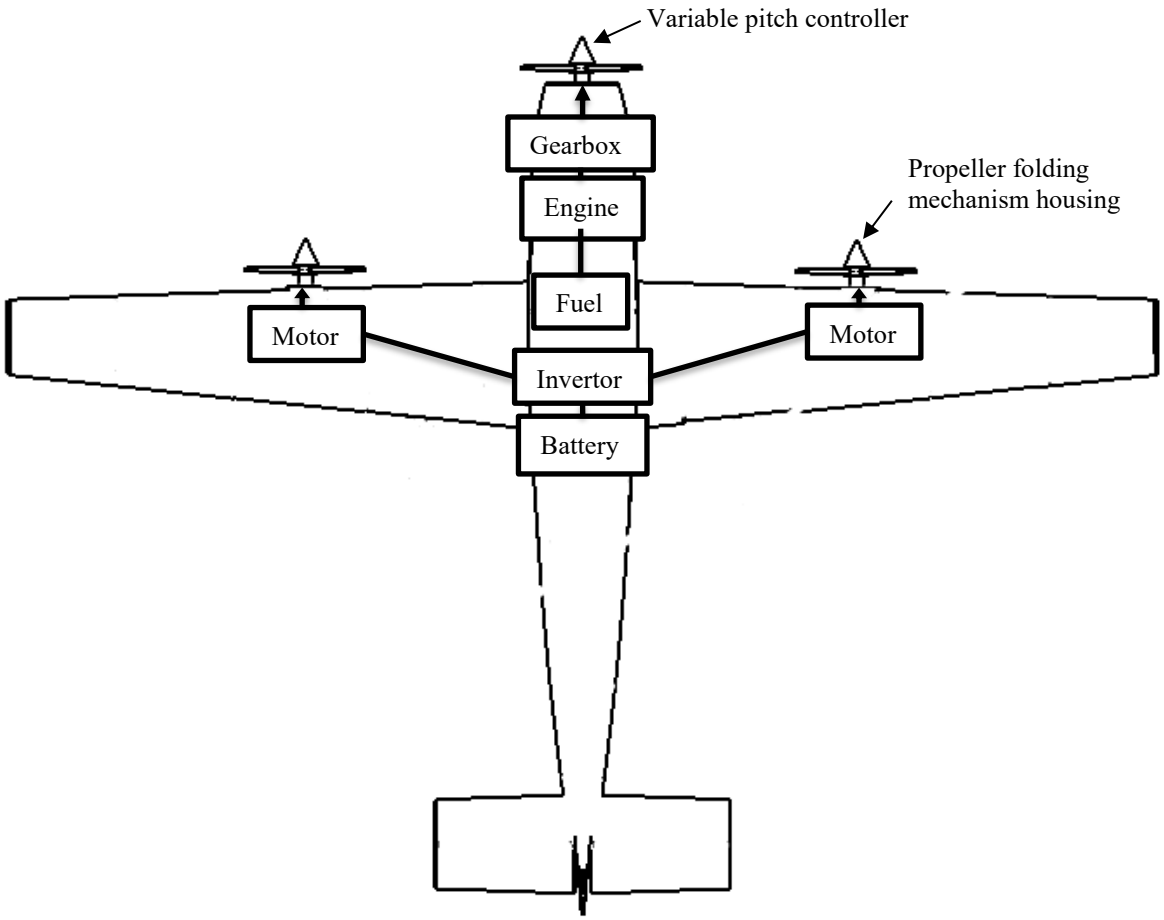

3.2. Aerodynamics

3.2.1. Wing Planform

Class II aerodynamic design began with a refinement of the wing planform. Analysis showed that a family common wing planform was suboptimal for both variants. The 4-seat variant cruise performance benefits from a smaller wing area. However, this would result in an unacceptably high 6-seat wing loading at MTOW. Therefore, it was necessary to design optimized wing planforms for both missions. The class II 4 and 6-seat planforms have areas of 155 ft^2 and 180 ft^2 respectively.

Rectangular planforms were specified for simplicity in the class I design process. However, a tapered wing has a more efficient lift distribution that results in lower induced drag. Furthermore, a tapered composite wing does not suffer the same manufacturing complexity as a tapered aluminum wing. Therefore, the wing was specified with a taper of 0.5

While having two planform areas was optimal for cruise performance, it was desirable to maintain as much commonality between the wings as possible. Therefore, the HEGAAsus family share a common inboard wing section, with the 6-seat variant receiving a wingtip extension. Figure 19 shows the wing planform in the 4-seat configuration. Figure 20 shows the wing planform in the 6-seat configuration, including the additional wing tip extension. This design approach allows the HEGAAsus family wing to remain as common as possible, whilst being optimized for both cruise missions.

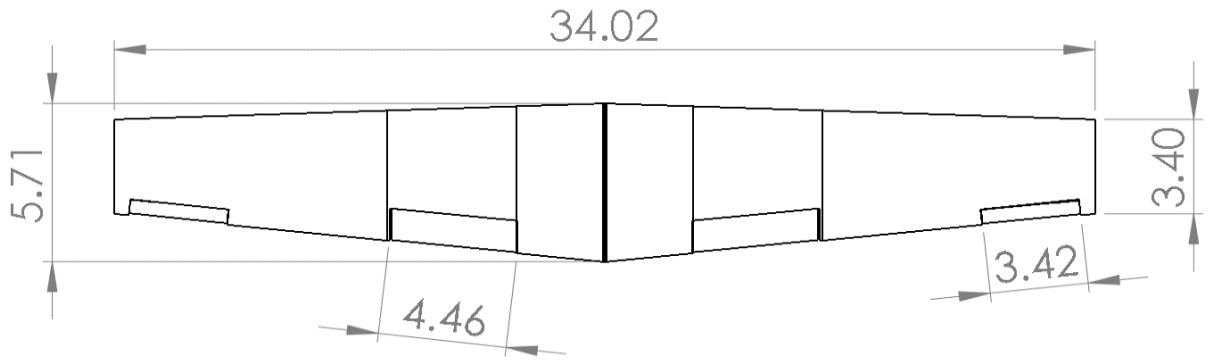

Figure 19 - HEGAAsus 4-seat wing planform dimensions

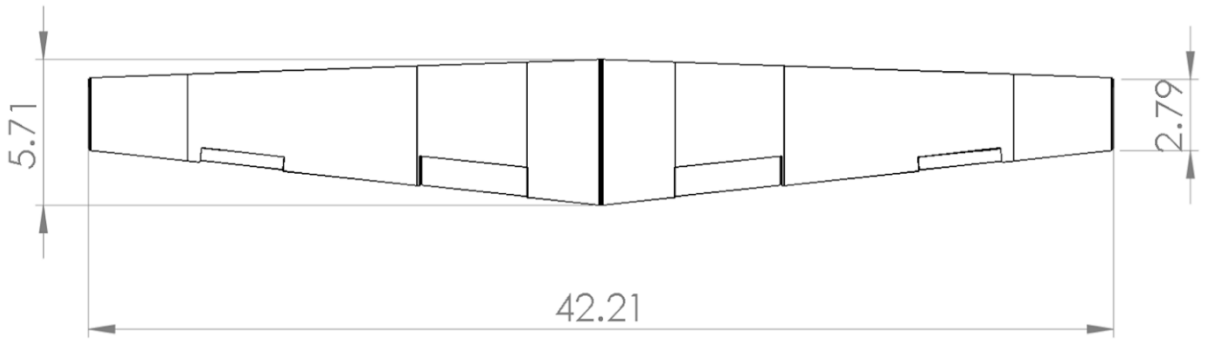

Figure 20 - HEGAAsus 6-seat wing planform dimensions

3.2.2. Airfoil Selection

The class II wing design continued with the selection of an airfoil. The airfoil design was constrained by several factors identified in preliminary analysis including:

- The optimum 2D design lift coefficient in cruise was identified to be 0.33.
- To minimize the wing drag profile in cruise, the chosen airfoil had to achieve the cruise lift coefficient at a low positive angle of attack.
- A 2D maximum lift coefficient greater than 1.7 was needed to reach the required takeoff/landing distances.
- As elevator trim is required to balance the aerodynamic moment induced by the zero angle of attack lift, the chosen airfoil should have a zero angle of attack lift coefficient no greater than 0.3 to ensure excessive elevator trim drag is avoided.
- The airfoil requires sufficient internal volume to accommodate fuel and other subsystems.

Table 19 shows the range of airfoils that were analyzed and considered. Each airfoil is designed for use in incompressible flight and has a documented history of use in general aviation or experimental aircraft. These preliminary numbers were computed using the open-source program Xfoil.

Table 19 - Airfoil analysis data

	NACA 23015	NACA 4415	NASA GA(W)-1	NLF 416
Cl_0	0.13	0.40	0.51	0.48
Cl_{max}	1.80	1.83	2.03	1.80
Cd_0	0.0058	0.0059	0.0044	0.0047

Based on the design constraints, the NACA 23015 airfoil was selected for the HEGAAsus wing, the profile of which is shown Figure 21.

Figure 21 - HEGAAsus airfoil profile: NACA 23015

3.2.3. High Lift Devices

The class II aerodynamic wing design concluded with the specification of high-lift devices. The HEGAAsus family exceeds its takeoff requirements without the need for high-lift devices. However, the emphasis on high wing loading for optimal cruise performance resulted in a large ground distance covered between a 50-foot obstacle and touchdown. Therefore, a simple hinged flap system is specified for the HEGAAsus family. The use of a flap system gives the HEGAAsus a slower approach speed, reducing the ground distance covered between a 50-foot obstacle and touchdown. The flap system was designed to achieve a 1,500 ft landing distance at MTOW for the 4-seat variant. The flap system was designed using the method outlined by Gudmundsson [69] and is summarized in Table 20.

Table 20 - HEGAAsus flap design parameters

Flap design parameter	Value
Span wise Length	4.5 ft
Chordwise Depth	1.63 ft
TO Deflection	15°
Landing Deflection	60°

3.3. Structures

Extensive use of carbon fiber composites throughout the design allow for a novel approach to manufacturing structural components. Where traditionally frames, ribs, spars, and longerons would be forged separately and riveted to the skin of the aircraft, the main structural components (wing box, fuselage plugs, and empennage sections) of the HEGAAsus are manufactured as one piece. This approach yields benefits such as reduced part count, reduced component molds, increased reliability and increased strength. Although the main structural components are molded as one piece, the different regions of the structure are considered to carry the loads in a traditional sense. Therefore, throughout this section the different regions of the structure will be treated as their traditional counterparts when referring to structural design textbooks and methods.

It should be noted that if the aircraft were to go into service this would not be the final structural design and several more iterations would occur enabling further weight saving opportunities and detailed design of the carbon fiber layup to optimize the structural properties

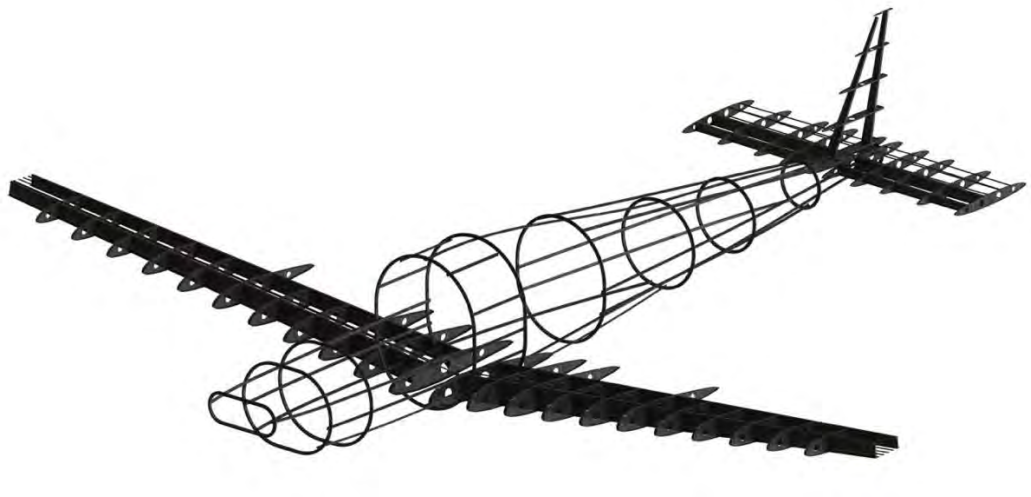

Figure 22 - Structural lay up (skin is hidden to show additional detail)

3.3.1. Wing

The wing's internal structures were designed using recommendations by Roskam [70]. The wing box design was chosen that comprised of two spars located at 25 percent and 60 percent chord and eight stringers, as shown in Figure 23. The wing skin was chosen to be 0.1 inches to provide it with damage tolerance and is supported by a T stringer with a width of 0.1inches and height of 0.2 inches.

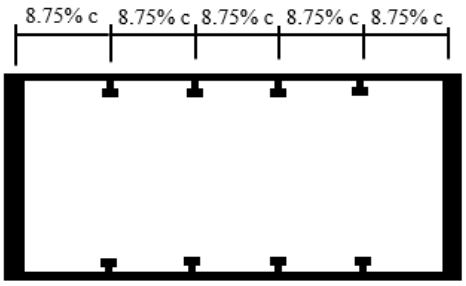

Figure 23 - Wing box structure

This box beam was tested using Euler-Bernoulli beam bending theory and the application of two distributed forces to simulate a 3.8 g flight case and 1g ground case. For the 3.8 g flight case, 10% of the fuel was assumed to be present in the wing in order to simulate minimal relief from fuel, while the 1 g ground case was for a fully loaded 6-seat variant. After each test an iteration to the spar thickness and span wise position of the engine was made until an optimum design was reached. This was determined to be when the spar thickness is 0.58 inches and the wing motor position 10 feet and 4.1 inches from the center line.

Ribs were positioned to prevent buckling of the skin, it was determined that the buckling would first occur at the root of the wing near the fuselage. Ribs spaced 20 inches apart are required to support the skin. Therefore, to allow for a margin of safety and in alignment with Roskam, a rib spacing of 18 inches was chosen. The full structural design of the wing and a cross section of the spar can be seen in Figure 24.

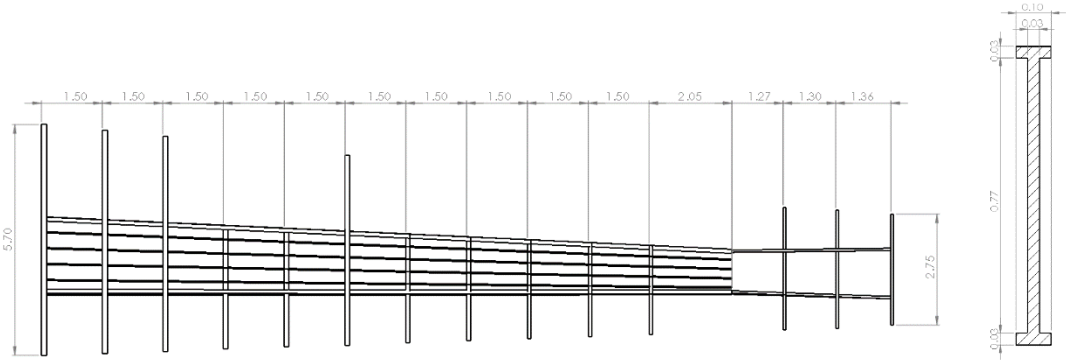

Figure 24 - Wing internal structure

3.3.2. Fuselage

The fuselage internal structures were designed using recommendations by Roskam [70]. A recommended frame pitch of 24” and longeron pitch of 15” was aimed for, with some margin allowed to accommodate cut outs for doors and

windows. Because of the partial pressurization of the cabin, a rounded rectangle design of frame was opted for to reduce the hoop stress while maintaining a large cabin volume, this frame design and the fuselage structure can be seen in Figure 25, all dimensions are in feet.

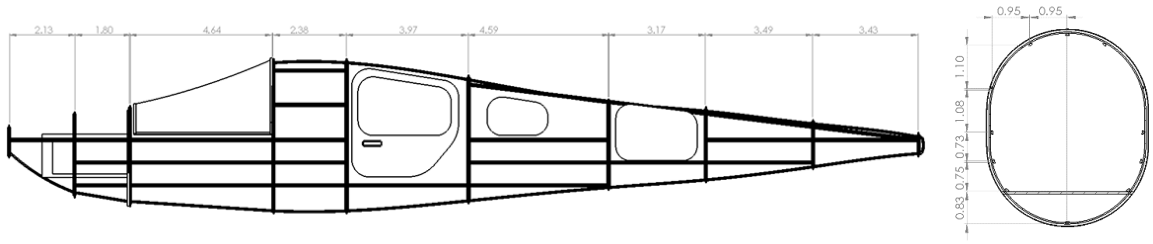

Figure 25 - Frame and longeron design

3.3.3. Empennage

The empennage internal structure was sized using the same method as the main wing. Using the same initial starting design for the wing box, shown in Figure 23, an iterative process was used to optimize the spar thickness. As there was no change to skin thickness, the rib separation remained at 18 inches. The internal structure for the empennage can be seen in Figure 26. All dimensions are in feet and the leading edge is to the left.

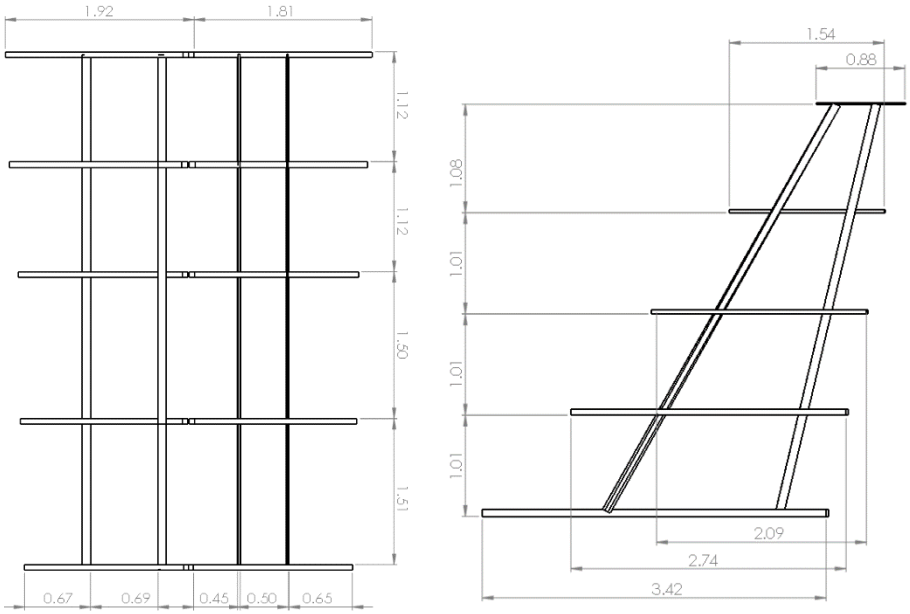

Figure 26 - Empennage structure

3.3.4. Landing gear

The HEGAAsus family employs a fixed tricycle landing gear configuration that is common for both aircraft variants. Fixed gear was selected because it was found that on average, they cost 50 percent less to insure, and 20 percent less maintain than their retractable counterparts [71]. In addition, fixed gear are traditionally lighter and more affordable than retractable gear. This coupled with the use of wheel fairings to reduce the drag of the main gear by up to 50 percent, and the possible weight and production costs, lead to the selection of fixed gear [71]. Lastly, to reduce the risk of loss of directional control a tricycle layout was selected.

The landing gear was sized using the design constraints outlined by Roskam [72], the design constraints are shown below. Figure 27 shows the landing gear configuration with key parameters shown in Table 21.

- Maintain 7 inches of propeller ground clearance whilst undergoing 1.6' oleo strut displacement (FAR 23.925)
- Nose gear to support 8%-15% of aircraft weight (For maneuverability on ground)
- Main gear to CG angle 10°-25° [73]
- Turnover angle greater than 45°
- Tip back angle greater than 16°

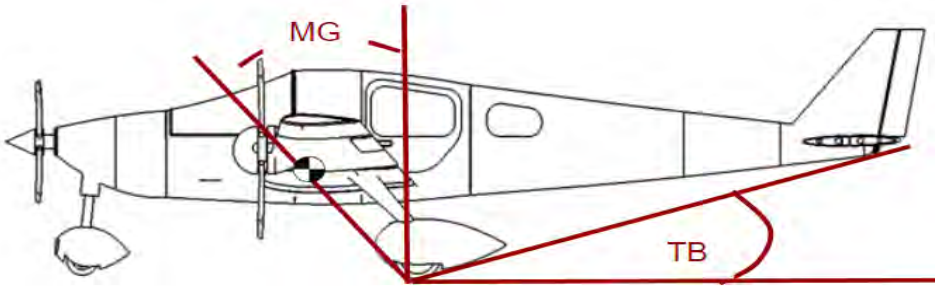

Figure 27 - Landing gear configuration

Table 21 - Landing gear parameters

Parameter	Value
Tip back angle (TB)	16.7°
Angle from center of gravity to vertical of main gear (MG)	12.0° - 23.5°
Nose Gear Location	2.7' aft of nose
Main Gear Location	13.0' aft of nose
Nose Gear Tire Diameter	19.5"
Nose Gear Tire Width	6.7"
Main Gear Tire Diameter	13.0"
Main Gear Tire Width	4.9"
Distance from main gear to centerline	6.2'
Turnover angle	45.0°

3.4. Control and Stability

3.4.1. Horizontal stabilizer

There were four primary design drivers for the horizontal stabilizer class II design: static stability, trim characteristics, stall characteristics, and an acceptable center of gravity (CG) envelope. Aircraft stability derivatives were determined iteratively using in-house code, with initial volumes from Class I estimates. The horizontal stabilizer was optimized by varying its design parameters until the desirable performance was achieved.

An aircraft is statically stable when the zero-lift moment is positive and the moment decreases with increasing angle of attack, providing a point where the moment becomes zero and the lift equals the weight to trim the aircraft. The moment slope is negative when the center of gravity is forward of the neutral point. Therefore, it was necessary to calculate the position of the neutral point to constrain the CG travel in the design process. Due to their similarity, the neutral point was estimated as 49% of the mean aerodynamic chord (MAC) for both HEGAAsus variants.

Roskam [72] suggests a minimum static margin of 10 percent, which constrains the aft limit of the CG location. The forward limit of the CG location was constrained by the aircraft trim capability at its stall angle of attack. This is

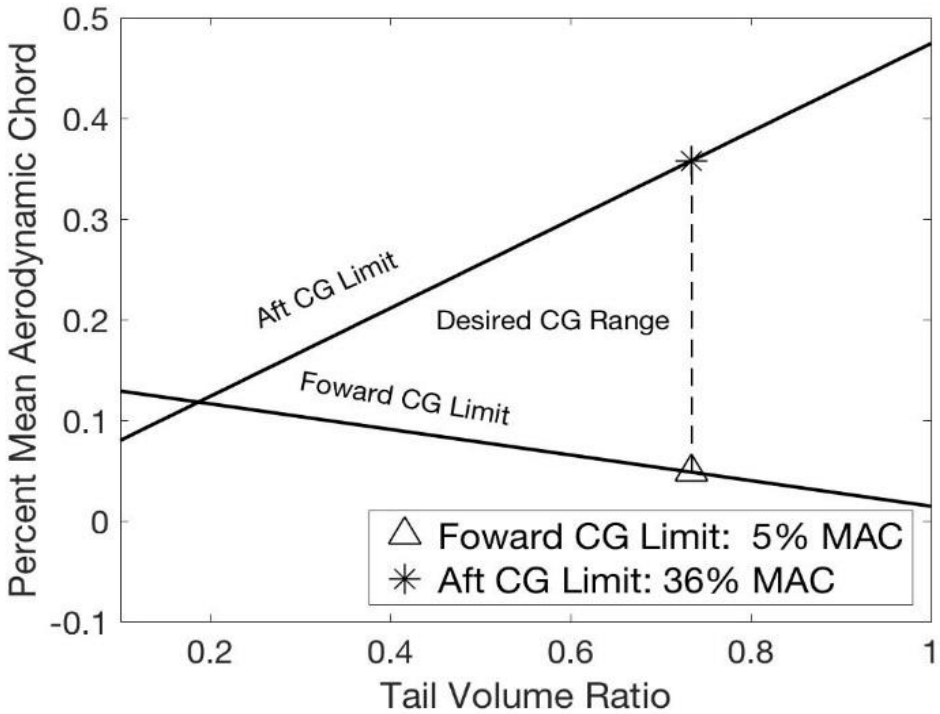

Figure 28 - Tail volume constraints diagram

necessary for take-off and landing maneuvers. By analysis of comparator aircraft CG envelopes, a CG range of 1.2 ft. was selected. A constraints diagram was constructed to determine the tail volume ratio to achieve the desired range, represented in percent mean aerodynamic chord in Figure 28. A tail volume ratio of 0.8 was chosen to provide a factor of safety.

A horizontal stabilizer incidence angle of 2° was chosen to minimize the trim elevator deflection during cruise. A horizontal stabilizer airfoil was chosen with the constraint that it would stall after the main wing. The angle of attack (AOA) of the horizontal stabilizer was calculated at the point when the main wing stalls using equation (5).

$$\alpha_{ht} = \left(1 - \frac{\partial e}{\partial \alpha}\right)\alpha - e_o - i_t \quad (5)$$

Where $\frac{\partial e}{\partial \alpha}$ is the change in downwash with respect to angle of attack, e_o is the downwash from the wing at zero angle of attack, α is the angle of attack of the aircraft, and i_t is the incidence angle of the tail which is positive when deflected downward. A NACA 0012 airfoil was chosen for the horizontal stabilizer to ensure this angle was below the stall angle of the airfoil, the study is summarized in Table 22.

Table 22 - Horizontal stabilizer airfoil selection study

Aircraft Stall AOA	Corresponding Horizontal Stabilizer AOA	NACA 0012 Stall AOA
18°	7.8°	18°

3.4.2. Vertical stabilizer

The two primary design drivers for the vertical stabilizer were the capability to takeoff and land in cross winds and airfoil selection to prevent stall of the vertical stabilizer when flying in cross winds. FAR part 23.233 [74] requires the aircraft to be capable of takeoff and landing in 90° cross wind speeds of at least $0.2V_{stall}$. This capability is determined by rudder size. Therefore, it was necessary to specify a vertical stabilizer capable of housing the necessary sized rudder.

The taper ratio of the vertical stabilizer was chosen to ensure there was enough room for the rudder whilst also decreasing the aerodynamic and structural loads at the tip. From observing comparator aircraft, it was determined that a rudder that encompasses 50% of the tip chord allows enough room for actuators and structures. The final selected taper ratio is shown in Table 24.

An airfoil was selected to ensure the vertical stabilizer does not stall whilst flying in a cross wind, the relative angle of attack of the vertical tail was computed using equation (6). Where $\frac{\partial\sigma}{\partial\beta}$ is the change in sidewash with respect to sideslip and β is the sideslip angle of the aircraft. A NACA 0009 was chosen to keep the vertical tail thin and reduce weight while ensuring it does not stall whilst enduring the design cross wind. The analysis is summarized in Table 23.

$$\alpha_{vt} = \left(1 - \frac{\partial\sigma}{\partial\alpha}\right)\beta \tag{6}$$

Table 23 - Vertical stabilizer airfoil selection study

Take-off Side Slip Angle	Relative Vertical Stabilizer AOA	NACA 0009 Stall AOA
9.46°	9.45°	11.5°

Table 24 - Empennage class II geometric parameters

	Horizontal Stabilizer	Vertical Stabilizer
Tail Volume Coefficient	0.8	0.04
Aspect Ratio	3	1.3
Taper Ratio	0.9	0.4
Span	10.5 ft	3.9 ft
Area	35.8 ft^2	20 ft^2
Incidence	1°	-
Trailing Edge Sweep	-	10°
Moment Arm	14.8 ft	14.2 ft
Airfoil	NACA 0012	NACA 0009

3.4.3. Control surface sizing

The horizontal tail effectiveness parameter was determined to increase the forward limit of the center of gravity location and take precautions to ensure take-off rotation. Figure 29 was taken from Aircraft Design: A Systems Engineering Approach [51], was used to translate the horizontal and vertical effectiveness parameters into control surface sizes.

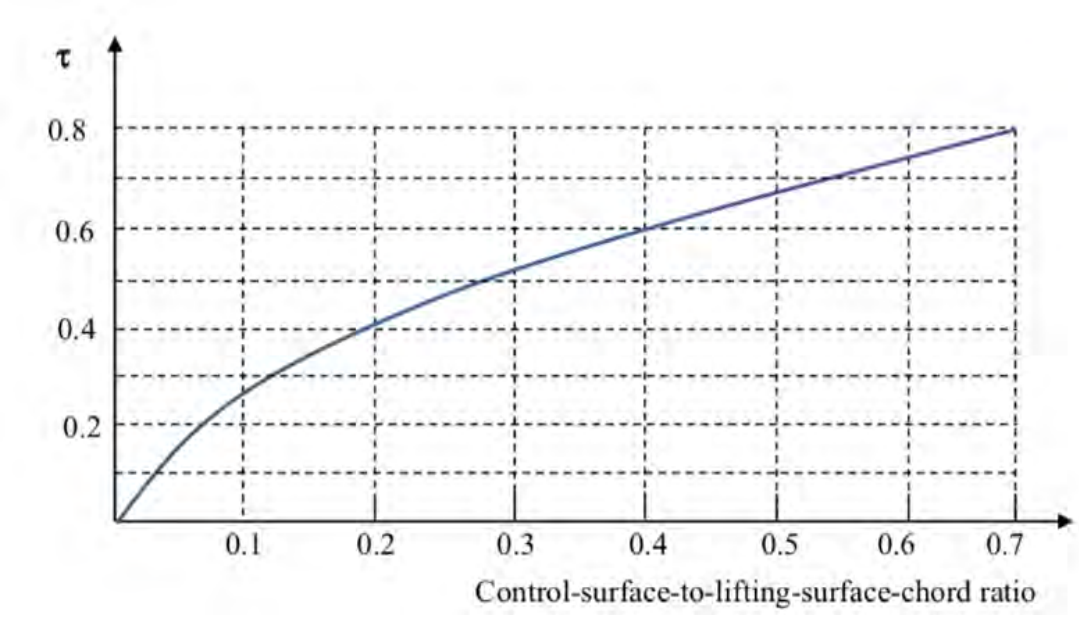

Figure 29-Control Surface to Lifting Surface Chord Ratio

Aileron sizing was an iterative process. According to Roskam [75], the ailerons are generally 20% of the wingspan and 15% of the wing chord. These values were used as the initial design. Gudmundsoon [69], suggests that proper control surface sizing enables the aircraft to take-off in crosswinds without extreme control surface deflections. This allows the pilot to respond to gusts. For satisfactory performance, the aileron chord length was increased to 25 percent of the wing chord. The control surface deflections for the 6-seat variant subjected to crosswinds during take-off are summarized in Table 25. The control surface sizes for the 4 and 6-seat variants are shown in Table 26. For reference, the aileron span is length of the aileron on one wing.

Table 25- Control surface deflection when the aircraft is subject to 15 knot crosswinds during take-off.

Coefficient term	Requirement	HEGAAsus
δa	$\leq 0.25\ \delta a_{max}$	$0.27\ \delta a_{max}$
δr	$\leq 0.75\ \delta r_{max}$	$0.05\ \delta r_{max}$
δe	$\leq 0.50\ \delta e_{max}$	$0.03\ \delta e_{max}$

Table 26- HEGAAsus Control surface sizes

Parameter	Elevator	Rudder	Aileron
Chord	1.5 ft	0.94 ft	0.84 ft
Span	10.5 ft	4 ft	4.1 ft

To mitigate the risk of flutter instabilities, the hinge locations for all control surfaces were placed at the center of gravity of the control surface [103]. If imbalances are found on a control surface after the final parts are manufactured, a control horn can be placed on the surface to move the CG forward and dampen out these effects.

3.5. Subsystems

This section of the report describes the subsystem architectures specified for the HEGAAsus family, each subsystem is common to both the 4 and 6-seat variants unless specified.

3.5.1. Flight control architecture

Mechanical linkages, fly-by-wire, and fly-by-light (fiber optic system) were all considered as potential flight control architectures [51]. First mechanical and electronic systems were compared. The advantages of electronic systems were found to outweigh the cost and increased control feedback of a mechanical system, some of these advantages are:

- Reduction in weight
- Increased redundancy
- Ease of integration with future technologies, such as autonomy
- Pilot workload reduction
- Increased potential for automated safety features

At present there are two electronic flight control architectures. Research showed that Fly-by-light offers several advantages over fly-by-wire, including:

- Increased redundancy due to the number of fibers per bundle
- Increase in transmission speeds
- Ease of incorporation with future systems due to a larger bandwidth
- Increased reliability due to its immunity to electro-magnetic interference

The downside to fly-by-light is the increased cost over fly-by-wire. However, data shows that this cost should decrease significantly in the next ten years [57]. For these reasons, supported by fly-by-light of TRL 8 (low risk to the 2028 EIS), it was decided that fly-by-light would be the flight control architecture implemented on the HEGAAsus [57].

3.5.2. Avionics

The avionics suite of the HEGAAsus is centered around the Garmin G1000 flight deck, including a Garmin GFC 700 autopilot [76]. This system meets the current requirements for VFR and IFR flight in all classes of airspace and is Automatic dependent surveillance-broadcast (ADS-B) compliant, which will become mandatory in 2020 and allows for flight in both controlled and uncontrolled airspace. In addition, to meet FAR part 91.205 requirement, a Standby Attitude Module is installed on the aircraft. This system includes all primary flight instruments and includes an independent, self-contained power supply. The all glass cockpit displays, and backup flight displays can be seen in Figure 30. Table 27 lists all the standard avionic equipment included on the aircraft to allow VFR and IFR flight.

Figure 30 - Cockpit avionics layout

Table 27 - VFR/IFR avionic equipment

Required Instruments	Provided Instruments
VFR (Day)	
Airspeed indicator	GDC air data computer and GDU display
Altimeter	Garmin G1000 (GDC air data computer and GDU display)
Magnetic direction indicator	Garmin G1000 (Horizontal Situation Indicator and GDU display)
Tachometer for each engine	Garmin G1000 (Engine Display)
Oil pressure gauge for each engine using pressure system	Garmin G1000 (Engine Display)
Temperature gauge for each liquid cooled engine	N/A
Oil temperature gauge for each air cooled engine	Garmin G1000 (Engine Display)
Manifold pressure gauge for each altitude engine	Garmin G1000 (Engine Display)
Fuel gauge indicating the quantity of fuel in each tank	Garmin G1000 (Engine Display)
Landing gear position indicator (if retractable)	N/A
Approved aviation red or white aviation anti-collision light system	To be specified in the detailed design phase
Emergency locator transmitter (if operated for hire)	ARTEX's ELT 345
VFR (night)	
Approved position lights	To be specified in the detailed design phase
Landing Light	To be specified in the detailed design phase
All instruments required for VFR (day)	Garmin G1000
IFR	
All instruments required for VFR (night)	Garmin G1000
Two-way radio and navigation equipment	Garmin G1000 (GIA integrated avionics unit)
Gyroscopic rate of turn indicator	Garmin G1000 (Turn rate indicator)
Slip-skid indicator	Garmin G1000 (Attitude Indicator)
Sensitive altimeter adjustable for barometric pressure	Garmin G1000 (Altimeter)
Clock	Garmin G1000 (Mission Timmer)
Gyroscopic pitch and bank indicator	Garmin G1000 (Attitude Indicator)
Gyroscopic direction indicator	Garmin G1000 (Attitude Indicator)
General	
Back up Primary Instruments	Standby Attitude Module from MidContinent

3.5.3. Ice protection

The HEGAAsus ice protection system is specified to prevent ice formations on the leading edge of the wing, empennage, propeller blades and cockpit windows. An Electro-Mechanical Expulsion Deicing System (EMEDS) is used on the leading edge of the wing and empennage. This system is certified by the FAA for flight into known icing conditions and offers several advantages over competitor systems including [77]:

- Reduced mass and maintenance burden when compared to weeping wing systems
- Reduced electrical energy requirement compared to electric thermal mat solutions
- Improved robustness when compared to pneumatic deicing systems
- Better deice performance than all alternative systems (minimum thickness 0.05 inches, no upper limit)

EMEDS is an automatic system that is triggered when ice is detected on the wing, reducing the workload on the pilot. The system utilizes an electro-thermal strip to heat the leading edge of the wing, which ensures the liquid freezes at a point on the airfoil that is less sensitive to ice formation. The EMEDS actuators then deflect the airfoil skin to break and remove the ice. The system schematic is shown Figure 31.

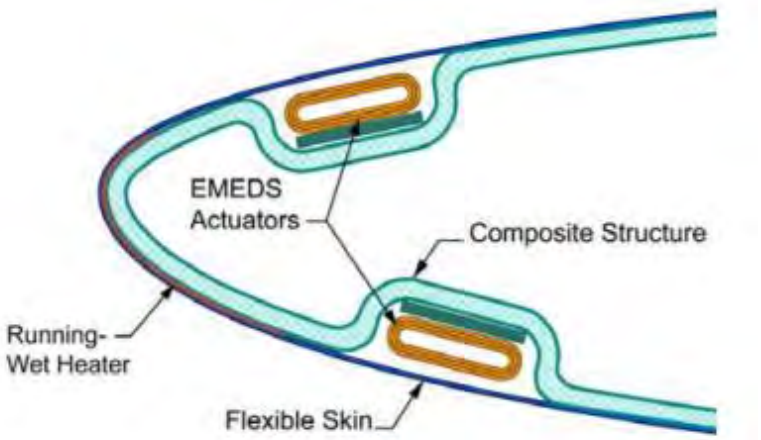

Figure 31 – Electro-mechanical expulsion deicing system

The HEGAAsus ice protection system is specified with several other components to enable flight into known icing conditions. These systems include an annunciator light to inform the pilot of ice formation, an ice detector light to allow the pilot to illuminate the leading edge of the wing, an electrically heated cockpit window, propeller blades, propeller spinner, engine intakes, and air data sensors. The ice protection system allows the aircraft to fly into known icing conditions as defined by FAA 14 CFR Part 23.

3.5.4. Cabin conditioning

To enable the aircraft to cruise at altitudes up to 23,500 ft, a partial pressurization system is specified to maintain the cabin altitude below 12,000 ft and ensure passenger comfort. A partial pressurization system was selected instead of supplemental oxygen. It was considered that this would contribute to the luxury appeal of the design by removing the requirement for a cannula or mask fed oxygen supply. Partial pressurization has been proven in service by the Cessna Centurion, which is the bestselling 6-seat aircraft by volume [78].

The cabin conditioning system uses a pump to maintain a pressure differential of 3.35psi relative to local ambient pressure. During ground operation, the cabin conditioning system will provide cooling air for battery thermal management. Figure 32 shows the cabin conditioning system architecture. In case of a failure of the cabin conditioning

system, emergency oxygen will be supplied from under seat oxygen masks. The oxygen bottle will be sized for the aircraft passenger capacity and provide oxygen for the duration of a rapid descent from 23,500 ft to 12,000 ft.

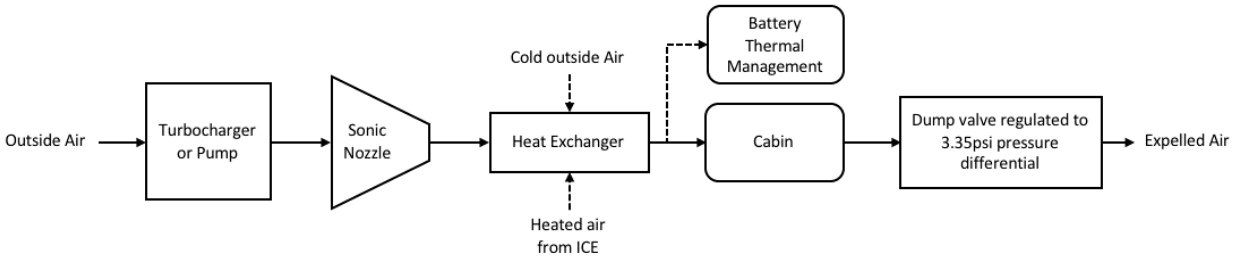

Figure 32 - Cabin conditioning schematic

3.5.5. Energy storage

Energy for flight is provided by batteries and fuel in the HEGAAsus family. Both of these systems are located on the aircraft centerline to minimize moment of inertia impacts. The fuel tank boundaries include the front spar, rear spar and inboard edges of rib three. There are three battery packs mounted fore of the front spar, aft of the rear spar and aft of the rear bulkhead. Each of these battery packs weighs 50 lbs and each battery storage location is accessible via a hatch. In this way, it is easy and convenient for the operator to remove or replace batteries in the field. Figure 35 shows a location schematic of the energy storage system.

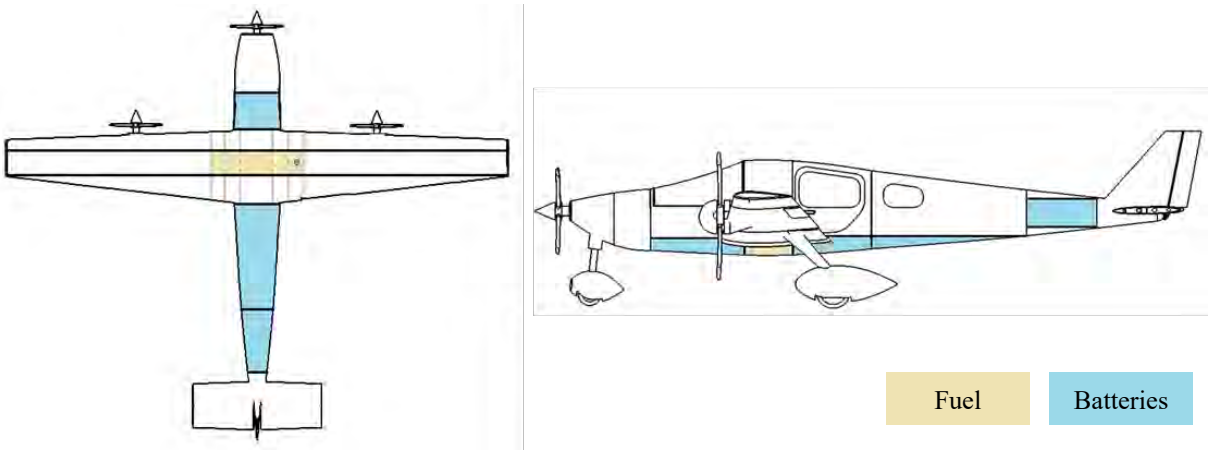

Figure 33 - Energy storage location schematic

Fuel

Final performance calculations from section 6.2 determined that 63.4 gal of fuel was required to achieve the mission. A fuel system fill factor of 0.85 was included to account for the thermal expansion of fuel and unusable fuel in the tank system and pipework, providing an additional design constraint. The requirements and constraints resulted in a minimum fuel tank inner mold line volume of 79.3 gal. The available space in the defined fuel tank is 80.6 gal, which

is sufficient to meet the mission requirement with some margin. A schematic of the fuel system is shown in Figure 34. The schematic shows the vent system that prevents pressurization of the airspace within the tank, two center mounted electric pumps that supply the engine and an over wing refueling port. Pressure refueling was determined to be unnecessary due to the low fuel capacity of the aircraft.

Battery

It was determined that 103kwh and 117kwh of battery energy were required to complete the 4-seat and 6-seat missions respectively. However, a common battery pack was designed to reduce certification and manufacturing cost. Additionally, this design decision gives the 4-seat aircraft an improved emergency range. A depth of discharge factor of 80% was applied to the required battery energy to represent the usable storage capacity of batteries in service [33], resulting in a target capacity of 146kwh. The battery pack was designed using the physical dimensions of the Panasonic Li-Ion 18650 cells [79] with weight estimated using the assumed 230wh/lb battery selected for the HEGAAsus (see Table 2).

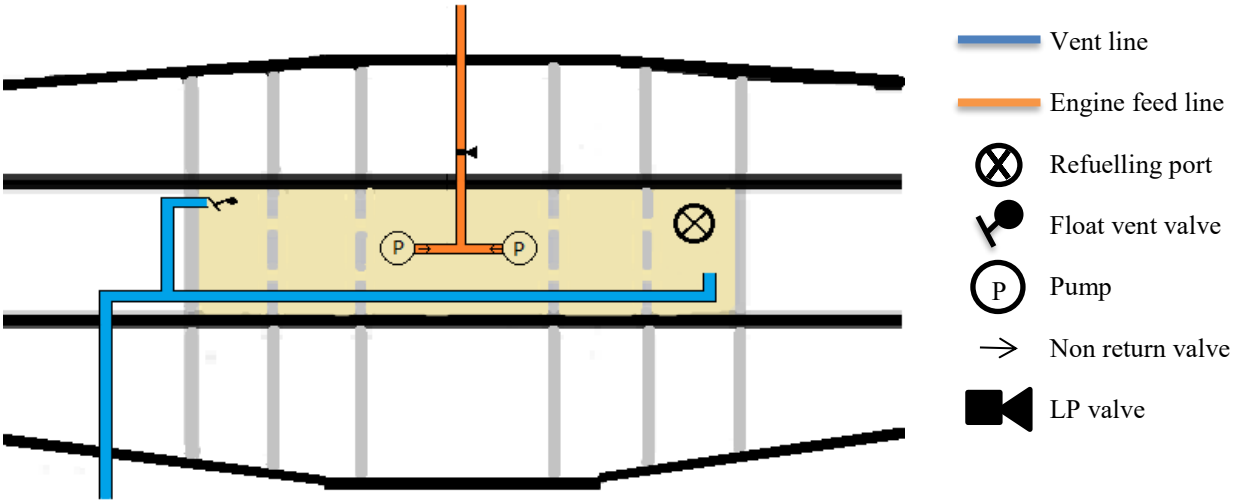

Figure 34 - Fuel system schematic diagram

To produce a voltage of 580V required by the Siemens electric motors, 157 cells are wired in series to create one battery module. To achieve the target capacity, 84 modules are wired in parallel. Figure 35 shows the physical arrangement of the battery pack and Table 28 summarizes each battery pack specification.

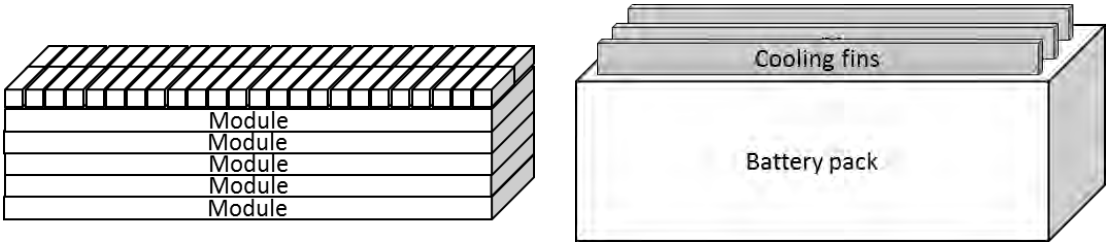

Figure 35 - Battery pack construction

Table 28 - Battery pack specifications

Parameter	Battery pack values		
	Fore	Mid	Aft
Voltage (V)	581	581	581
Capacity (kwh)	69.7	48.8	27.9
Number of cells	6280	4396	2512
Number of modules	40	28	16
Dimensions (L" x W" x H")	63 x 22 x 7	43 x 22 x 7	39 x 12 x 8
Weight (lbs)	348	244	141

3.5.6. Thermal management

During aircraft operations, there are several sources of waste heat including the internal combustion engine, electric wing motors and battery packs. To ensure optimum performance and in the case of the battery packs, to prevent thermal runaway, it is necessary to specify a cooling system to manage these thermal heat loads.

Internal combustion engine

As the Higgs engine specified is not currently commercially available and is under-going a certification process, little information is available on the thermal properties, so exact sizing of any radiators or cooling systems has not been undertaken at this time. However, using methods outlined by Roskam [80] the air inlet size can be estimated using the below equation (7). Where A is the air inlet size in m^2, P is engine horsepower, T is temperature in cruise in Kelvin, V is cruise speed in kts, ρ is air density at cruise.

$$A_{inlet} = \frac{P^{1.2}T}{(\frac{V}{2}\rho)^{1.4}11500} = \frac{350^{1.2}*242}{50^{1.4}*11500} = 0.1m^2 = 1.07ft^2 \quad (7)$$

Electric wing motors

The Siemens SP260D electric motors located in the aircraft wings have a nominal efficiency of 95% [81]. Based on the mission profile motor power requirement, the maximum rejected heat expected is 6 kW per motor. The motors utilize direct-cooled conductors, which remove waste heat from the motor windings using an electrically non-

conductive cooling liquid, silicon oil. This ensures the motor remains at its optimum operating temperature of 203°F [82]. The motor cooling silicon oil circuit must be integrated with a heat exchanging system to remove the excess heat. The HEGAAsus design is specified with an oil to air radiator system based on representative and readily available automotive components. A design methodology provided by cooling system manufacturer Mocal [83] was followed to size the HEGAAsus motor cooling system. An iterative approach was taken to the specification of the cooling system, with the analysis presented representing the final iteration. Parameters required for the specification of the cooling system are summarized in Table 29.

Table 29 - Motor cooling design parameters

Parameter	Summary
Oil flowrate per radiator row	Determined from the oil pump flow rate and the specified radiator design.
Extreme temperature difference	The difference between the oil temperature entering the radiator and the ambient temperature
Matrix face air velocity	The velocity of air through the radiator, assumed to be 20% of the freestream velocity at radiator inlet

Mocal produce radiators in various configurations ranging in cooling capability, dimension and weight. Seeking to ensure minimal system weight, the smallest radiator possible was specified for the HEGAAsus system with the details shown in Table 30.

Table 30 - Motor radiator parameters

Number of Rows	Height (inch)	Capacity (gal)	Weight (lb)
10	3.00	0.03	0.86

Typical cooling systems are powered by high flowrate oil pumps connected to an ICE gearbox. However, as the HEGAAsus motors are not collocated with the ICE it is necessary to specify an electric oil pump. Electric oil pumps of comparable flow rate to mechanically driven pumps are prohibitively heavy. Therefore, multiple lightweight electric pumps operating in parallel were necessary.

Figure 36 shows a heat transfer graph relating matrix face air velocity to the heat dissipated in each radiator tube, for various radiator tube flow rates, provided by Mocal [83].

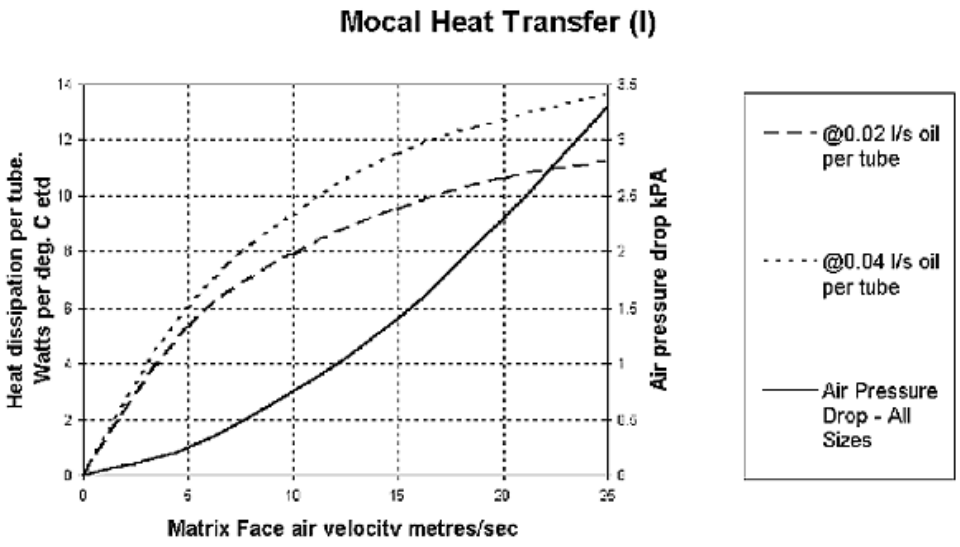

Figure 36 - Heat transfer relationship

Assuming the HEGAAsus system would take the higher flow rate of 0.04 l/s/tube (0.63 gal/min/tube), the performance requirement of the oil pumps can be calculated. Mocal produce a 3.1lb electric pump specified for a range of 1.1 to 2.0 gal/min [83]. For the 10-tube radiator chosen, a total flow rate of 3.2 gal/min is necessary to supply the radiator, requiring 4 pumps operating in parallel. However, it is reasonable to assume that development in the performance of electric oil pumps would allow a reduction in the number by the aircraft certification date.

The motor cooling inlet is positioned in the motor fairing behind the wing propellers. Therefore, the inlet velocity was approximated as the propeller outlet velocity. Considering the performance envelope for the wing propellers, 360ft/s is the most suitable value for the initial system sizing. Using the Mocal velocity ratio assumption, the matrix face air velocity would be 72ft/s.

The extreme temperature difference ($\Delta T_{extreme}$) is calculated as the difference between the oil entering the radiator (assumed to be 212ºF) and the highest expected ambient temperature (assumed to be 122 ºF).

Given the previously determined design parameters, Figure 36 was used to establish the heat dissipated per radiator tube (Q_{tube}). For the design condition, each of the 10 radiator tubes dissipates 13 W/tube/ºC.

The total heat dissipated by the radiator ($Q_{radiator}$) is found using the following expression, where N_{tube}.is the number of radiator tubes equation (8) [83]:

$$Q_{radiator} = Q_{tube} \cdot N_{tube} . \Delta T_{extreme} \quad (8)$$

Table 31 summarizes the performance of the cooling system across various operational conditions. The analysis shows that in the worst case considered in normal operation (2 pump failures at ambient temperature = 77 °F), the design would still function as required.

Table 31 - Cooling performance at various operating conditions

Operational Condition	Ambient Temperature (°F)	Heat dissipated by radiator (kW)	Nominal System Safety Factor
Design	122	6.5	1.08
RFP Design	77	9.75	1.63
1 pump failure	77	8.8	1.47
2 pump failures	77	8.1	1.35

As this is an initial calculation, the system redundancy is subject to revision with future detailed design. Furthermore, this analysis does not consider the motor oil flowrate requirements, as this data was not commercially available. Future design effort is required to ensure the cooling requirements at the motor windings is matched with the proposed radiator cooling system.

Battery packs

Batteries produce waste heat when discharging due to the exothermic reaction that produces the electric current and the internal resistance of the battery. Due to the large current draw of a high power electrical system, significant internal resistance losses are expected in the HEGAAsus system. To deal with the rejected heat, prevent thermal runaway and maintain the batteries within optimum operational limits a thermal management system has been specified.

The HEGAAsus battery thermal management system uses direct air cooling taken from a ram air scoop when the aircraft is in flight or from the air conditioning system when stationary or taxiing. This system has an advantage over liquid-air cooling as it minimizes the use of mechanical components such as oil pumps, radiators, valves and pipework, but the mechanical simplicity comes with the tradeoff of reduced heat removal capacity in operation. However, the thermal management analysis shows that the simpler air cooling system is sufficient for the thermal loads experienced by the battery packs.

Heat balance equations 9-12 were used to model the thermal management system [84]:

$$m_{cell}C_{cell}\frac{dT_{cell}}{dt} = Q_P + Q_S - Q_B \quad (9)$$

$$Q_P = I\left(V_{open\ circuit} - V_{nominal}\right) \quad (10)$$

$$Q_S = T_{cell}\Delta S\frac{I}{nF} \quad (11)$$

$$Q_B = Ah(T_{cell} - T_{local}) \quad (12)$$

Where Q_P is the over potential heat (internal resistive losses), Q_S is the heat generated due to entropy changes and Q_B is the heat removal by the thermal management system cooling fins. Table 32 shows the general parameters used in the thermal model.

The entropy change (ΔS) is dependent on the battery state of charge can be approximated using the second order polynomial shown in equation 13 [85] .

$$\Delta S = -179(SOC)^2 + 274.29(SOC) - 116 \quad (13)$$

A heat transfer coefficient (h) can be estimated using the Nusselt number and the application of the Dittus-Boelter correlation [86], as shown by equation 14:

$$h = \frac{k(0.03{Re_x}^{0.8}{P_r}^{0.3})}{L} \quad (14)$$

In the system of equations 9-14, the fin cooling area (A) is the unkown variable to be found by iteration.

Table 32 - Thermal management parameters

Parameter	Symbol	Value
Cell weight (lb)	m_{cell}	0.05
Cell specific heat capacity (J/lbK)	C_{cell}	409
Open circuit voltage (V)	$V_{open\ circuit}$	4.3
Nominal voltage(V)	$V_{nominal}$	3.7
Charge number	n	1
Faradays constant (sA/mol)	F	96485.33
Current (A)	I_{taxi}	41
	$I_{takeoff/climb}$	201
Local temperature (°F)	T_{local}	$T_{ambient} - (0.0058 \times altitude)$
Cooling airspeed (ft/s)	v_{air}	$v_{aircraft} \times 0.7\ (blockage\ factor)$

The 6-seat aircraft has a longer climb duration and higher taxi power requirement making it the constraining design case. Three design cases for the 6-seat aircraft were considered for the battery thermal management including hot day (120 °F), nominal day (70 °F) and cold day (0 °F). The upper and lower limits are extreme cases and based on average

temperatures across America. It is noted that additional design cases such as storage in hot conditions should be considered but were deemed out of the scope of this report.

The results of the final iteration of the battery cooling system design is summarized in Table 33. Sizing of the ram air intake was calculated for the cross-sectional area of airflow past the cooling fins, with a blockage factor to account for boundary layer build up and adverse pressure gradients [30] .

Table 33 - Battery cooling system sizing

Parameter	Battery pack		
	Fore	Mid	Aft
Length (inch)	39	39	39
Height (inch)	0.35	0.39	0.37
Number of fins	40	25	15
Cooling fin area (ft^2)	7.75	5.32	3.07
Air scoop intake (W" x H")	22 x 0.50	22 x 0.55	12 x 0.53

Figure 37 shows the analysis of the system across the 3 design cases. Figure 37 shows that it is necessary to reduce the cooling air flow speed to ensure the batteries remain within operating limits, depending on the ambient conditions. The cooling air flow is controlled by varying the air scoop intake area. The air scoop intake positions are presented in Table 34 as a percentage closed, where 100% describes the fully closed condition.

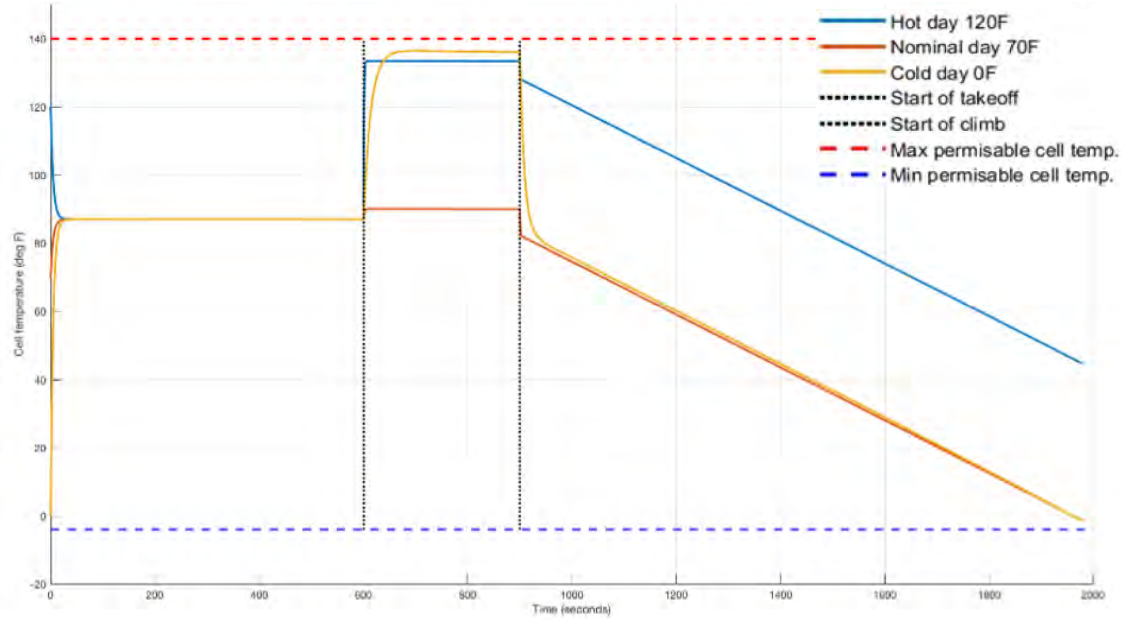

Figure 37 - Battery thermal loads at different operational conditions

Table 34 - Battery cooling operational conditions

Conditions	Cold day	Nominal day	Hot day
Ambient temperature (°F)	0	70	120
Air scoop position	95%	40%	0%

3.5.7. Autonomy

Addressing the future expectations of aircraft autonomy, the HEGAAsus is designed to integrate the necessary software and hardware architectures to provide safe and reliable autonomous flight. The HEGAAsus fly-by-light system provides redundancy in fiber optic bundling, with minimal weight increase. This allows for the installation and integration of wing tip mounted pods that will house autonomous sensor packages in future.

Radar and multi-band LiDAR sensors will provide synthetic vision for the HEGAAsus [87], as visualized in Figure 40. Synthetic vision will determine the terrain for takeoff, landing, and low altitude maneuvering as stationary obstacles do not have trajectories that require tracking or prediction. The primary components of a LiDAR sensor pack are shown in Figure 39.

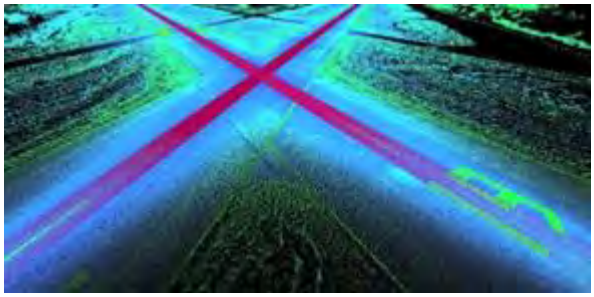

Figure 38-Demonstration of Airport Runway LiDAR Detection by ESP Associates[88]

LiDAR is currently implemented in the autonomous vehicle industry at a technology readiness level of 8 for stationary object detection and avoidance. LiDAR (Figure 39) operates by emitting spray of laser bands to capture a cone of "sight" through an accurate, close-range point cloud for real-time obstacle proximity sensing. Simultaneously, a radar signal gathers a long-range point cloud to assist the autonomous architecture with obstacle detection in low visibility conditions by means of vision-independent radio waves.

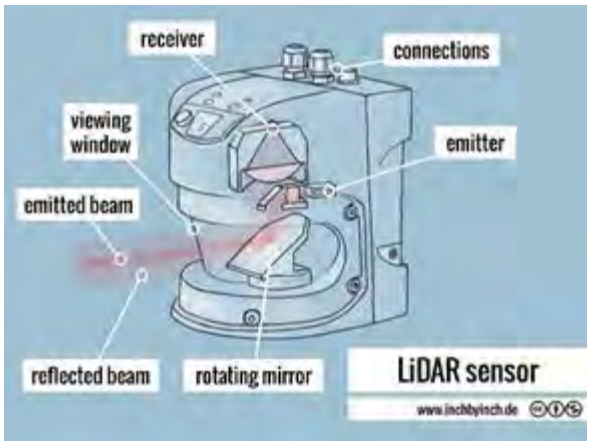

Figure 39- LiDAR Sensor Technology Diagram [89]

These sensors communicate with the HEGAAsus flight computer and integrate with existing auto-pilot systems such as that provided in the G1000 flight suite. This will allow the HEGAAsus to navigate its mission while maintaining proper balance of the hybrid electric powertrain through the existing FADEC.

Automatic Dependent Surveillance-Broadcast (ADS-B), an upcoming requirement for FAA compliance of general aviation aircraft, is discussed further in section 5.5.2 and will be the primary tool for path prediction and de-confliction with other aircraft [90]. As aircraft will be the focal point of obstacle-in-motion avoidance, the de-confliction aspect of autonomous flight will be far narrower in scope than that which an autonomous ground vehicle may encounter. Professional advisement [91] from Autonomous Ground Vehicle expert and CEO of TORC Robotics, Michael Fleming, provided the team with confidence that these integrated subsystems will offer sufficient architecture to enable full autonomy of the HEGAAsus upon the development of appropriate and certified software.

The primary future consideration of enabling an autonomous architecture is the legal ramifications of integrating autonomous critical decision making in atypical environments. This will impact the timeline of a suitable software bundle being loaded into the existing flight computer. The HEGAAsus family will integrate such software and its corresponding hardware when the systems have been developed, tested, and certified by separate entities with an expertise in autonomy. The exact architecture will be dependent on the specification of regulations as this becomes available through the certifying authorities.

4. DESIGN VERIFICATION

4.1. Structural Analysis

To verify the structure was capable of withstanding the forces applied to it a range of critical load cases, shown in Table 35, were determined from FAR Part 23 regulations [74].

Table 35 - Structural load cases

Load case	FAR section
Fully loaded on the ground	FAR 23.473
Towing fully loaded	N/A
Max pull-up (3.8g)	FAR 23.337
Min Dive (1.52g)	FAR 23.337
No fuel while at max cruise speed	FAR 23.343
Gust loads	FAR 23.341
MTOW landing	N/A
One gear landing	FAR 23.483
Level landing	FAR 23.479
Take-off with high lift devices	FAR 23.345
Max aileron deflection	FAR 23.349
Max rudder deflection at cruise	FAR 23.351
All speed and lift control devices deployed	FAR 23.373

To accurately test these cases, the moment of inertia and cross-sectional area of the structure was required. This was calculated using the structural model generated in SolidWorks. The moment of inertia was calculated for various points along the wing and empennage. Using a numerical technique, an empirical function was fit to the measured moments of inertia and cross-sectional area. This function was applied with Euler-Bernoulli beam bending theory to calculate the stress at each load case. Table 36 shows how the various loading conditions stress the structure. Note that the second column is the percent of the max yield stress for the material with a factor of safety of 1.5 has been applied.

An additional consideration that is required for the fuselage loading is the +3.35psi pressurization of the cabin. For the verification of this pressure force, the fuselage was assumed to be a cylindrical pressure vessel with hoop stress calculated using the equation 15. Where P is the pressure inside the pressure vessel, r is the radius of the cylinder, and t is the skin thickness.

$$\sigma_{Hoop} = \frac{P\,r}{t} \tag{15}$$

Using the largest radius of the fuselage for r gives the maximum stress due to pressurization. The calculated hoop stress is equivalent to 1.80% of the yield stress of Hexply 8552 [43].

Table 36 - Structural analysis results

Load Case	Percent Max Yield Stress	Location of Max Stress
Fully loaded on the ground	29.6%	Wing Box Juncture
Towing fully loaded	40.2%	Nose Gear Juncture
Max pull-up (3.8g)	23.5%	Wing Box Juncture
Max Dive (1.52g)	6.9%	Wing Box Juncture
No fuel while at max cruise speed	2.5%	Wing Box Juncture
Gust loads	N/A	Discussed in Vn Diagram
MTOW landing	31.5%	Wing Box Juncture
One gear landing	62.5%	Wing Box Juncture
Level landing	31.7%	Wing Box Juncture
Take-off with high lift devices	23.8%	Wing Box Juncture
Max aileron deflection	27.4%	Wing Box Juncture
Max rudder deflection at cruise	38.1%	Vertical Stabilizer Juncture
All speed and lift control devices deployed	19.6%	Wing Box Juncture

This initial analysis showed that the structure of the HEGAAsus is capable of withstanding all constraining design loads with a margin of safety exceeding 1.5.

4.1.1. Gust loading

A V-n diagram was constructed for the HEGAAsus family using FAR part 23.333-23.337 requirements for normal category aircraft. Figure 40 shows the V-n diagram for the 6-seat variant at sea level. Gust loads were also computed and were determined to be the factor that determined the maximum design load factors, resulting in a maximum load factor of 3.5 and a minimum load factor of -1.7. Design speeds are summarized in Table 37.

Table 37 – Design speeds

Performance parameter	Speed (knots)
Stall Speed	74
Maneuver Speed	140
Cruise Speed	200
Dive Speed	244

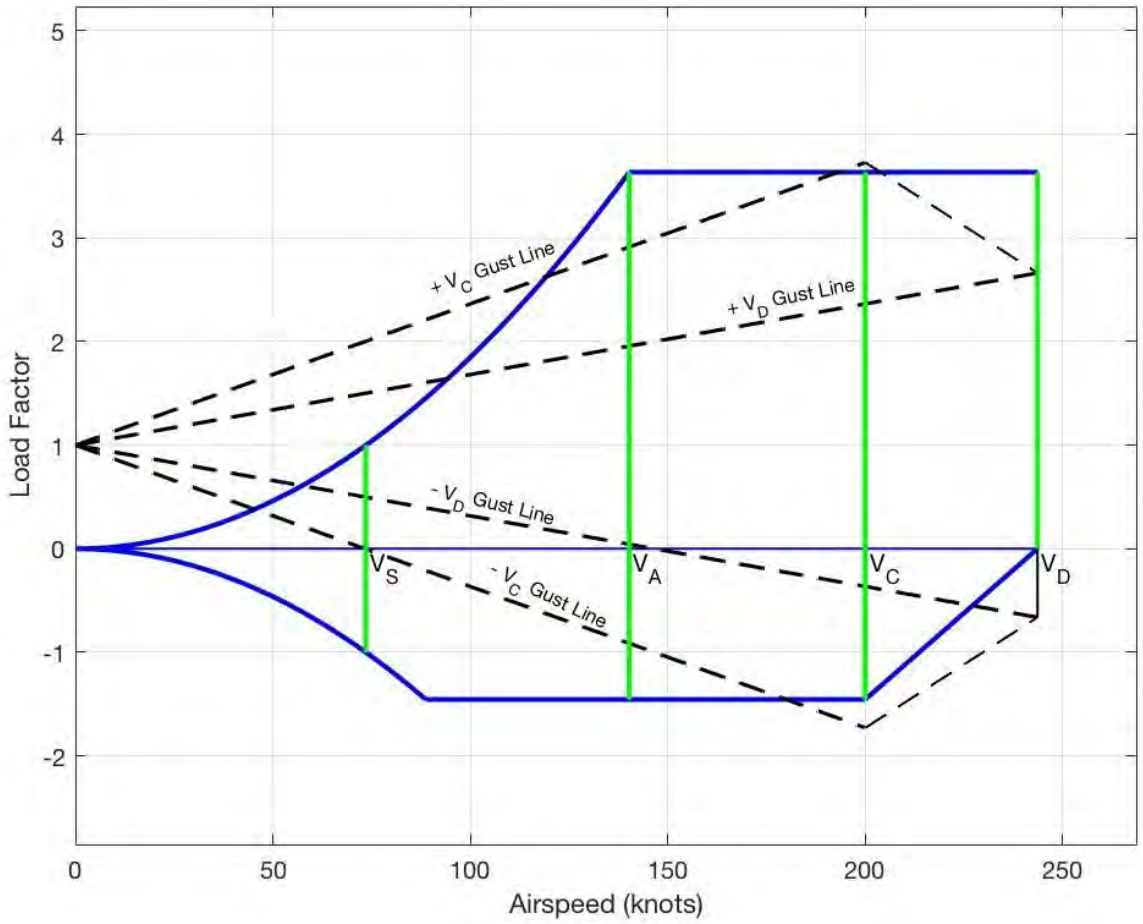

Figure 40 – HEGAAsus family V-n diagram

4.2. Weight and CG Limits

Weight estimates were developed from the Class I estimates by including known weights of identified components and updated aircraft geometry. The center of gravity location of each component is identified relative to the nose in Table 38. The chosen design has allowed for significant use of common structures and systems, with only the cabin furnishings and wing tip modification differing from the four to 6-seat variants. This means the two variants are 95% common by empty weight.

Table 38 - Weight and CG verification

Weight item		Weight estimation method	Weight (lb)		X CG position (ft)	
			4-seat	6-seat	4-seat	6-seat
Group I - Structure weight	Wing	*Class I*	322	373	13.0	13.0
	Empennage	*Class I*	74	74	27.9	27.9
	Fuselage	*Class I*	260	260	14.8	14.8
	Nacelle Components 1	*Class I*	33	33	10.0	10.0
	Nacelle Components 2	*Class I*	33	33	10.0	10.0
	Main Landing Gear 1	*Class I*	69	69	13.1	13.1
	Main Landing Gear 2	*Class I*	69	69	13.1	13.1
	Nose Landing Gear	*Class I*	59	59	2.7	2.7
Group II - Powertrain Weight	Engine	*Known Weight*	302	302	1.8	1.8
	Engine install	*Class I*	6	6	1.8	1.8
	Air induction system	*Class I*	14	14	0.0	0.0
	Generator	*Estimate*	88	88	4.3	4.3
	Controller	*Class I*	55	55	3.0	3.0
	Power Inverter	*Known Weight*	55	55	3.0	3.0
	Charger	*Known Weight*	49	73	15.7	15.7
	Cables	*Estimate*	55	55	14.8	14.8
	Motors	*Known Weight*	110	110	10.2	10.2
	Motors	*Known Weight*	110	110	10.2	10.2
	Motor install	*Class I*	1	1	10.2	10.2
	Motor install	*Class I*	1	1	10.2	10.2
	Thermal Management	*Estimate*	55	55	9.8	9.8
	Nose Propeller	*Class I*	110	110	0.0	0.0
	Wing Propeller 1	*Class I*	66	66	10.0	10.0
	Wing Propeller 2	*Class I*	66	66	10.0	10.0
	Fuel System	*Class I*	97	97	13.0	13.0
Group III - Fixed Equipment Weight	Flight Control system	*Class I*	109	109	12.5	12.5
	Hydraulic system	*Class I*	99	99	21.3	21.3
	Electrical system	*Class I*	154	154	12.5	12.5
	Electronics	*Class I*	26	26	14.8	14.8
	Avionics	*Known Weight*	82	82	3.0	3.0
	Air systems	*Class I*	53	53	21.3	21.3
	Furnishings	*Class I*	199	298	15.9	15.9
	Supplemental Oxygen	Known Weight	9	9	24.6	24.6
	Trapped fuel and oil	*Class I*	75	75	13.0	13.0
Empty weight			**2963**	**3138**		
Group IV – Variable Payload Weight	Forward Passengers	*Known Weight*	380	380	9.8	9.8
	Back Passengers	*Known Weight*	380	760	19.2	15.9
	Front Baggage	*Known Weight*	0	60	9.8	9.8
	Back Baggage	*Known Weight*	119	120	22.3	22.3
	Fuel	*Estimate*	441	441	13.0	13.0
	Forward Batteries	*Estimate*	602	602	11.7	11.7
	Aft Batteries	*Estimate*	134	134	25.6	25.6
Max takeoff weight			**5019**	**5635**		

Once the weights were known, the average component CGs were positioned in the aircraft to compute the aircraft CG location. Weight and balance was an iterative process between placing these weights where volume and functionality allowed and adjusting the landing gear and empennage design to have the CG range incorporate the various loading conditions. Stability and landing gear constraints were place on the CG travel to ensure the safety and functionality of the aircraft was preserved on the ground and in the air for both variants. The final forward limit and aft limits were constrained by the landing gear design.

With constraining CG limits identified throughout the Class II design section, a CG excursion diagram was constructed. This is shown in Figure 41. The variation in CG location for the 6-seat mission is shown in Figure 42.

.

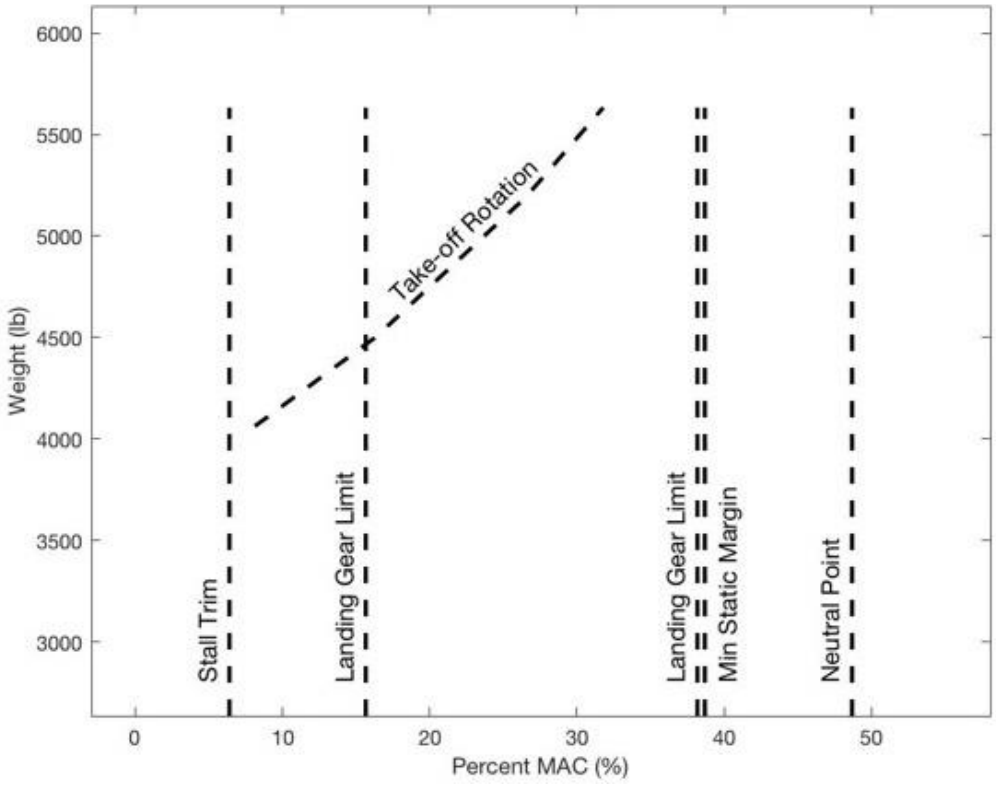

Figure 41 - Center of gravity limits

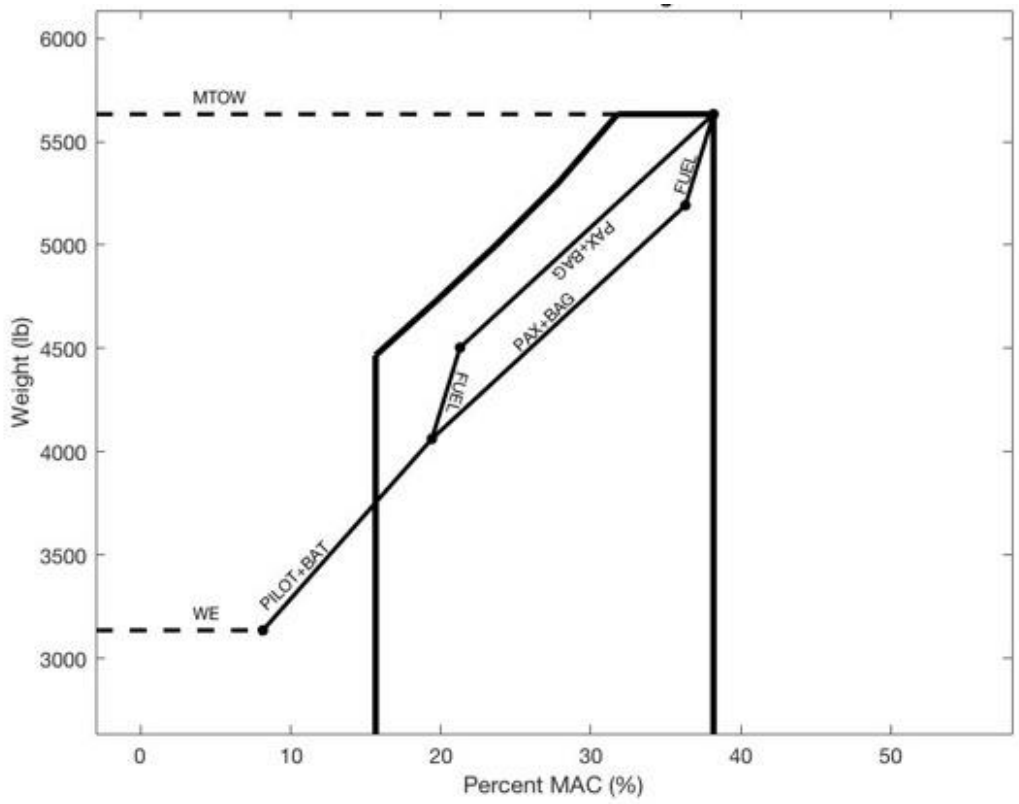

Figure 42 - Variation of center of gravity during the 6-seat design mission

4.3. Aerodynamic Analysis

4.3.1. Drag breakdown

An analysis of the aircraft drag breakdown during a long-range cruise at 22,500ft was undertaken. Using the drag relationship below, a 3D drag coefficient for the wing was estimated.

$$C_{L3D} = \frac{C_{L2D}}{1+\frac{2}{AR}} \tag{16}$$

Drag coefficients of the fuselage and empennage were estimated using the Skin Friction Drag code from the Virginia Tech Aerodynamics and Design Software Collection. The drag coefficient of the landing gear with their aerodynamic pods was estimated using the method outlined by Kundu [92]. Figure 37 shows the buildup of the total aircraft drag coefficient. Using a method developed by Scholz, it was possible to estimate the span loading efficiency on the wing and thus estimate the induced drag to be 0.053 and 0.039 for the 4 and 6-seat wings [50].

Table 39 - Drag breakdown

C_{D0}	4-Seat	6-Seat
Wing	0.0047	0.0050
Horizontal Stab.	0.0020	0.0020
Vertical Stab.	0.0016	0.0016
Fuselage	0.0030	0.0030
Landing Gear	0.0024	0.0024
Total	**0.0137**	**0.0139**

During the preliminary design phases an assumed C_{D0} value of 0.015 was used. This analysis shows that, not only was this a reasonable assumption, the drag on the HEGAAsus is lower than expected. Drag polar diagrams are shown in Figure 43.

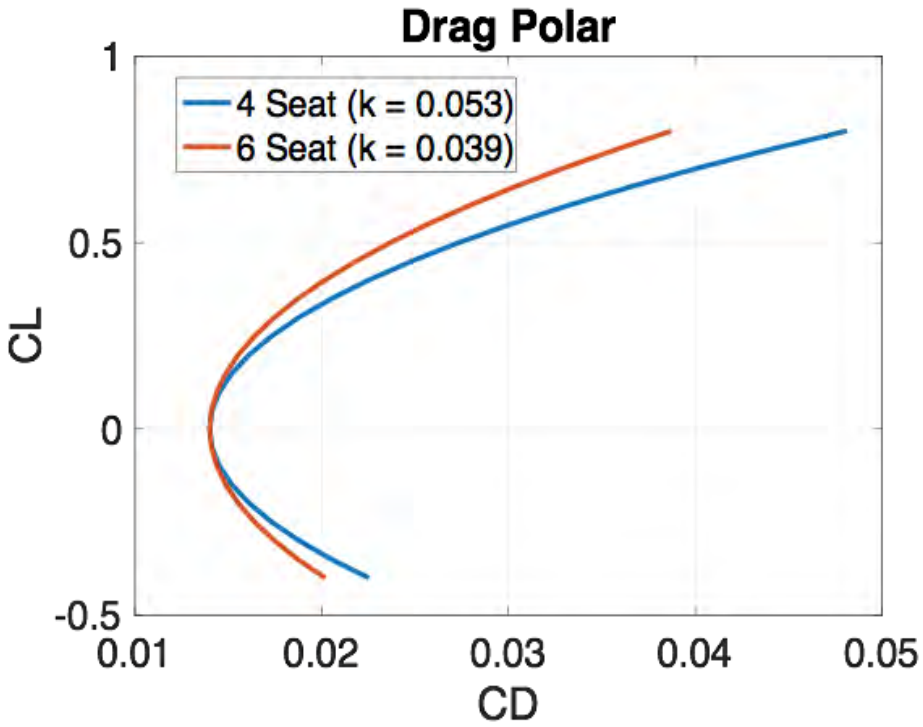

Figure 43 - Drag polar diagram

4.3.2. Propeller wash analysis

To validate lift distribution assumptions used in performance calculations, an assessment of the variation in lift distribution when the wing propellers were active in take-off and climb and inactive in cruise was undertaken. Using a modified VLM code WASPE, developed by Rajkumar [93], it was possible to account for the velocity profile behind the propeller and its impact on the wing loading. The propeller velocity profile was modeled using JavaProp [94]. The

results were compared with lift distribution without wing propellers, using the open source program Tornado [95]/ Estimations for the 6-seat variant are provided in Figure 44.

The estimated total lift coefficient of the wing is 0.279 in cruise and 0.281 for takeoff and climb. Due to the small variation, for the purposes of performance evaluation, it was deemed that lift coefficient is independent of propeller effects.

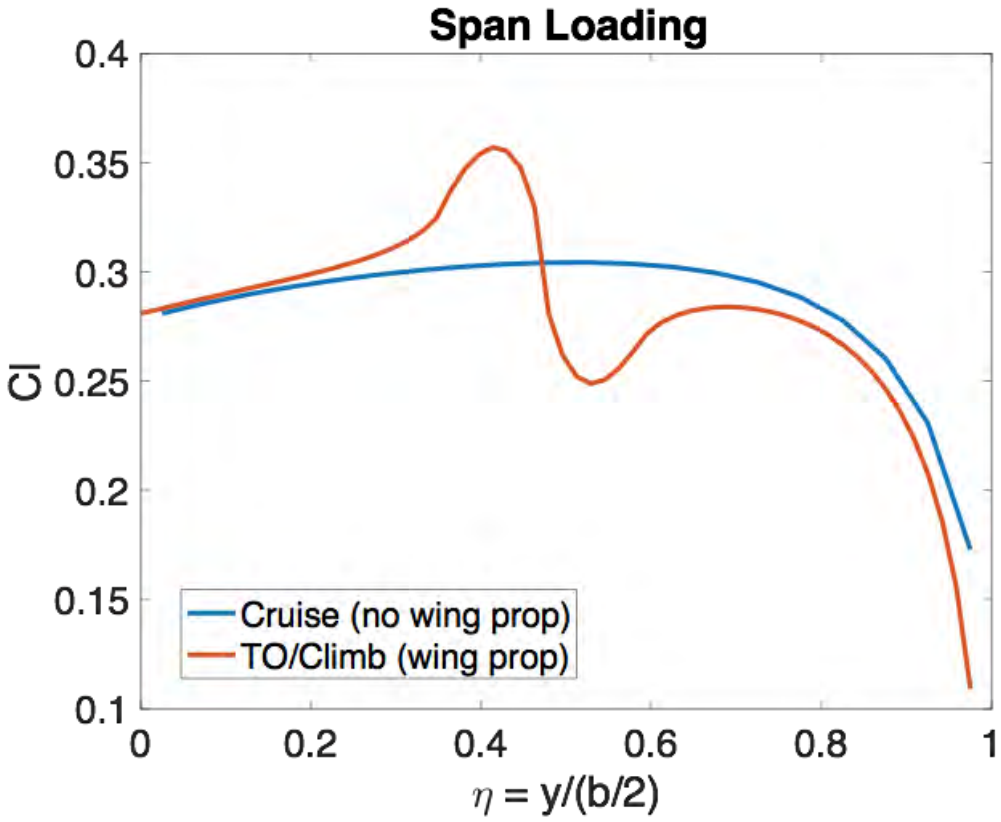

Figure 44 – Propeller wash impact on lift distribution

4.4. Performance Calculations

4.4.1. Cruise Speed

The RFP states a required cruise speed of 174 knots with a target of 200 knots. Cruise speeds for the HEGAAsus were calculated for two conditions: a high-speed cruise (HSC) utilizing 80% throttle and a long-range cruise (LRC) using

60% throttle. The variation in cruise speed with altitude can be seen inFigure 45, at the selected cruise altitude of 22,500ft all cruise configurations exceeds the minimum requirement of 174kts outlined in the RFP.

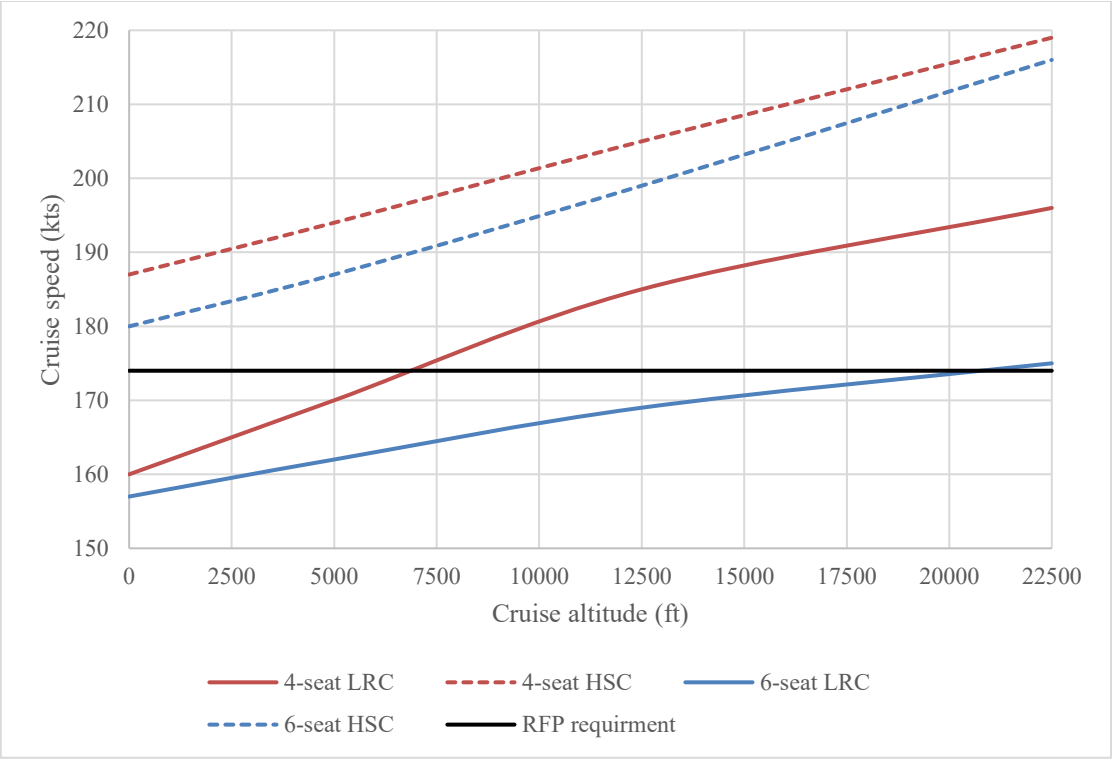

Figure 45 - Cruise speed variation with altitude

4.4.2. Rate of Climb

The airspeed for best climb rate were calculated as 104kts and 94kts for the 4 and 6 seat aircraft using methods from Gudmundssonn [69]. The climb rate were then determined from the excess available power and are summarized in Table 40.The airspeed for best climb rate were calculated as 104kts and 94kts for the 4 and 6-seat aircraft using methods from Gudmundssonn [69]. The climb rates were then determined from the excess available power and are summarized in Table 40.

Table 40 - Initial climb rates

4-seat	6-seat
2,561 fpm	2,351 fpm

4.4.3. Range

Payload-range diagrams were created to show the operational capabilities of the HEGAAsus. A payload-range diagram consists of four points, defined as follows:

A. The furthest left point represents the aircraft loaded with its maximum payload but no fuel, and therefore no range.
B. The second point represents the aircraft loaded with its maximum payload and as much fuel as can be added before reaching MTOW. The area between points A and B represent all of the mission ranges that can be flown with maximum payload.
C. The third point represents the design condition; the aircraft is loaded with full fuel and design payload. The area between points B and C represents the mission ranges that can be flown at MTOW.
D. The final point represents the maximum possible range; the aircraft is loaded with full fuel but no payload. The area between points C and D represent all the mission ranges that can be flown with full fuel.

The numerical values for the above conditions for both variants of the HEGAAsus at cruise conditions at 22,500 ft can be seen in Table 41.

Table 41. Payload Range Conditions

Condition	4 Seat Payload (lbs)	Corresponding Range (nm)	6 Seat Payload (lbs)	Corresponding Range (nm)
Max Payload, No fuel	1,098	0	1,538	0
Max Payload, MTOW	1,098 (+166 lbs fuel)	430	1,538 (+166 lbs fuel)	390
Max Fuel, MTOW	878 (+440 lbs fuel)	1,000	1,318 (+440 lbs fuel)	893
Max Fuel, No Payload	0 (+440 lbs fuel)	1,127	0 (+440 lbs fuel)	1,107

This data makes up the payload-range diagram, seen in Figure 48. Note that the weight on the y-axis is payload weight only.

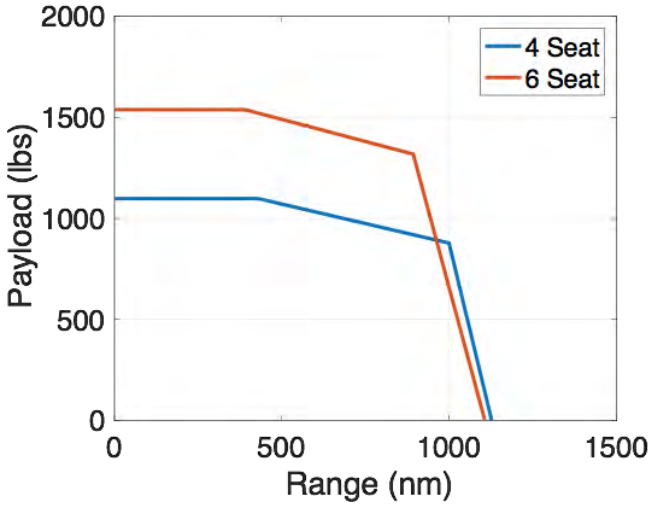

Figure 46 - Payload range diagram

4.4.4. Takeoff

Takeoff distances were calculated using the method outlined by Gudmundsson [69]. This method breaks the takeoff run into four phases: ground roll, rotation, transition, and climb to 50 ft obstacle. As per the RFP, calculations were made for sea-level plus 18° F on dry pavement, 5,000 ft above sea-level on pavement, and 5,000 ft on grass. The key assumptions used in these calculations are shown in Table 42 and the resulting take off distances in Table 43.

Table 42 - Takeoff distance assumptions

Parameter	Variant	
	4-seat	6-seat
Friction Coefficient Pavement	0.04	
Friction Coefficient Grass	0.08	
Propeller Efficiency	0.70	
CL	1.80	
CD	0.19	0.14
V_{rotate} at Sea Level (knots)	73	73
V_{rotate} at 5,000 ft (knots)	85	84

Table 43 - Takeoff distances

	4-Seat TO Distance (ft)	6-Seat TO Distance (ft)
Sea Level + 18° F, Paved	1,413	1,499
5,000 ft, Paved	2,010	2,140
5,000 ft, Grass	2,043	2,182

4.4.5. Landing

Landing distances were calculated using the method from Gudmundsson [69]. The landing run is split into four phases: approach, flare, free roll, and braking. As per the RFP, calculations were made at sea-level plus 18° F on dry pavement, 5,000 ft above sea-level on dry pavement, and 5,000 ft on grass. The key assumptions made for these calculations are listed in Table 44 and the resulting landing distances in Table 45.

Table 44 - Takeoff distance assumptions

Parameter	Value	
	4-seat	6-seat
Glideslope	3°	
CL (4-seat/6-seat)	2.27	2.38
V_{TD} (4-seat/6-seat) (knots)	71	73
Braking Coefficient Paved	0.5	
Braking Coefficient Grass	0.2	

Table 45 - Landing distances

	4-Seat LDG Distance (ft)	6-Seat LDG Distance (ft)
Sea Level + 18° F, Paved	1,474	1,607
5,000 ft, Paved	1,529	1,674
5,000 ft, Grass	1,692	1,987

4.4.6. Emergency Performance

In line with FAA regulations, the design mission carries fuel reserves for 45 minutes of flight. Calculations were made to show what overland distance this would translate to at best endurance speed [69] and an altitude of 5000 ft. The RFP also calls out the emergency range possible on only electric power in the event of ICE failure at 5000 ft. These calculations were made assuming that the batteries were at 20% charge at the time of ICE failure, as . Recognizing that emergency performance is important to the customer, calculations were also made to demonstrate that the HEGAAsus can takeoff, climb out, go around, and land if either of the two propulsion systems were to fail on takeoff. Table 46 lists the emergency performance characteristics of the HEGAAsus.

Table 46 - Emergency procedures

	4-Seat	6-Seat
45 min IFR Reserve Range (nm)	84	76
ICE Only TO Distance (ft)	2,131	2,300
Electric Only TO Distance (ft)	2,001	2,056
ICE Only RoC (ft/min)	885	861
Electric Only RoC (ft/min)	1,021	982

4.5. Stability and Control Validation

4.5.1. Stability Validation

Initial estimates of the stability derivatives were calculated using class II analytical methods outlined in Roskam [75]. To verify the class II calculations an open source software, called XFLR5 was used to perform 3D vortex panel method to compute the stability derivatives. Results for the 6-seat variant are summarized in Table 47. Additionally, the neutral point was also found to be at 51% and 49% MAC for the 4 and 6-seat aircraft. Initial estimates used a 49% MAC neutral point, thus validating the assumption previously used.

Table 47 - Verification of stability derivatives

	$C_{L_{(.)}}$	$C_{m_{(.)}}$
0	0.06	0.085
α	5.3	-0.5
δe	0.5	-1.7
q	8.6	-14.7

	$C_{Y_{(.)}}$	$C_{l_{(.)}}$	$C_{n_{(.)}}$
β	-0.04	-0.1	0.003
δa	0.06	0.1	0
δr	0.02	0	-0.02
p	-0.2	-0.5	-0.1
r	0.08	0.2	-0.02

The trim characteristics of the aircraft were computed by setting the lift equal to the weight and the moment to zero. The results for cruise conditions are summarized in Table 48.

Table 48 - Cruise trim settings

	4-Seat Variant	6-Seat Variant
Trim Angle of Attack (α)	4.3°	3.8°
Trim Elevator Deflection (δe)	0.7°	1.8°

4.5.2. Control Surface Validation

Various maneuvers outlined in FAR 23 [74] were analyzed to ensure the control surfaces were sized correctly, including:

A. Using the forward center of gravity limit to demonstrate takeoff rotation can occur in less than five seconds.

B. On approach demonstrate a roll performance from -30° to 30° in 4 seconds.

C. Demonstrate ability to fly in a $0.2V_{stall}$ 90° crosswinds during take-off.

D. Demonstrate ability to perform a 3.8g coordinated turn.

The results [75] for the 6-seat variant, the more difficult design, are displayed in Table 49.

Table 49 - Control surface validation

Requirement	δa	δr	δe	δa_{max}	δr_{max}	δe_{max}
Rotation on takeoff	0°	0°	25°	+/- 30°	+/- 30°	+/- 25°
Roll on approach	8°	0°	0°			
Crosswind at take-off	8°	1.5°	-0.7°			
3.8g coordinated turn	0.0°	-0.6°	-4.4°			

4.5.3. Dynamic Stability and Handling Qualities

To assess dynamic stability during cruise, the dynamics of the aircraft were linearized, and the eigenvalues computed. The dynamics of the aircraft can then be expressed in state space form as shown in equation (17).

$$\dot{\delta x} = A\delta x + B\delta u \tag{17}$$

Where A and B are given by either equation (18), for longitudinal dynamics, or equation (19) for linearized lateral dynamics. The original dynamics of the aircraft can then be represented by the eigenvalues of A.

$$A_{Lon} = \begin{pmatrix} -0.0096 & 0.08 & 0 & -9.81 \\ -0.27 & -0.86 & 73.1 & 0 \\ 0.0002 & -0.037 & 1 & 0 \\ 0 & 0 & 1 & 0 \end{pmatrix} \quad B_{Lon} = \begin{pmatrix} -0.44 & 0.98 \\ -18.7 & 0 \\ -26.6 & 0 \\ 0 & 0 \end{pmatrix} \tag{18}$$

$$A_{Lat} = \begin{pmatrix} -0.007 & -0.26 & 73.9 & 9.81 \\ -0.89 & -24.36 & 9.62 & 0 \\ 0.14 & 3.13 & -1.52 & 0 \\ 0 & 1 & 0 & 0 \end{pmatrix} \quad B_{Lat} = \begin{pmatrix} 0.78 & 0.2 \\ 89.3 & 1.630 \\ -1.77 & -0.93 \\ 0 & 0 \end{pmatrix}$$

The Cooper-Harper pilot rating scale provides a connection between pilot satisfaction while flying an aircraft and flying qualities. A level I rating reflects flying qualities that are adequate for the flight phase, a level 2 rating is adequate but involves an increase in pilot workload, and a level 3 rating means the aircraft is controllable but requires excessive pilot workload. According to Roskam [96], the handling qualities in Table 50 result in a level one rating.

The specified avionic architecture allows the HEGAAsus handling qualities to be improved with an augmented stability system. By assuming that all states could be sensed, a full-state feedback control was designed. The state-space model of the aircraft dynamics becomes. (Equation (19)-(21))

$$\dot{\delta x} = A\delta x + B(\delta u_{aug} + \delta u_{pilot}) \tag{19}$$

$$\text{Where, } \delta u_{aug} = -K\delta x \tag{20}$$

$$\dot{\delta x} = (A - BK)\delta x + B\delta u_{pilot} = A_{closed-loop}\delta x + B\delta u_{pilot} \tag{21}$$

$A_{closed\text{-}loop}$ represents the aircraft dynamics with the stability augmentation system. The desired handling qualities in Table 50 were transformed into desired eigenvalues for each mode and the gains K (equation (22) and (23)) were chosen to achieve these eigenvalues.

$$K_{Lon} = \begin{pmatrix} 0.0035 & -0.0009 & -0.1212 & -0.0471 \\ 0.498 & -0.2804 & -0.0449 & -10.0359 \end{pmatrix} \quad (22)$$

$$K_{Lat} = \begin{pmatrix} 0.0021 & -0.1974 & -0.1212 & -0.0471 \\ 0.1415 & -2.9972 & -0.0449 & -10.0359 \end{pmatrix} \quad (23)$$

With the aid of augmented stability, the HEGAAsus is able to meet all of the requirements for level I flying qualities, as shown in Table 50.

Table 50 - Handling qualities validation

Mode	Short Period	Phugoid	Sprial	Roll	Dutch-Roll
Handling Quality	ζ	ζ	T_{half}	τ	$\zeta\omega_n$
Level I	> 0.04	0.3 - 2	>20 s	< 1 s	> 0.35 rad/s
HEGAAsus	0.05	0.8	69 s	0.067 s	0.45 rad/s

5. AIRCRAFT INTERNAL CONFIGURATIONS

As requested by the RFP, the HEGAAsus product portfolio is offered in 4 and 6-seat passenger variants. The following sections outline the internal configurations of the HEGAAsus product portfolio.

5.1. Cockpit

The HEGAAsus cockpit is common across all variants. Figure 47 shows a render of the internal cockpit. The Garmin avionic suite specified in section 3.5.2 is shown as installed in the HEGAAsus instrument array. The HEGAAsus windshield is positioned to provide standard field of view angles, as presented by Sadraey [51]. Figure 48 shows the windshield arrangement relative to the pilot's position. Table 51 summarizes the windshield field of view angles.

Figure 47 - HEGAAsus cockpit render

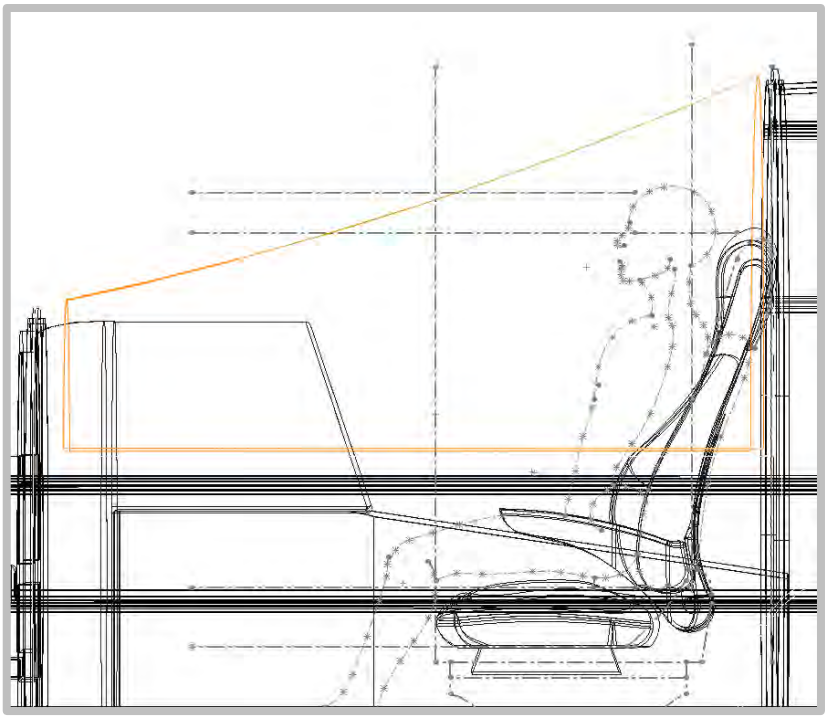

Figure 48 - HEGAAsus windshield positioning

Table 51 - Windshield field of view specification

Field of view component	Angle (degrees)
Above horizontal	15
Below horizontal	20
Left of heading	135
Right of heading	115

5.2. Passenger Variants

Figure 49 shows the seating configuration of the 4-seat variant. Figure 50 shows the seating configuration of the 6-seat variant. Table 52 gives the volume allocation for passengers and cargo.

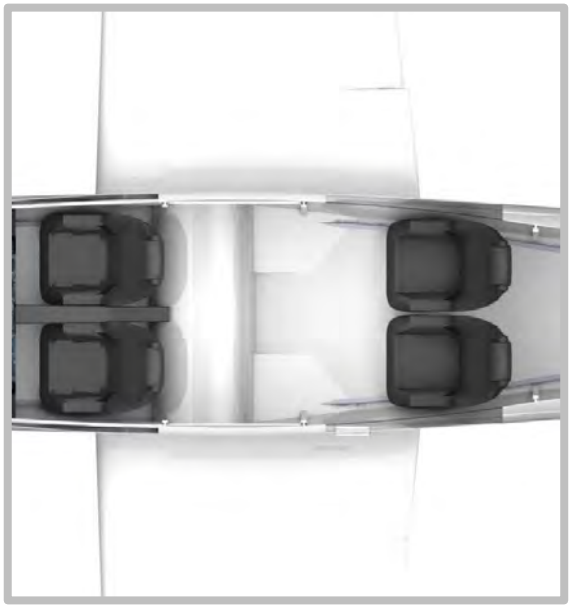

Figure 49 - HEGAAsus 4-seat internal configuration

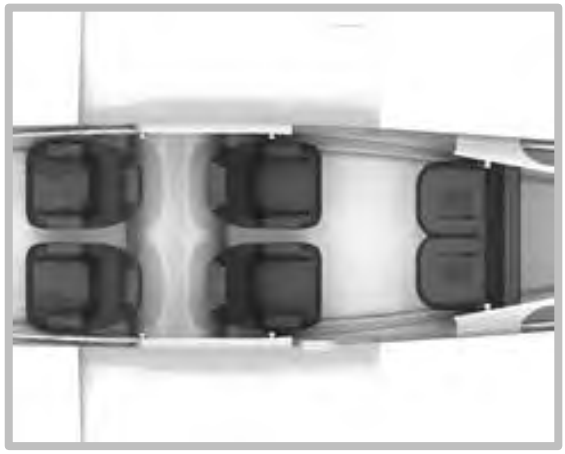

Figure 50 - HEGAAsus 6-seat internal configuration

Table 52 - HEGAAsus passenger variant internal volumes

	4-seat volume (ft^3)	6-seat volume (ft^3)
Passenger compartment	85	85
Cargo	28	28

6. CERTIFICATION

A novel approach to certification has been taken reflecting the use of the hybrid powertrain and the family airframe commonality and is described in this section. When describing an aircraft to the certification authorities, manufacturers commonly use the Air Transport Association (ATA) numbering system standard [97]. This approach has been taken for the HEGAAsus family. Where referenced, ATA'XX' refers to an existing ATA standard.

6.1. Hybrid Powertrain Certification Plan

There is currently no standardized means to certify a hybrid powertrain as there has been no precedent. Therefore, it is proposed that the HEGAAsus hybrid powertrain model is defined as a single internal combustion engine (ATA71) with propulsive augmentation (ATA84) provided by electric motors. As the aircraft demonstrates compliance to Part 23 without power augmentation, the HEGAAsus family of aircraft will be certified as 'Level 2 single engine aircraft' under FAA Part 23 regulations [74].

Both the ATA71 and ATA84 systems are to be controlled by FADEC, which is designed to ensure compliance with Part 23.24. To prevent unsafe flying conditions, a failure of one motor will result in the opposing motor being automatically shutdown to prevent adverse yaw effects. A failure of the combustion engine will automatically activate the wing motors, using all remaining battery energy to increase the glide slope of the aircraft, giving the pilot more time to find a suitable ditching location or to conduct an emergency landing. As the FADEC unit is critical for flight it will be shown to have a probability of failure 10^{-12}/flight hour.

The HEGAAsus team received an expert opinion from FAA Designated Engineering Representative, Alan Lawless, that such a certification plan to demonstrate single engine compliance was sound.

6.2. Airframe Type Certificate

To reduce the cost of certification, the basic airframe (without the wing tips) will be type certified for the 6-seat maximum takeoff weight and passenger occupation. By showing compliance to the more difficult design mission, the airframe will share a common type certificate for both the 4 and 6-seat variants. A wingtip modification will be certified separately to the airframe and will be a standard fit on the 6-seat variant. Section 9.5 outlines the cost saving benefit of this certification plan.

7. BUSINESS AND SALES

7.1. Product Portfolio

The HEGAAsus product portfolio consists of 4 and 6-seat passenger variants. The 4 and 6-seat variants are designed with high structural and system commonality, utilizing the same fuselage, empennage and base wing plan. The 6-seat variant mission profile is achieved with a modification package introducing a wingtip extension. The HEGAAsus product portfolio approach leverages benefits for the cost of certification and manufacturing. Certifying both products under one type certificate has a direct effect on the program cost by reusing design data and minimizing administrative rework. By manufacturing most of the aircraft on the same production line, greater economies of scale can be achieved and production cost can be minimized. This allows the HEGAAsus product portfolio to remain competitively priced when considered against comparator aircraft.

7.2. Supply and Demand

The general aviation market was negatively affected by the global recession between 2007 and 2009. GA aircraft deliveries fell from a peak of 4,277 in 2007 to a recent low of 2,024 in 2010. A small growth in global deliveries has been seen in the period 2010-2016, with a reported 2,268 deliveries in 2016 [98]. As of 2016, the FAA predicted an average annual growth of 1.7% across piston and turbine powered GA aircraft market between 2016 and 2037 [53]. An analysis of reported deliveries in 2016 showed that across all piston and turbine powered GA aircraft, 31% (692) were 4-seat vehicles and 10% (228) were 6-seat vehicles [98]. The following assumptions were made to predict the market size at point of entry.

- The global yearly growth of all piston and turbine powered GA aircraft deliveries will be equal to the overall average yearly growth of the GA market – 1.7%.
- The percentage of 4 and 6-seat GA aircraft forming all piston and turbine powered GA aircraft deliveries will remain constant from 2016 values, 31% and 10% respectively.

Based on these assumptions and data provided for 2016, Table 53 summarizes the predicted market size in the initial 4-seat (2028-2033) and 6-seat (2030-2035) production runs.

The RFP calls for an initial production run or 4-10 aircraft per month. To establish the viability of this range a market trade study was completed. Table 53 summarizes the yearly deliveries required to satisfy the upper and lower monthly production rate range, and resultant percentage of predicted global deliveries this would gain over the initial 5-year production runs.

Table 53 - Percentage of global deliveries captured by monthly production rates

Monthly production rate	Yearly deliveries	Percentage of predicted global 4-seat deliveries over 5 years	Percentage of predicted global 6-seat deliveries over 5 years
1	12	1.1%	3.3%
10	120	11.3%	33.1%

Table 53 and Table 54 show the estimated deliveries of comparable 4 and 6-seat aircraft in the period 2014-2016 [98], ordered by increasing average.

Table 54 - Estimated 4-seat competitor deliveries 2015-17

Aircraft	Number of seats	2015	2016	2017	Average
Mooney Ovation ultra	4	3	1	3	2
Money Acclaim Ultra	4	-	6	4	5
Piper PA 44 Seminole	4	17	10	17	15
Tecnam 2010P Twenty Ten	4	20	22	18	20
Tecnam 2006T	4	24	24	19	22
Cessna TTx	4	44	31	23	33
Cirrus SR20	4	31	35	46	37
Diamond DA42	4	44	34	36	38
Cessna Skylane	4	33	50	46	43
Piper PA28 Archer III	4	30	49	81	53
Diamond DA40	4	75	48	60	61
Cessna Skyhawk	4	143	100	129	124
Cirrus SR22	4	128	133	135	132
Cirrus SR22T	4	142	149	174	155

Table 55 - Estimated 6-seat competitor deliveries 2015-17

Aircraft	Number of seats	2015	2016	2017	Average
Piper PA 34 Seneca	6	8	3	1	4
Piper PA46 M500	6	27	12	12	17
Beechcraft Bonanza G36	6	23	25	13	20
Beechcraft Baron G58	6	18	20	23	20
DiamondDA62	6	2	30	33	22
Piper PA 46 M350	6	34	26	9	23
Piper PA46 M500	6	-	22	35	29

As a new manufacturer attempting to disrupt the market by delivering a new technology, it was reasonable to assume that the HEGAAsus product portfolio would not capture the highest percentage of global deliveries initially. Table 54 and Table 55 show that the highest number of deliveries are held by established manufacturers and models (Cessna, Cirrus and Piper), with the majority of deliveries belonging to 3 aircraft in both seating variants. Based on these factors, the probability of achieving similarly high deliveries in the first 5-year production run is low. Therefore, an initial constraint of 2 to 6 aircraft in both seating variants was applied.

The HEGAAsus production rates were further constrained by considering the ratio of market demand for 4-seat and 6-seat aircraft. To ensure either variants of the HEGAAsus did not exceed the probable number of deliveries, a production rate range of 1-2 aircraft per month was selected for the 6-seat variant. This value constrained the 4-seat production rate range to 3-6 aircraft per month, via the ratio. However, additional analysis of the product portfolio cost model was required to constrain the production rates to single values.

7.3. Flyaway cost

The unit flyaway costs for the 4 and 6-seat HEGAAsus variants are shown in Table 56 and is estimated using the Eastlake model approach [69]. The cost of certification and production of both variants is shared across all models manufactured due to the high degree of commonality. The cost of the wingtip certification and manufacturing is only shared across the number of 6-seat variants manufactured.

Table 56 - HEGAAsus family flyaway costs

Cost Factor	4-seat	6-seat
	Unit Cost / $	Unit Cost / $
Engineering	$114,483	$150,859
Development support	$3,906	$4,900
Flight test operations	$294	$810
Tooling	$51,816	$68,169
Manufacturing labor	$247,355	$304,098
Quality control	$48,234	$59,299
Materials/equipment	$26,743	$31,643
Fixed landing gear discount	-$4,749	-$4,749
Power train	$92,885	$94,493
Avionics	$9,500	$9,500
TOTAL COST TO PRODUCE	**$590,466**	**$719,023**
Manufacturers liability insurance	$100,379	$122,234
FLYAWAY COST	**$690,845**	**$841,257**

7.4. Cost Model

The HEGAAsus primary project costs were estimated using the Eastlake Model [69]. This is a variant of the DAPCA-VI model that has been adapted for the development of GA aircraft, accounting for design and manufacturing complexity such as composite materials and pressurization with correction factors [69]. The model estimates the cost of required engineering, tooling, and manufacturing man-hours based on the expected airframe weight and maximum level airspeed. As the Eastlake model does not account for the additional novelty and cost of a hybrid electric architecture, the HEGAAsus cost model was augmented with fixed value predictions where appropriate. The program cost prediction accounts for the shared airframe and wingtip design approach according to equations (24) and (25):

$$4 - \text{Seat Unit Cost} = \frac{(\text{Fixed cost+Variable cost})_{airframe}}{N_4+N_6} + \text{PLI} \tag{24}$$

$$6 - \text{Seat Unit Cost} = \frac{(\text{Fixed cost+Variable cost})_{airframe}}{N_4+N_6} + \frac{(\text{Fixed cost+Variable cost})_{wingtip}}{N_6} + \text{PLI} \tag{25}$$

Where subscript *airframe* refers to the common (4-seat and 6-seat) airframe, subscript *wingtip* refers to the 6-seat variant wingtip extension, N_4 and N_6 are the number of 4-seat and 6-seat variants produced in 5 years, and PLI is Product Liability Insurance.

Fixed development cost refers to the cost of engineering, developmental support, flight test operation, and tooling man-hours required for certification. Primary design cost parameters are the structural weight, maximum level airspeed, airworthiness certification method (LSA or CFR Part 23), wing taper, flap system complexity, composite material manufacturing, and hull pressurization [69].

The Eastlake Model accounts for variable product costs with two sub groups: manufacturing cost and equipment cost. Manufacturing cost accounts for labor, materials, equipment, and product quality control. Equipment cost accounts for additional hardware required to deliver an operable aircraft and includes landing gear, powertrain, propeller(s), and avionics systems [69].

Equipment costs are subject to a Quantity Discount Factor (QDF), which accounts for the number of units produced and the development of manufacturing experience. It is assumed that the unit equipment cost will be reduced by leveraging economies of scale and that the increasing experience of the labor force will reduce manufacturing times. The value for QDF is found according to equation (26):

$$\text{QDF} = (F_{EXP})^{1.4427 \cdot \ln N} \quad (26)$$

Where F_{EXP} represents the increasing labor experience and N is the number of units produced. Given that the HEGAAsus product family would be delivered from a new production facility by a start-up business, a value of F_{EXP} = 0.95 was selected [69].

Product liability insurance (PLI) is required by manufacturers to cover their products in use. The cost of PLI is a function of the number of products sold and their accident rate, but is usually estimated in the range of 12-17% of the total unit cost [69]. Given that the HEGAAsus product family will deliver a currently unproven technology, it is reasonable to assume PLI = 17%.

7.5. Price vs Production Rate

The production rate of both HEGAAsus variants determine the minimum selling price of the product portfolio. Table 57 shows the change in minimum selling price for the 4-seat and 6-seat HEGAAsus variants, within the production rate constraints of the supply and demand study.

Table 57 - Minimum selling price analysis of HEGAAsus product portfolio

		Monthly Production rate							
		3		4		5		6	
		4-seat	6-seat	4-seat	6-seat	4-seat	6-seat	4-seat	6-seat
6-seat monthly production rate	1	$981,701	$1,211,445	$873,480	$1,103,197	$795,618	$1,025,314	$736,324	$966,002
	2	$870,553	$1,020,984	$793,395	$943,807	$734,539	$884,934	$690,850	$841,260

As shown in Table 57, within the constraints imposed by the supply and demand study a monthly production rate for the 4-seat and 6-seat variants of 6 and 2 respectively produces the lowest minimum selling price.

7.6. Design, fabrication, and certification cost

Using the adapted Eastlake cost model, the total cost of certifying the common airframe and 6-seat wingtip extension at monthly production rates of 6 and 2 for the 4 and 6-seat variants respectively is shown in Table 58.

Table 58 - HEGAAsus product porfolio certification cost

	Man-hours		Rate, $/hr	Total cost	
	Airframe	**Wingtip**		**Airframe**	**Wingtip**
Engineering	261,330	20,759	$92	$54,951,677	$4,365,159
Development support	-	-	-	$1,874,919	$119,238
Flight test operations	-	-	-	$141,260	$61,926
Tooling	178,391	14,075	$53	$24,871,735	$1,962,391
TOTAL COST OF CERTIFICATION				**$81,839,591**	**$6,508,714**

7.7. Manufacturing

The HEGAAsus product portfolio takes advantage of outsourcing of composite manufacturing and the high commonality of the airframe to reduce production cost. Due to the high capital investment required for composite manufacturing capability, all major structural components of the HEGAAsus are outsourced to composite production facilities. These components are delivered to the HEGAAsus assembly facility where they are distributed to material storage areas until required. This approach allows the HEGAAsus production facility to operate on a lean "Just in Time" inventory strategy [99], where parts are delivered to fulfil known orders, as well as a "Level Loading" inventory model in which aircraft are constantly built at a sustainable pace to meet expected orders [100]. In addition, due to the high design commonality, the HEGAAsus family can be assembled on the same manufacturing line.

Due to the extensive outsourcing of large components and the relatively low rate of production, the HEGAAsus assembly line does not utilize the production line automation [101]. This minimizes the production line capital investment. However, automated production methods could be integrated in the assembly line at a future date, should the production rate warrant the investment. Figure 51 shows a schematic of the HEGAAsus manufacturing facility production flow [102].

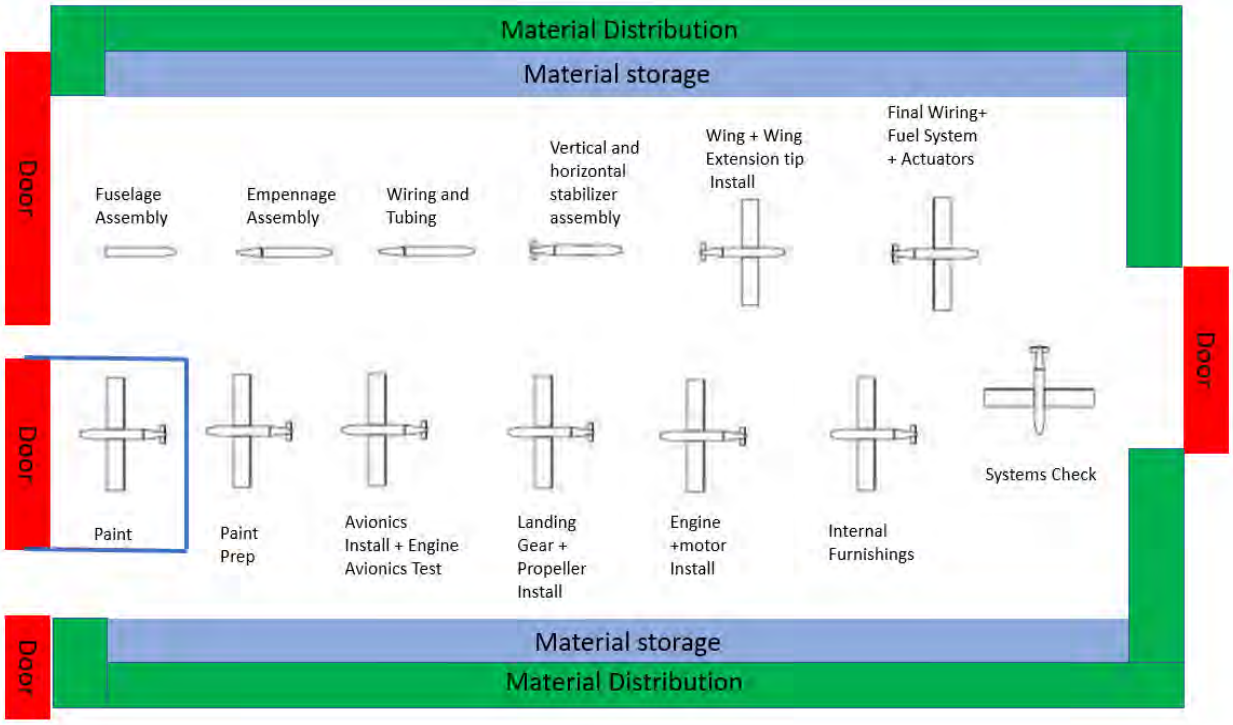

Figure 51 - HEGAAsus manufacturing facility production flow schematic

7.8. Operating costs

The operating costs for the HEGAAsus product portfolio have been estimated using the Eastlake Model, adapted to consider the novelty of a hybrid powertrain. The cost of financing the purchase of the aircraft has been omitted from the hourly cost estimation in line with industry standard. Table 59 summarizes the operational costs of both HEGAAsus passenger variants. The number of take-off cycles is required in addition to total flying hours to account for the recharging of the hybrid system batteries. The number of take-off cycles is calculated based on the number of flight hours and the flight duration based on the RFP range and target cruise speed.

Table 59- HEGAAsus product portfolio operating costs

Operation Cost Parameter	4-seat	6-seat
Annual Flight hours	*300*	
Annual Take-off cycles	*60*	*80*
Annual Aircraft maintenance cost, $	$7,839.00	$7,839.00
Annual Storage cost, $	$3,000.00	$3,000.00
Fuel flow @ cruise, gal/hr	*9.56*	*8.57*
Unit fuel cost, $ / gal	*4.50*	
Annual Fuel cost, $	$12,911.73	$11,572.62
Average electricity price, $ / kWh	0.1016	
Annual Battery charging cost, $	$5,242.56	$5,527.04
Annual Insurance cost, $	$11,825.00	$18,200.00
Annual inspection cost $/year	$500.00	$500.00
Annual Engine Overhaul fund, $/year	$3,000.00	$3,000.00
Total Yearly cost, $	**$44,318.29**	**$49,638.66**
Cost per flight hour	***$147.73***	***$165.46***

7.9. Pricing, Breakeven and Profitability

The pricing of the HEGAAsus product portfolio is based on factors including the cost of production, market price sensitivity and program profitability. A market trade study was completed to determine the acceptable purchase price for 4-seat and 6-seat GA aircraft. Comparator aircraft purchase prices were determined and plotted against aircraft advertised range and cruise speed. Linear best fit lines were drawn through the comparator 4-seat and 6-seat data sets. The HEGAAsus variants cruise speed and range were then used to determine an appropriate market price point. Figure 52 and Figure 53 show the price sensitivity data sets for this analysis. Table 60 summarises the price points for cruise and range, the average of both and the HEGAAsus price points

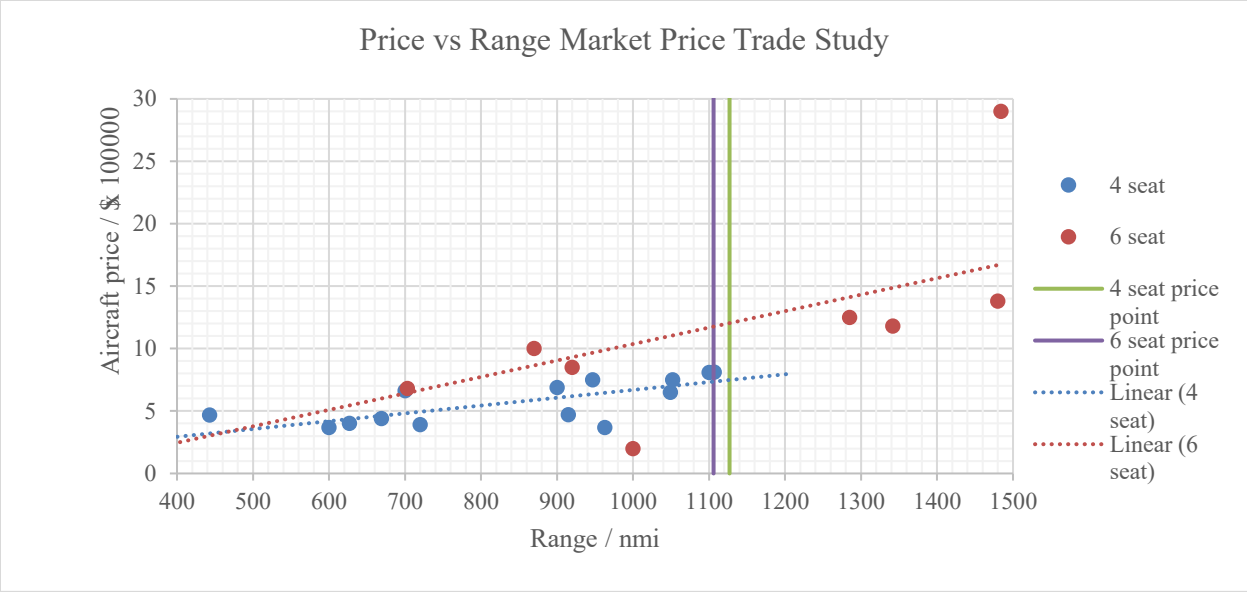

Figure 52- Price sensitivity analysis: range vs price

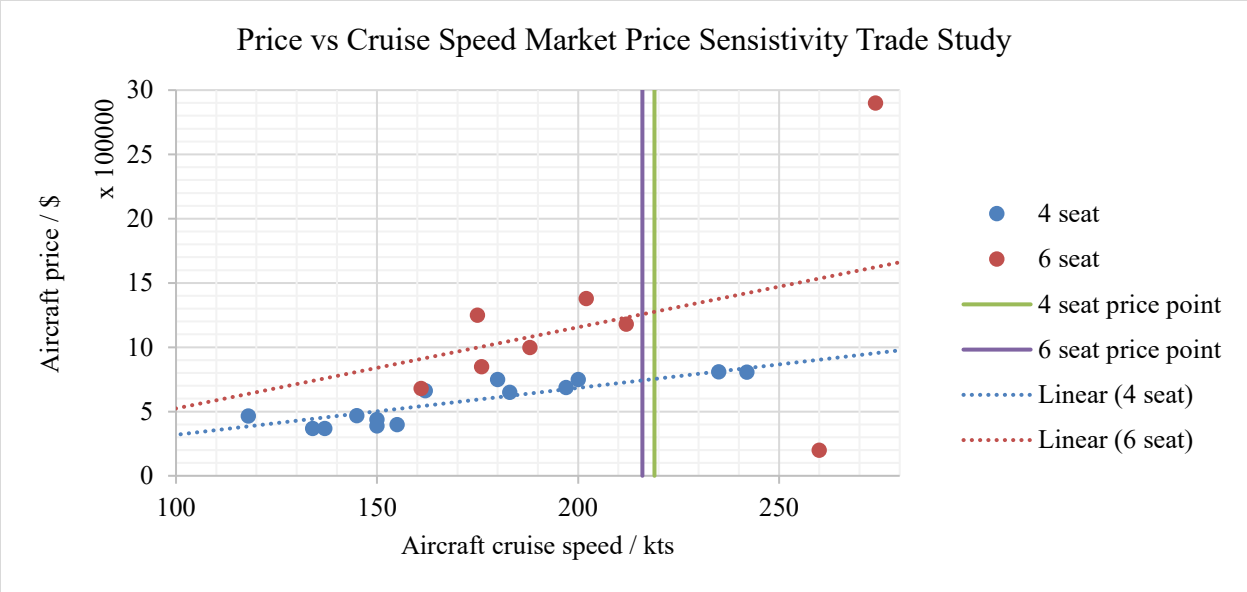

Figure 53 - Price sensitivity analysis: cruise speed vs price

Table 60 - HEGAAsus price point analysis results

HEGAAsus Variant	Range Price Point	Cruise Speed Price Point	Average Price Point	HEGAAsus price point
4-seat	$748,391	$753,333	$750,862	$755,000
6-seat	$1,176,305	$1,256,613	$1,216,459	$1,180,000

The minimum selling price (flyaway cost) represents the price at which the aircraft would have to be sold to breakeven over the initial 5-year production run, at production rates of 6 HEGAAsus 4-seat variants and 2 HEGAAsus 6-seat

variants a month. To achieve a minimum program gross profit of 15% over 5 years the retail price must be increased above the minimum selling price. The price point for the 4-seat HEGAAsus variant is $755,000, in agreement with the average predicted market expectation. The price point for the 6-seat HEGAAsus variant is $1,180,000, below the predicted average market expectation. The program gross profit margin is most sensitive to the 4-seat variant price point as the majority (360 vs 120) of aircraft produced will be in this configuration. The fall in gross revenue generated by reducing the 4-seat retail price below the predicted market expectation cannot be recovered within the limits of the 6-seat market price expectation, whilst maintaining a 15% gross profit margin. Pricing the 6-seat variant below market expectation will also account for the smaller predicted market size relative to the 4-seat market, and the subsequent larger market share it is required to achieve.

Figure 54 shows the breakeven analysis result for the initial production run of the HEGAAsus portfolio, with revenue from the Minimum Selling Price and selected retail price. Figure 54 shows that the HEGAAsus portfolio will break even after 280 (210/70) aircraft, equating to 35 months production, when sold at the chosen retail price. The program gross profit for the 5-year production run is predicted to be $63,744,900, resulting in a 15.4% gross profit margin on a total revenue of $413,000,000. This analysis assumes that both HEGAAsus variants are produced and sold over the same 5-year period, and is therefore an initial estimate.

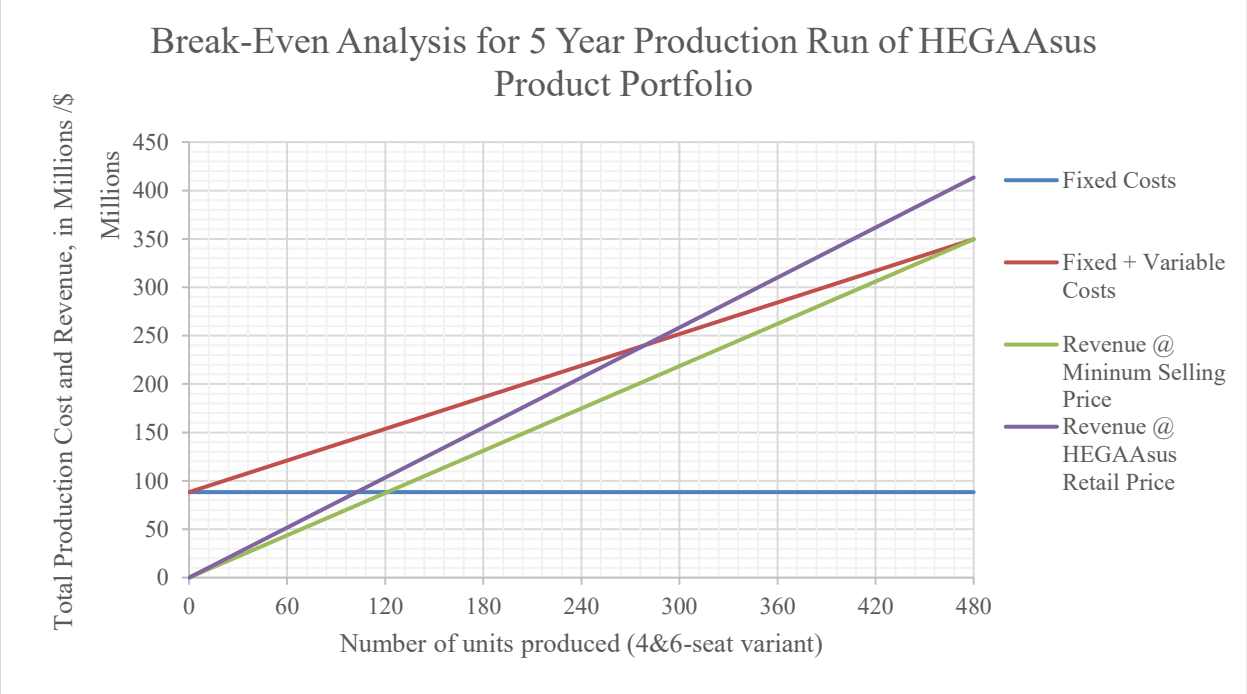

Figure 54 - HEGAAsus breakeven analysis for initial 5-year production run

8. GENERAL ARRANGEMENT DRAWINGS

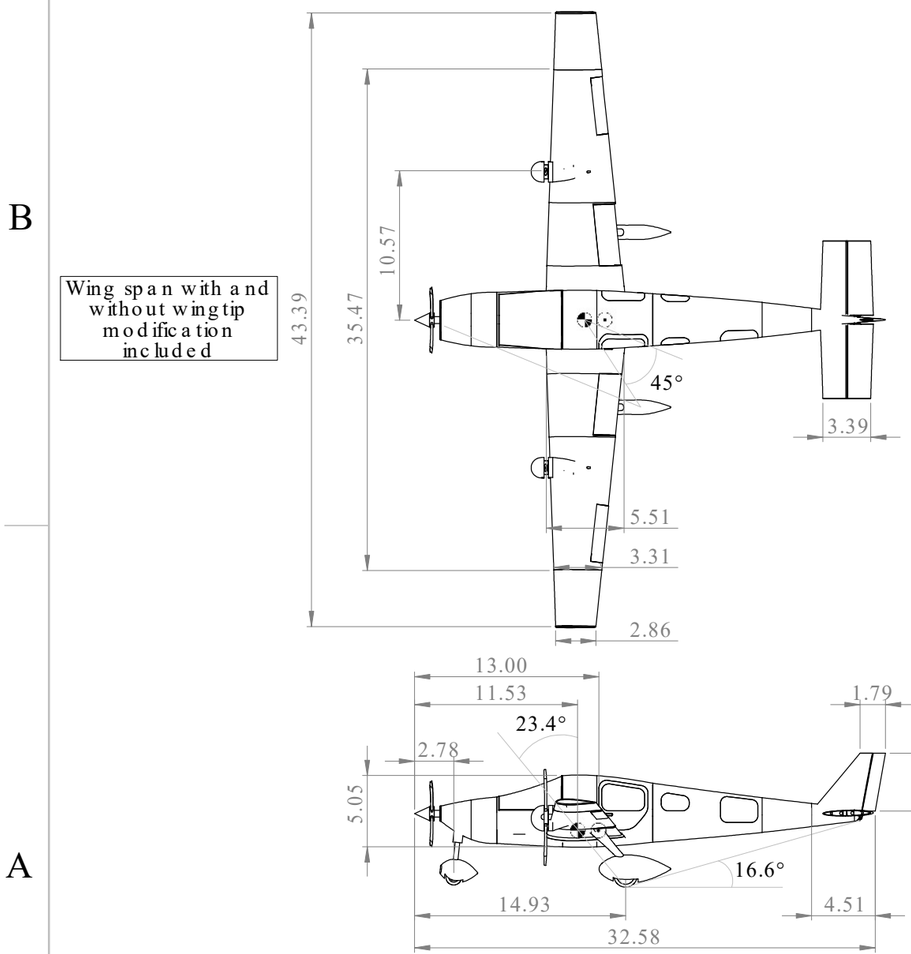

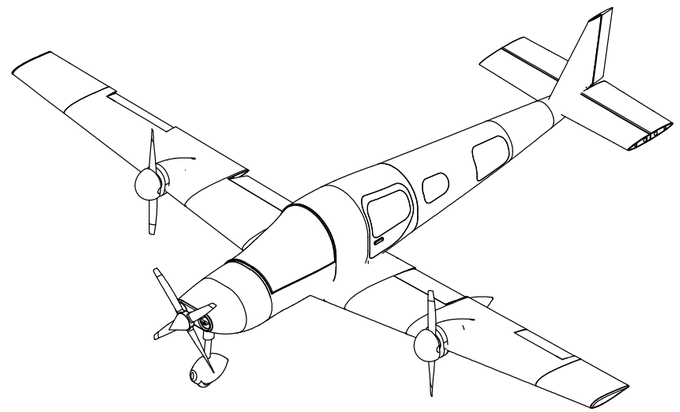

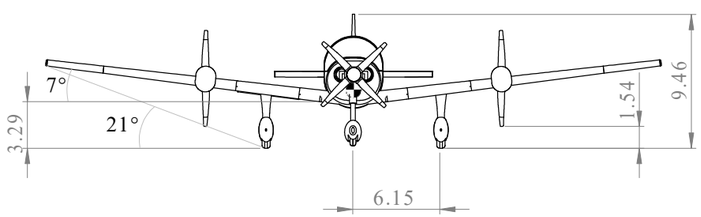

TITLE: HEGAAsus 3-View		
DATE: 4/29/18	AUTHOR: Samantha Rocker	REV: 1
SCALE: 1:100	UNITS: feet, ft	SHEET 1 OF 1

9. REFERENCES

[1] S. Aviation, "ACARE Explained," 2015. [Online]. Available: http://www.sustainableaviation.co.uk/wp-content/uploads/2015/09/SBAC-Aviation-and-Environment-Briefing-Paper-–-ACARE-Explained.pdf. [Accessed: 14-Nov-2017].

[2] Trade-A-Plane, "Trade-A-Plane: Aircraft for Sale," *Trade-A-Plane Aircraft Listings*, 2017. [Online]. Available: https://www.trade-a-plane.com/. [Accessed: 20-Oct-2017].

[3] General Aviation Manufacturers Association, "GENERAL AVIATION, Statistical Databook & Industry Outlook," 2011.

[4] B. Landsberg, "WHEN IS AN AIRCRAFT TOO OLD?," *AOPA News*, 2000. [Online]. Available: https://www.aopa.org/news-and-media/all-news/2000/july/pilot/when-is-an-air. [Accessed: 15-Nov-2017].

[5] Transparency Market Research, "Hybrid Cars Market Estimated to Reach US$ 398.90 Bn by 2024; Global Industry Analysis, Size, Share, Growth, Trends, and Forecast 2016 - 2024: Transparency Market Research," *Cision*. [Online]. Available: https://www.prnewswire.com/news-releases/hybrid-cars-market-estimated-to-reach-us-39890-bn-by-2024-global-industry-analysis-size-share-growth-trends-and-forecast-2016---2024-transparency-market-research-615068924.html. [Accessed: 14-Apr-2018].

[6] P. Jackson, *Jane's All the World's Aircraft*, 100th ed. Jane's Information Group, 2013.

[7] C. Campbell *et al.*, "Design of a Hybrid Electrical Propulsion System," *52nd AIAA/ASME/ASCE/AHS/ASC Struct. Struct. Dyn. Mater. Conf.*, no. April, pp. 1–10, 2011.

[8] Siemens, "World's first serial hybrid electric aircraft to fly at Le Bourget," *Joint press release by Siemens, Diamond Aircraft and EADS*. [Online]. Available: https://www.siemens.com/press/en/pressrelease/?press=/en/pressrelease/2011/corporate_communication/axx20110666.htm. [Accessed: 10-Nov-2017].

[9] B. S. Gunston Bill, Willis David, Munson Kenneth , Peacock Lindsay T., Jackson Paul, *Jane's All the World's Aircraft: Development & Production 2015-2016 2015-2016*, 104th ed. IHS Jane's;

[10] The Telegraph, "What is The Airbus E-Fan? In 60 seconds." [Online]. Available: https://www.telegraph.co.uk/news/aviation/11730235/What-is-The-Airbus-E-Fan-In-60-seconds.html. [Accessed: 30-Apr-2018].

[11] Airbus, "The E-Thrust concept with Rolls Royce," *Airbus Newsroom*, 2017. [Online]. Available: http://company.airbus.com/responsibility/airbus-e-fan-the-future-of-electric-aircraft/technology-tutorial/E-Thrust.html. [Accessed: 15-Nov-2017].

[12] A. Dubois, M. Van Der Geest, J. Bevirt, J. Aviation, S. Cruz, and N. Glenn, "Design of an Electric Propulsion System for SCEPTOR," 2017.

[13] Aurora Flight Sciences, "LIGHTNING STRIKE, INNOVATION FOR RUNWAY INDEPENDENCE," 2016. [Online]. Available: http://www.aurora.aero/wp-content/uploads/2016/07/LightningStrike_brochure.pdf. [Accessed: 05-Nov-2017].

[14] R.- Royce, L. Term, C. Aircraft, P. System, J. Whurr, and P. Beecroft, "Vision 20," *Proc. 27th ISABE Conf.*, pp. 1–19, 2017.

[15] G. Hawley, "UNDERSTANDING TESLA'S LITHIUM ION BATTERIES," *EVANNEX*. [Online]. Available: https://evannex.com/blogs/news/understanding-teslas-lithium-ion-batteries. [Accessed: 12-Nov-2017].

[16] R. Matheson, "Doubling battery power of consumer electronics," *MIT*, 2016. [Online]. Available: http://news.mit.edu/2016/lithium-metal-batteries-double-power-consumer-electronics-0817.

[17] J. B. . Braga, M. H., Grundish, N. S., Murchison, A. J., and Goodenough, "Alternative strategy for a safe rechargeable battery," *Energy Environ. Sci.*, vol. 10, pp. 331–336, 2016.

[18] GRABAT, "Clean and Sustainable Energy for All." [Online]. Available: https://www.grabat.es/en. [Accessed: 12-Dec-2017].

[19] AOPA, "OXYGEN USE IN AVIATION," 2018. [Online]. Available: https://www.aopa.org/training-and-safety/pic-archive/pilot-and-passenger-physiology/oxygen-use-in-aviation. [Accessed: 29-Apr-2018].

[20] P. Aircraft, "Panthera Aircraft News," *Panthera Aircraft News*, 2017. [Online]. Available: http://www.pipistrel.si/plane/panthera/overview. [Accessed: 21-Oct-2017].

[21] P. Aircraft, "Welcome to the Seneca," 2017. [Online]. Available: http://www.piper.com/aircraft/trainer-class/seneca-v/. [Accessed 21 October 2017]. [Accessed: 21-Oct-2017].

[22] T. Avaiation, "Cessna Turbo Stationair HD brochure," 2017. [Online]. Available: http://cessna.txtav.com/-/media/cessna/files/piston/stationair/stationair_brochure.ashx. [Accessed: 08-Nov-2017].

[23] Textron Aviation, "Beechcraft Bonanza G36 Brochure," *Beechcraft Aircraft Website*, 2017. [Online]. Available: http://beechcraft.txtav.com/en/bonanza-g36. [Accessed: 21-Oct-2017].

[24] B. Cox, "Choosing A Six-Seater Fixed Gear Retractables," *Plane & Pilot*, 2010. [Online]. Available: http://www.planeandpilotmag.com/article/choosing-a-six-seater. [Accessed: 18-Oct-2017].

[25] F. Staff, "Six Classic Utility Aircraft," *Fyingmag*, 2013. [Online]. Available: https://www.flyingmag.com/aircraft/six-classic-utility-aircraft. [Accessed: 18-Oct-2017].

[26] Honda, "Statistics & Specifications for Honda's Advanced Light Jet - HondaJet." pp. 1–10, 2017.

[27] J. W. Tallman, "ROOM ENOUGH FOR ALL," *Aircraft Owners and Pilots Association News*, Nov-2013. [Online]. Available: https://www.aopa.org/news-and-media/all-news/2013/november/pilot/room-enough-for-all. [Accessed: 18-Oct-2017].

[28] T. Whaling, "What is the best 6 seat airplane ?," 2017. [Online]. Available: quora.com. [Accessed: 14-Nov-2017].

[29] C. on A. E. P. (CAEP), "Information related to the tenth meeting of the comitee on Aviation Environmental Protection (CAEP/10)," *Commitee on Aviation Environmental Protection (CAEP)*, 2016. [Online]. Available: https://www.icao.int/ENVIRONMENTAL-PROTECTION/Pages/CAEP.aspx. [Accessed: 25-Oct-2017].

[30] D. P. Raymer, *Aircraft Design: A Conceptual Approach*, 2nd ed. Washington: AIAA Education Series, 1992.

[31] Siemens, "Integrated inverter and DC/DC converter – A modular and scalable platform." [Online]. Available: https://w3.siemens.com/topics/global/de/elektromobilitaet/PublishingImages/antriebe-

pkw/pdf/sivetec-pes-siemens_en.pdf. [Accessed: 27-Mar-2018].

[32] Siemens AG, "Aerobatic Airplane 'Extra 330LE,'" 2016. [Online]. Available: https://www.siemens.com/press/pool/de/events/2016/corporate/2016-12-innovation/inno2016-aerobatic-airplane-e.pdf. [Accessed: 05-Nov-2017].

[33] G. Cinar *et al.*, "Sizing, Integration and Performance Evaluation of Hybrid Electric Propulsion Subsystem Architectures," *55th AIAA Aerosp. Sci. Meet.*, no. January, pp. 1–18, 2017.

[34] Heintje Wyczisk and Claus Zeumer, "HYPSTAIR – System Architecture, Certifiability and Safety Aspects Symposium E^2-Fliegen 2016, Stuttgart," *Symp. E^2-Fliegen 2016*, 2016.

[35] "Tranmissions," in *Cost, Effectiveness, and Deployment of Fuel Economy Technologies for Light-Duty Vehicles*, National Academies Press, 2015, pp. 167–172.

[36] MIT, "11.7 Performance of Propellers." [Online]. Available: http://web.mit.edu/16.unified/www/FALL/thermodynamics/notes/node86.html. [Accessed: 06-Mar-2018].

[37] C. Cessna and C. Tt, *Pilot Operating Handbook & Flight Manual - Columbia 400 / Cessna Corvalis TT*, no. Rev. 101113-01. X-Plane by Laminar Research.

[38] B. University, "Charging LI-ion batteries." [Online]. Available: http://batteryuniversity.com/learn/article/charging_lithium_ion_batteries. [Accessed: 15-Jan-2018].

[39] D. Galeon, "Fast Chargin EVS," *NBC News*. [Online]. Available: https://www.nbcnews.com/mach/science/carmaker-sees-ultrafast-charging-2022-electric-vehicles-ncna824576. [Accessed: 27-Apr-2018].

[40] Z. Lu, X. Yu, L. Zhang, X. Meng, L. Wei, and L. Jin, "Experimental investigation on the charge-discharge performance of the commercial lithium-ion batteries," *Energy Procedia*, vol. 143, pp. 21–26, 2017.

[41] E. Calculation, "kWh to Ah Conversion Calculator." [Online]. Available: http://everydaycalculation.com/kwh-ah.php. [Accessed: 27-Apr-2018].

[42] F. Hexcel, "Hexcel ready to fly on the A350 XWB," *Reinf. Plast.*, vol. 57, no. 3, pp. 25–26, 2013.

[43] Hexcel, "HexPly ® 8552 - Product Data Sheet - EU Version." Hexply, pp. 1–6, 2016.

[44] Toray Composite, "Toray 3900 PREPREG SYSTEM 3900-series," 2017. [Online]. Available: http://www.toraycma.com. [Accessed: 05-Mar-2018].

[45] G. Norris and M. Wanger, *Boeing 787 Dreamliner*, 1st ed. Minneapolis: Zenith Press;, 2008.

[46] K. Bernetich, "Personal Advisment: Karl Bernetich, Material and Manufacturing Engineering for Boeing Co." p. Composite materials selection and manufacturing, j, 2018.

[47] A. Comparison, "Aircraft Comparison Cessna 350 Cessna 400 Cirrus SR22 Cirrus SR22 Turbo." Cessna Aircraft company, 2008.

[48] Piper, *Pilot's Operating handbook 1999kg Seneca II*, 1st ed. Vero Beach 1: Piper, 1980.

[49] M. Nita and D. Scholz, "Estimating the Oswald Factor from Basic Aircraft Geometrical Parameters," *Dtsch. Luft- und Raumfahrtkongress*, vol. 281424, pp. 1–19, 2012.

[50] B. S. de Mattos, "Fuselage Design.," *ITA - Technol. Inst. Aeronaut.*, pp. 1–21, 2009.

[51] M. H. Sandraey, *Aircraft Design: A Systems Engineering Approach*. Chichester: Wiley, 2013.

[52] D. J. Roakam, *Airplane Design Part V: Volume 5*. Design, Analysis and Research Corporation (DARcorporation), 2015.

[53] FAA, "FAA Aerospace-Forecast-General-Aviation-Data-Tables-2017-2037." 2016.

[54] EPS, "EPS Fuel Economy," 2017. [Online]. Available: https://eps.aero/the-eps-engine/fuel-consumption/. [Accessed: 06-Mar-2018].

[55] D. Chen and J. H. A. Chuang, "RED A05," 2014. [Online]. Available: https://www.red-aircraft.com/wp-content/uploads/2012/07/RED-A051.pdf. [Accessed: 06-Mar-2018].

[56] C. Aircraft, "Explore the SR22," 2018. [Online]. Available: https://cirrusaircraft.com/aircraft/sr22/. [Accessed: 06-Mar-2018].

[57] N. Moll, "AIN Exclusive: The Higgs Diesel," *AIN Online*, 2016. [Online]. Available: https://www.ainonline.com/aviation-news/general-aviation/2016-11-08/ain-exclusive-higgs-diesel. [Accessed: 06-Mar-2018].

[58] C. Engines, "CE-2017-202 Diesel engine for aircraft propulsion system," vol. 169, no. 2, pp. 7–13, 2017.

[59] A. Aero, "JET-A Solutions," 2018. [Online]. Available: http://www.ac-aero.com/jet-a/. [Accessed: 06-Mar-2018].

[60] Lycoming, "iE2 Engine." [Online]. Available: https://www.lycoming.com/engines. [Accessed: 22-Feb-2018].

[61] Continential, "Type Certificate E3SO ENGINE SPECIFICATIONS IO-550-N," *Continential*, p. 634675.

[62] R.- Royce, "The most versatile turboshaft engine in its class," *2018*. [Online]. Available: https://www.rolls-royce.com/products-and-services/defence-aerospace/uavs/m250-turboshaft.aspx#/. [Accessed: 06-Mar-2018].

[63] C. Motors, "Continental ® Aircraft Engine Maintenance Manual IO-360," *Continential*, 2011.

[64] Tesla, "Induction Versus DC Brushless Motors." [Online]. Available: https://www.tesla.com/en_GB/blog/induction-versus-dc-brushless-motors?redirect=no. [Accessed: 14-Nov-2017].

[65] I. Precision Electric, "NEED A VARIABLE FREQUENCY DRIVE TO CONTROL THE SPEED / SOFT START YOUR AC OR DC MOTOR?" [Online]. Available: https://www.precision-elec.com/difference-between-ac-and-dc-motors/. [Accessed: 14-Nov-2018].

[66] S. E. Electrial Engineering, "Why does a Tesla car use an AC motor instead of a DC one?," 2013. [Online]. Available: Why does a Tesla car use an AC motor instead of a DC one? [Accessed: 14-Nov-2017].

[67] V. Der Hoeven, "Development of Superconducting and Cryogenic Power Systems and Impact for Aircraft Propulsion," vol. 1115, no. 1963, pp. 1322–1328, 1964.

[68] T. Theodorsen, *The theory of propellers.* Langley Field: Langley Aeronautical Laboratory, 1994.

[69] S. Gudmundsson, *General Aviation Aircraft Design, Applied Methods and Procedures*. Elsevier, 2014.

[70] J. Roskam, *Airplane Design Part III: Layout Design of Cockpit, Fuselage, Wing and Empennage: Cutaways and Inboard Profiles: Volume 3*, 5th ed. Kansas: DARcorporation, 2017.

[71] T. H. E. Drag, O. F. Airplane, W. Fairings, L. Gears, P. Retractable, and L. Gears, "NATIONAL

ADVISORY COMMITTEE FOR AERONAUTICS REPORT No . 518 THE DRAG OF AIRPLANE WHEELS , WHEEL FAIRINGS II-NONRETRACTABLE AND PARTLY RETRACTABLE II-NONRETRACTABLE AND PARTLY RETRACTABLE," no. 518, 2018.

[72] J. Roskam, *Airplane Design Part IV: Layout Design of Landing Gear and Systems: Volume 4*, 7th ed. Kansas: DARcorporation, 2017.

[73] P. Raj, "AOE 6045: Aircraft Design- Aircraft configuration." Viginia Technology University, 2017.

[74] FAA, "Part 23 - Small Airplane Certification Process Study," pp. 0–89, 2009.

[75] J. Roskam, *Airplane Design Part VII: Determination of Stability, Control and Performance Characteristics: Volume 7*, 4th ed. Kansas: DARcorporation, 2017.

[76] Garmin, "Aviation, Avionics, Autopilot," 2018. [Online]. Available: https://buy.garmin.com/en-GB/GB/p/70143. [Accessed: 06-Mar-2018].

[77] C. and Company, "Low Power Ice Protection Systems," 2015. [Online]. Available: http://www.coxandco.com/products/low_power_ice_protection_systems.html. [Accessed: 10-Apr-2018].

[78] Disiplines of flight, "The Cessna 210 Centurion: Arguably the best high performance single ever produced." [Online]. Available: https://disciplesofflight.com/cessna-210-centurion/. [Accessed: 15-Apr-2018].

[79] Panasonic, "Specifications for NCR18650GA Specifications Discharge rate characteristics of NCR18650GA." [Online]. Available: https://na.industrial.panasonic.com/sites/default/pidsa/files/ur18650zta.pdf. [Accessed: 13-Apr-2018].

[80] L. M. N. G. E. Carichner, *Fundamentals of Aircraft and Airship Design, Volume 1 – Aircraft Design*. AIAA Education Series, 2010.

[81] K. Petermaier, "Electric propulsion components with high power densities for aviation." pp. 1–16, 2015.

[82] T. Lombardo, "Inside Siemens' Record-Breaking Electric Aircraft Motor," *engineering.com*, 2016. [Online]. Available: https://www.engineering.com/ElectronicsDesign/ElectronicsDesignArticles/ArticleID/12805/Inside-Siemens-Record-Breaking-Electric-Aircraft-Motor.aspx. [Accessed: 19-Apr-2018].

[83] Mocal Oil Coolers, "Oil Coolers," *Mocal Products*, 2017. [Online]. Available: http://www.mocal.co.uk/products-oilcoolers.html. [Accessed: 19-Apr-2018].

[84] K. Onda, O. Ohsihma, M. Nakayma, K. Fukunda, and T. Araki, "Thermal behaviour of small lithium-ion battery during charge and dicharge cycles," *Jounal of Power sourcres*, p. 8, 2015.

[85] I. Chimie, "Thermal Hazard Technology." [Online]. Available: http://www.inforlab-chimie.fr/doc/document.fichier.279.pdf. [Accessed: 19-Apr-2018].

[86] Y. . Cegel, *Heat Transfer: a Practical Approach*, 2nd ed. McGraw-hill, 2003.

[87] S. Cole, "Synthetic vision systems on the way for military avionics," 2017. [Online]. Available: http://mil-embedded.com/articles/synthetic-systems-the-for-military-avionics/. [Accessed: 29-Apr-2018].

[88] ESP Associates, "Airports," 2018. [Online]. Available: http://www.espassociates.com/markets/transportation/airports.

[89] Inch, "LiDAR sensor." [Online]. Available: https://inchbyinch.de/pictorial/lidar-sensor/. [Accessed: 29-Apr-

2018].

[90] FAA, “Automatic Dependent Surveillance-Broadcast (ADS-B).” [Online]. Available: https://www.faa.gov/nextgen/programs/adsb/. [Accessed: 29-Apr-2018].

[91] M. Fleming, “Personal Advisment: Micheal Fleming Full Autonomey.” .

[92] A. . Kundu, *Aircraft Design*, 1st ed. Cambridge: Cambridge University Press, 2010.

[93] V. Rajkumar, “Personal Advisment: V.G.Rajkumar WAPSE.” Crofton Department of Aerospace and Ocean Engineering Virginia Polytechnic Institute and state university, Blackburg.

[94] JavaProp, “Design and Analysis of Propellers.” [Online]. Available: https://www.mh-aerotools.de/airfoils/javaprop.htm. [Accessed: 20-Apr-2018].

[95] Tornado, “A vortex Lattice Method implemented in MATLAB,” 2015. [Online]. Available: http://tornado.redhammer.se/. [Accessed: 20-Apr-2018].

[96] D. J. Roakam, *Airplane Design Part I: Volume 1*, 5th ed. Kansas: DARcorporation, 2015.

[97] IATA- Honeywell, “ATA Chapter List.” [Online]. Available: https://havrel.honeywell.com/docs/inforesources/ATA_Chapter_Descriptions.PDF. [Accessed: 29-Apr-2018].

[98] Woolworths Limited, “General Aviation Manufacturers Association - 2017 Annual Report,” pp. 1–57, 2017.

[99] Investopedia, “Just In Time - JIT,” 2018. [Online]. Available: https://www.investopedia.com/terms/j/jit.asp. [Accessed: 19-Apr-2018].

[100] Quality America Inc., “Level Load Balancing.” [Online]. Available: http://qualityamerica.com/LSS-Knowledge-Center/leansixsigma/level_load_balancing.php. [Accessed: 19-Apr-2018].

[101] Precision Automated Technolgy Inc, “Labor vs Automation Infographic: How Robotics Can Increase Your Bottom Line.” [Online]. Available: https://p-a-t.com/blog/labor-vs-automation-infographic-how-robotics-can-increase-your-bottom-line/. [Accessed: 19-Apr-2018].

[102] K. Stone, V. President, and P. Executive, “Aircraft Manufacturing Facility Design,” *Austin Co.*, pp. 1–13.

[103] R. Boynton, K. Weiner, "Measuring Mass Properties of Aircraft Control Surfaces"